Effect of lateral density variations of topographical masses in improving geoid model accuracy over Canada

Zdeněk Martinec, 1993

Contents

List of Figures

List of Tables

Preface

This is the final report prepared for the Energy, Mines and Resources of Geodetic Survey Division of Canada under the term of contract DSS No. 23244-2-4356/01-SS (DSS file No. 032SS.23244-2-4356). The Scientific Authority for this contract was Dr. André Mainville.

Acknowledgements

The work reported here was prepared while the author was on leave from the Faculty of Mathematics and Physics, Charles University in Prague, Czech republic. I am grateful to Prof. Dr. Petr Vaníček for the hospitality enjoyed during my stay at the Department of Surveying Engineering at the University of New Brunswick (UNB). I appreciate his constant support and encouregement throughout the research.

I wish to take this opportunity to thank the Scientific Authority, Dr. André Mainville, for his exemplary cooperation and repeated help.

I wish to express my gratitude to Mr. Mehdi Najafi for careful reading all the progress reports and a draft of the final report, and his effort to improve understandability of the text. I extend my indebtedness to Peng Ong for his help with finding out the series of Geological Maps of Canada.

Dr. Marc Véronneau has contributed to the success of this investigations by making available to me data sets of the digital terrain model of Canada.

Introduction

Today's effort of geodesists is devoted to compute the geoid with an absolute accuracy of 1 cm. To achieve such an accuracy, the theory of solving a geodetic boundary value problem for geoid determination used up to now to compute the geoid with an accuracy of about 50 cm has to be precised. There is a lot of theoretical problems that have to be highlighted for computing such an accurate geoid. Let us introduce a couple of questions which should be answered in this context. How to continue the gravity data from the topography to the geoid through the topographical masses in order the traditional Stokes's integral could be applied to gravity anomalies? How to incorporate the truncation error of Stokes's integration into the geoidal height corrections? How many terms of the Taylor series expansion of the gravitational potential of the topographical masses are to be taken into consideration for a precise computing the gravitational effect of the topographical masses?

In this report we focus our attention on the problem of the influence of lateral changes of the density of the topographical masses (masses between the geoid and the earth's surface) on geoidal height computation. Up to now all theories computing the gravitational effect have assumed that the topographical masses were homogeneous. The density was considered constant, equal to a mean value $\varrho_0 = 2.67$ g/cm^3. This is too approximate especially near and in mountaineous areas. Geological and geophysical knowledge about the earth's crust indicates that there are lateral density variations of the order of 10% at least. In contrast with deeper parts of the earth, the radial changes of the density of the topographical masses are unimportant. The reason is that the mass density of deeper parts of the earth is influenced by pressure and temperature changing strongly radially, whereas the density of topographical masses is determined by geological factors (geological formation, age, porosity, previous history, etc.) which differs from place to place.

The report aims to answer the question: Are corrections to geoidal heights due to laterally varying density of topographical masses important for a 1-cm geoid determination? And, if so how to modify the existing theories for the topographical effect computation to take into consideration lateral density inhomogeneities.

Theoretically, we will investigate three problems connected with these questions.

1. What are the correct forms of expressions describing the effect of topographical masses on geoidal heights?

2. How to remove a weak singularity of the Newton integral kernel if a 2-D topographical density is considered?

3. How large is the truncation error of Stokes integration and how to remove a weak singularity of Stokes's function?

The gravitational effect of topographical masses on geoid heights is described by three terms (Heiskanen and Moritz, 1967; Wichiencharoen, 1982; Vaníček and Kleusberg, 1987; Wang and Rapp, 1990; Sideris and Forsberg, 1990; Heck, 1992; Martinec and Vaníček, 1993a,b; Martinec et al., 1993a; Martinec, 1993a-c): the *direct topographical effect on gravity* which is the gravitational attraction of topographical masses at a point on the topography, the *primary indirect topographical effect on potential* which is the gravitational potential of topographical masses at a point on the geoid, and the *secondary indirect topographical effect on gravity* which is the gravitational effect of topographical masses on the anomalous gravity on the geoid.

Nevertheless, in geodetical literature there are large differences in formulae for describing these terms. Mixing the gravitational attraction of topographical masses with the downward continuation of gravity anomalies (Wang and Rapp, 1990) is one reason of discrepancies of formulae for the direct topographical effect on gravity. Misunderstanding planar approximation of the geoid (Wichiencharoen, 1982; Vaníček and Kleusberg, 1987; Wang and Rapp, 1990) is a source of severe errors in formulae for the primary indirect topographical effect on potential (Martinec and Vaníček, 1993a). Chapter 1 of the report is thus devoted to derive theoretical formulae for the above topographical terms in the forms which they possess in a boundary condition of the boundary-value problem for geoid determination.

The weak singularity of the Newton kernel makes difficulty in computing the direct topographical effect on gravity as well as both the indirect topographical effects. The traditional way (Moritz (1968, 1980); Wichiencharoen (1982); Vaníček and Kleusberg (1987); Wang and Rapp (1990); Sideris and Forsberg (1990); Heck (1992); Martinec and Vaníček (1993a,b)) of removing the singularity on the Newton kernel is as follows. First, the Newton kernel is expanded by means of Taylor's series expansion, then the integral over the vertical coordinate is carried out analytically, and finally the singularity is removed in each individual terms of Taylor series.

A questionable point of the above procedure, pointed out e.g. by Heck (1992), is whether the Taylor series expansion converges or not, and if so, how many terms of the infinite Taylor series should be taken into consideration to describe the gravitational potential with a prescribed accuracy. Geodesists (Moritz, 1968; Vaníček and Kleusberg,1987; Sideris, 1990; Forsberg and Sideris, 1993) usually take only a few first terms of the Taylor series (most often only the first three) and believe that the rest of the series may be neglected. This seems to be a good approximation for a flat terrain when a grid of the topographical heights is sparse having a large step (e.g. 0.5 degree). Then a dummy point of integration in the Newton integral never goes too much close to the computation point and magnitudes of higher order terms of the Taylor series retain small.

The problems appear when the gravitational potential of the topographical masses is computed in a rugged mountaineous terrain such as the Rocky Mountains. In this case, a grid of topographical heights has to be considered fairly dense (e.g. 1km×1km) to fit rought shape irregularities of the terrain. A dummy point of the Newton integral may moves very close to the computation point, and thus magnitudes of higher order Taylor terms increase faster then magnitudes of lower order terms. As a result, higher order terms become dominant and the Taylor series expansion stops to converge (Martinec at al., 1993c)

Instead of expanding the Newton kernel into a Taylor series expansion and removing singularity of each series term separately, in this report (Chapter 2) we will remove the singularity of the Newton kernel immediately in the definition of the Newton integral. By subtracting and adding a value of the Newton kernel at the computation point to the Newton integrand, the singular point $\psi = 0$ may be left out from the integration domain, and thus the singularity can be overcome. The only necessity is to evaluate the

Newton integral over a fixed height and a fixed mass density. This can be done analytically resulting in the gravitational potential of a Bouguer shell.

In Chapter 3 we will show how to chose the condensation density of the Helmert condensation layer. A concrete form of the condesation density influences a condition for the existence of the solution of the boundary-value problem for geoid determination. An improper choise of the condensation density may cause that the boundary condition for an anomalous gravitational potential is singular, and consequently, the solution of the boundary-value problem does not exist in a 'classical' sense. Moreover, a condensation density significantly influences forms of the Bouguer terms of the direct as well as primary indirect topographical effect; different ways of condensation results in different expressions for the topographical terms. Therefore, attention should be paid to a way how to perform the condesation of the topographical masses.

To distinguish contributions to the geoidal heights generated by topographical masses of a constant density from those coming from the lateral changes, we will separate the density of topographical masses into a 'reference' part, which will be considered constant throughout all the topo-masses, and laterally varying 'anomalous' part. Lateral changes of the topographical density may appear due to different reasons. In Chapters 5 and 7 we will consider three of them: the density contrast of water in lakes, the Pratt-Hayford compensation density, and anomalous density of a given geological formation. The first type of lateral changes of topo-density is important in regions with large lakes (such as in the North America). By the second model of the lateral density, we will estimate the effect of compensation mechanism of topographical masses on the geoidal heights. Nevertheless, as already mentioned, the largest lateral changes of the topographical density are caused by geological factors. On a geological pattern of topographical masses from Purcell Mountains (the eastern part of the Canadian Rockies) we will demonstrate that the lateral densities may play an important role for an accurate geoid determination.

The direct topographical effect on gravity can be transformed to geoidal heights by applying the Stokes integration. To avoid the integration over the whole earth, Vaníček and Kleusberg (1987) suggested to separate the geoidal heights into low and high frequency parts. The low frequency part is assumed to be determined from satellite geodesy, whereas the high frequency part is computed by Stokes's integration with the spheroidal or the modified

spheroidal Stokes's function. Unfortunately, Vaníček and Kleusberg (1987) did not explore the truncation error of this 'partial' Stokes's integration quite properly. Therefore, one point under our interest is to give a formula and numerical values (over Canada) of this error. Theoretically, this requires to introduce the Molodensky truncation coefficients for the spheroidal and the modified spheroidal Stokes functions. The section 6.2 dealts with this problem.

All mentioned Stokes's functions have a weak singularity at the point $\psi = 0$. Hence, to evaluate the Stokes integral numerically, we meet with the same problems as in computing the Newton integral. The singularity at the point $\psi = 0$ may be treated by an analytical way (Heiskanen and Moritz, 1967, sect. 2.24) or may be removed by the same way as we do for Newton kernel. Vaníček and Kleusberg (1987) used the former possibility, but we will follow the latter possibility and remove the singularity of the Stokes function by subtracting and adding the gravity anomaly at the computation point to the gravity anomaly at an integration point. In such a way, the singular point $\psi = 0$ of Stokes's function will be removed from the integration domain.

The price paid for it is to evaluate the angular integral of the Stokes function analytically. When the integration domain of Stokes's integral is the full solid angle, then the angular integral of the Stokes function vanishes. Nevertheless, we will shrink the Stokes integration to a spherical cap of a small radius. In this case an incomplete integral of Stokes's function does not vanish; analytical formula for the primitive function of this integral is derived in section 6.4.

Chapter 1

Stokes-Helmert's boundary-value problem for geoid determination

This chapter is devoted to formulate the boundary-value problem for geoidal height determination. As was shown by many geodesists this problem can be characterized as a *free non-linear* boundary-value problem for the *internal non-harmonic* gravity potential. We will demonstrate that this problem can be transformed to a *fixed linearized* boundary-value problem for the *harmonic* Helmert anomalous potential.

We are specially interested in terms describing the effect of topographical masses on geoidal heights. We will show that this effect can be characterized by three terms, the direct topographical effect on gravity, the primary indirect topographical effect on potential, and the secondary indirect topographical effect on gravity. In geodetical literature there are large differences in formulae for descriptions of these terms. Let us mention the contraversy between Vaníček and Kleusberg's (1987) equation for the direct topographical effect and Wang and Rapp (1991)'s mixed formula for the direct topographical effect and the downward continuation of gravity anomaly. The planar approximation of the geoid caused that resulting equations for the primary indirect effect on potential derived e.g. by Wichiencharoen (1982) or Vaníček and Kleusberg (1987) are also significantly biased (Martinec and Vaníček, 1993a). Therefore, in Chapter 1 we will derive formulae for topographical terms in details.

1.1 Formulation of the problem

Let us start with reminding fundamental expressions related to geoid determination.

Gravity field. The gravity potential W is created by the gravitational potential V generated by the earth's masses and by the centrifugal potential Φ induced by the earth's rotation, i.e.,

$$W = V + \Phi \ . \tag{1.1}$$

The potentials will be described by spherical coordinates (r, Ω), where Ω stands for the pair of angular coordinates, co-latitude ϑ and longitude λ.

Geoid. As usual the geoid is defined as the equipotential surface of the gravity potential W of the earth corresponding to the mean sea level, i.e.,

$$W(r, \Omega) = W_0 \ , \tag{1.2}$$

where W_0 is the prescribed (known) value. This implicit definition of the geoid may be transformed to an explicit expression for the radial coordinate r of a point on the geoid,

$$r = r_g(\Omega; W_0) \ , \tag{1.3}$$

where $r_g(\Omega; W_0)$ is a non-linear function of both the variables Ω and W_0. The Bruns's formula (Heiskanen and Moritz, 1967, eqn.(2-144)) represents a linearized form of eqn.(1.3).

Topographical masses. The masses between the geoid and the earth's surface will be called the topographical masses. We will assume that the density ϱ of the topographical masses is known. In the reality, we have only innacurate models for it. Later we will see that by introducing the Helmert condensation layer, the requirement of accurate topographical density is greatly reduced and only a rough information about topographical density is sufficient to determine the gravity field inside the topographical masses with a sufficient accuracy.

Formulation of the problem. Let us assume that gravity measurements performed on the earth's surface result in data about the magnitude of gravity

acceleration $g = |\mathrm{g}|$. Let heights acquired from surface leveling have been converted to the orthometric heights H of the earth's surface above the geoid (Heiskanen and Moritz, 1967, sect.4). The transformation from the leveling heights to the orthometric heights may be run because we assume that the density of the topographical masses is known. Given two data sets on the earth's surface, $g = g(\Omega)$ and $H = H(\Omega)$, and the value W_0 of the gravity potential on the geoid, the problem is to determine the figure of the geoid and the gravity potential W outside the geoid. This problem may be classified as the free boundary-value problem for the gravity potential W.

1.2 Helmert's anomalous potential

Let us decompose the gravitational potential V generated by the earth into two parts:

$$V = V^g + V^t \,, \tag{1.4}$$

where V^g is the potential generated by the masses below the geoid and V^t is the potential generated by the topographical masses. Helmert (1884) suggested to approximate the topographical potential V^t by potential V^c of masses condensed on the geoid with surface condensation density $\sigma(\Omega)$. The difference between potentials V^t and V^c then defines the residual potential δV,

$$\delta V = V^t - V^c \,. \tag{1.5}$$

As shown in Martinec and Vaníček (1993a), the effect on geoidal undulations by the topographical potential V^t is of the order of 10^3 m, whereas the residual potential δV influences geoidal heights of only about 2 m. It means that the condensation potential V^c approaches the topographical potential V^t fairly well. As a consequence, the residual potential δV may be computed from relatively much less precise expressions, e.g., by evaluating the Newton volume integral using approximate estimates of the topographical density. Such estimates cannot be used in computing the condensation potential V^c, because they would cause errors in geoidal heights 3 orders of magnitude larger.

To make use of the above fact, the potential V^c together with the potential V^g will be considered as unknown quantities. The gravity potential $V^g + V^c + \Phi$ may be expressed as a sum of a normal gravity potential U generated by

a geocentric biaxial ellipsoid spinning with the same angular velocity as the earth and an anomalous potential T^h,

$$V^g + V^c + \Phi = U + T^h \ . \tag{1.6}$$

Inserting from eqns.(1.4)-(1.6) into eqn.(1.1), the gravity potential can be written as a sum of three terms:

$$W = U + T^h + \delta V \ . \tag{1.7}$$

Here we denote the anomalous gravitational potential T^h by a superscript h and will call it *Helmert anomalous potential* to differentiate it from the standard anomalous potential T (Heiskanen and Moritz, 1967, eqn.(2-137)). Eqn.(1.7) shows that T^h is related to T by

$$T = T^h + \delta V \ . \tag{1.8}$$

This formula may be thought of as another expression for the Helmert condensation decomposition (1.5).

The important consequence of eqn. (1.6) is that the Helmert anomalous potential T^h is harmonic outside the geoid, i.e., it satisfies Laplace's equation everywhere outside the geoid,

$$\nabla^2 T^h = 0 \qquad \text{outside the geoid} \ . \tag{1.9}$$

The free boundary-value problem for the gravity potential W formulated in sect. 1.1 will be transformed to a fix boundary-value problem for the Helmert anomalous potential T^h. Equation (1.9) shows that the latter problem is described by Laplace's equation valid outside the geoid. In the sequal, we will look for a boundary condition for T^h.

1.3 Bruns's formula

Let us re-derive the Bruns' formula (Heiskanen and Moritz, 1967, eqn.(2-144)) for the case when the Helmert decomposition (1.5) is employed. Let P_0 be a point on the geoid and Q be the corresponding point on the reference ellipsoid (lying on the same geocentric radius). Then the actual gravity potential of the Earth at the point on the geoid, W_{P_0}, can be written as

$$W_{P_0} \equiv W_0 = U_{P_0} + T^h_{P_0} + \delta V_{P_0} \ . \tag{1.10}$$

The normal potential on the geoid, U_{P_0}, can be expanded by the Taylor series expansion as:

$$U_{P_0} = U_Q + \left.\frac{\partial U}{\partial r}\right|_Q N + \frac{1}{2}\left.\frac{\partial^2 U}{\partial r^2}\right|_Q N^2 + \dots ,$$
$$= U_Q - \gamma_Q N + \varepsilon_N , \tag{1.11}$$

where γ_Q is the normal gravity on the reference ellipsoid and N is the geoid-ellipsoid separation called geoidal height. The magnitude of the correction term ε_N is of the order of $10^{-10} \times W_0$ (Vaníček and Martinec, 1993). Its contribution to the geoidal height N is at the most 1 mm. In the following text, this term will be omitted because we are interested only in one-centimeter geoid determination.

We will assume that the parameters of the reference ellipsoid have been chosen in such a way that the normal potential U on the reference ellipsoid has the same value as the actual gravity potential on the geoid, i.e.,

$$U_Q = W_0 . \tag{1.12}$$

Substituting from eqn.(1.12) into eqn.(1.11), we get

$$U_{P_0} \doteq W_0 - \gamma_Q N , \tag{1.13}$$

where we have omitted the correction term ε_N. Finally, substituting for W_0 from eqn.(1.10), the last equation becomes

$$N \doteq \frac{1}{\gamma_Q}\left(T^h_{P_0} + \delta V_{P_0}\right) . \tag{1.14}$$

This is a modified Bruns's formula for the case of Helmert's decomposition (1.5). The term

$$N^h = \frac{T^h_{P_0}}{\gamma_Q} \tag{1.15}$$

yields the separation between the so called co-geoid (Heiskanen and Moritz, 1967, Sec. 3-6.) and the reference ellipsoid, and the term

$$N_{pri} = \frac{\delta V_{P_0}}{\gamma_Q} \tag{1.16}$$

yields the separation between the geoid and co-geoid; it is the so-called primary indirect topographical effect on potential divided by γ_Q (ibid.). This term will be discussed in details in Chapters 4 and 5.

1.4 Linearized boundary condition for T^h

To evaluate the boundary condition for the Helmert anomalous potential T^h, let us apply the operator grad$\{\cdot\}$ to eqn.(1.7) and take the magnitude of the resulting vector. We get

$$|\mathrm{grad}W| = |\mathrm{grad}U| \left[1 + 2\,\frac{\mathrm{grad}U \cdot \mathrm{grad}(T^h + \delta V)}{|\mathrm{grad}U|^2} + \frac{|\mathrm{grad}(T^h + \delta V)|^2}{|\mathrm{grad}U|^2}\right]^{\frac{1}{2}} . \tag{1.17}$$

Using the binomial theorem, the right-hand side may be linearized to the form

$$|\mathrm{grad}W| \doteq \gamma - \frac{\partial T^h}{\partial r} - \frac{\partial\,\delta V}{\partial r} - \varepsilon_H \ , \tag{1.18}$$

where $\gamma = |\mathrm{grad}U|$ is the normal gravity. The magnitude of the correction term ε_H is of the order of 0.1 mGal at the most. In one-centimeter geoid computation this term should be considered as a correction to the first two terms. Its explicit form may be found in Vaníček and Martinec (1993).

The equation (1.18) is valid everywhere above the geoid. Let us consider it at a point P on the earth's surface.

$$\left.\frac{\partial T^h}{\partial r}\right|_P = -g_P + \gamma_P - \left.\frac{\partial\,\delta V}{\partial r}\right|_P - \varepsilon_H \ . \tag{1.19}$$

Normal gravity γ_P may be expressed by means of γ and its derivatives at the point Q on the reference ellipsoid lying on the same geocentric radius as the point P (Heiskanen and Moritz, 1967, sect. 2-14),

$$\begin{aligned}\gamma_P &= \gamma_Q + \left.\frac{\partial\gamma}{\partial r}\right|_Q (N + H) + \ldots \\ &\doteq \gamma_Q - 2\frac{\gamma_Q}{R}\,N - F - \varepsilon_\gamma \ ,\end{aligned} \tag{1.20}$$

where R is the mean radius of the earth, and F is the free-air reduction,

$$F = -\left.\frac{\partial\gamma}{\partial r}\right|_Q H \ , \tag{1.21}$$

and N is the geoidal height given by the Bruns formula (1.14). The explicit form of the ellipsoidal correction term ε_γ was derived among others by Moritz

(1980, sect.40.), Cruz (1986), Pavlis (1988) and Martinec (1990). Inserting eqns.(1.20) and (1.14) into eqn.(1.19) yields

$$\left.\frac{\partial T^h}{\partial r}\right|_P + \frac{2}{R} T^h_{P_0} = -\Delta g^F_P - \delta A - \delta P^{(2)} - \varepsilon_H - \varepsilon_\gamma \ . \tag{1.22}$$

The term

$$\Delta g^F_P = g_P - \gamma_Q + F \tag{1.23}$$

is the free-air gravity anomaly (Heiskanen and Moritz, 1967, eqn.(3-62)), the term

$$\delta A = \left.\frac{\partial \delta V}{\partial r}\right|_P \tag{1.24}$$

is the direct topographical effect on gravity (Heiskanen and Moritz, 1976, eqn.(3-59)), the term

$$\delta P^{(2)} = \frac{2}{R}\delta V_{P_0} \tag{1.25}$$

is the secondary indirect topographical effect on gravity (Heiskanen and Moritz, 1967, eq.(3-51)).

Adding and subtracting term $\partial T^h/\partial r\big|_{P_0}$ to the condition (1.22), we get

$$\left.\frac{\partial T^h}{\partial r}\right|_{P_0} + \frac{2}{R} T^h_{P_0} = -\Delta g^F_P - \delta A - \delta P^{(2)} - \varepsilon_H - \varepsilon_\gamma - Dg \ , \tag{1.26}$$

where

$$Dg(T^h) = \left.\frac{\partial T^h}{\partial r}\right|_P - \left.\frac{\partial T^h}{\partial r}\right|_{P_0} \tag{1.27}$$

is the difference of anomalous gravitation between the earth's surface and the geoid.

The geoid in the boundary condition (1.26) will be modelled by a sphere of radius R. It means that the left-hand side of eqn.(1.26) is linearized as follows:

$$\left.\frac{\partial T^h}{\partial r}\right|_{P_0} + \frac{2}{R} T^h_{P_0} = \left.\frac{\partial T^h}{\partial r}\right|_R + \frac{2}{R} T^h_R + \varepsilon_R \ , \tag{1.28}$$

where the subscript R denotes that terms are taken on a sphere of radius R. Since the relative error of spherical approximation of the geoid is 3×10^{-3},

the magnitude of the correction term ε_R may reach units of mGal. In one-centimeter geiod computation this correction has to be taken into account; its explicit form may be found Vaníček and Martinec (1993).

Considering eqn.(1.28), the boundary condition (1.26) takes the final linearized form

$$\left.\frac{\partial T^h}{\partial r}\right|_R + \frac{2}{R} T^h_R = -\Delta g^F_S - \varepsilon_{\Delta g} \ , \tag{1.29}$$

where

$$\varepsilon_{\Delta g} = \delta A + \delta P^{(2)} + \varepsilon_H + \varepsilon_\gamma + \varepsilon_R + Dg \ . \tag{1.30}$$

The term $\varepsilon_{\Delta g}$ represents corrections to the free-air gravity anomaly Δg^F_S; its magnitude is of the order of units of mgal at most, i.e., its contribution to geoidal heights may reach 2 m. Therefore, the geoid occuring in this term may be taken as a sphere of radius R; the error of such approximation will be 5 mm at most and may be neglected.

The correction $\varepsilon_{\Delta g}$ consists of terms of different origins: the topographical effect ($\delta A + \delta P^{(2)}$), the difference between the differentiation along the actual plumb line of gravity field and along the radial direction (ε_H), higher order terms in the normal gravity (ε_γ), spherical approximation of the geoid (ε_R), and downward continuation of anomalous gravitation from the topographical surface to the geoid (Dg). In this report we only focus our attention to treat the effect of topographical terms δA and $\delta P^{(2)}$ on geoidal heights.

The Laplace's eqn.(1.9) together with the boundary condition (1.29) represent a fixed linearized boundary-value problem for determination of the Helmert anomalous potential T^h outside and on the geoid. After finding the solution of this problem, the shape of the geoid is determined by means of the Bruns formula (1.14).

Since the correction ε_H and continuation term Dg depend on the potential T^h, the solution of the problem is necessary to search by an iterative approach described e.g. by Martinec and Vaníček (1993d). The zero-order iteration of T^h is given by Stokes's integral applied on the right-hand side of eqn.(1.29) where terms ε_H and Dg are left out. Higher-order iterations are expressed by Stokes's integral of gravity anomaly differences. This report is only concentrated to estimate the effect of the topographical terms δA and $\delta P^{(2)}$ on geoidal heights. Therefore, we will not describe the iterative approach in details and only find the Stokes integral of terms δA and $\delta P^{(2)}$ (see Chapters 4, 5, and 7).

Chapter 2

Newton's integral for topographical potentials

As outlined in sect. 1.2, the residual potential δV will be evaluated by means of the Newton integral. To do it, we will express the potential V^t of the topographical masses by the Newton volume integral and the potential V^c of the condensed masses by the Newton surface integral. Substituting the results to the Helmert decomposition (1.5), we obtain the integral representation of the residual potential δV.

Let the geocentric radius of the geoid be $r_g(\Omega)$ and the geocentric radius of the earth's surface be $r_g(\Omega) + H(\Omega)$. It means that $H(\Omega)$ is the height of the earth's surface above the geoid reckoned along the geocentric radius; this height, to a relative accuracy better than 5×10^{-6}, is equal to the ordinary orthometric height. We shall assume throughout the report that $H > 0$. The gravitational potential V^t induced by the topographical masses at a point (r, Ω) is given by the Newton volume integral

$$V^t(r,\Omega) = G \int_{\Omega'} \int_{r'=r_g(\Omega')}^{r_g(\Omega')+H(\Omega')} \varrho(r',\Omega') N(r,\psi,r') r'^2 dr' d\Omega' \ , \qquad (2.1)$$

where G is Newton's gravitational constant, $\varrho(r,\Omega)$ is the density of the topographical masses, $N(r,\psi,r')$ is the Newton kernel,

$$N(r,\psi,r') = \frac{1}{\sqrt{r^2 + r'^2 - 2rr'\cos\psi}} \ , \qquad (2.2)$$

ψ is the angular distance between the directions Ω and Ω', and the integration in eqn.(2.1) for Ω' is taken over the full solid angle.

We will abbreviate notations for the orthometric heights $H(\Omega)$ dropping the argument Ω. Therefore, we will use H instead of $H(\Omega)$ for the orthometric height of the topographical surface in direction Ω and H' instead of $H(\Omega')$ for the orthometric height of the topography in direction Ω'.

The potential of the condensation layer of radius $r_g(\Omega)$ may be expressed by the Newton surface integral:

$$V^c(r,\Omega) = G\int_{\Omega'} \sigma(\Omega')\, N\left(r,\psi,r_g(\Omega')\right) r_g^2(\Omega') d\Omega' \ , \tag{2.3}$$

where $\sigma(\Omega)$ is the surface density of the condensation layer. In Chapter 3 we will introduce how to choose the surface density σ for the Helmert condensation layer.

2.1 Approximations

As shown by Wichiencharoen (1982), Wang and Rapp (1990), or Martinec and Vaníček (1993a), the equipotential surface undulations generated by the residual potential δV for density of 2.67 g/cm^3 are of the order of 2 m. That is why, for the purpose of computing the residual potential δV, the geoid may be modelled by a sphere of radius R,

$$r_g(\Omega) = R \ , \tag{2.4}$$

where R is the mean radius of the Earth. This approximation is justifiable because the error in this spherical approximation is at most 3×10^{-3} which then causes an error of at most 6 mm in the geoidal height.

For the same reason, the density of the topographical masses in the residual potential δV may be modelled by an averaged value $\varrho(\Omega)$ of the actual density $\varrho(r,\Omega)$

$$\varrho(r,\Omega) = \varrho(\Omega) \ , \tag{2.5}$$

where $\varrho(\Omega)$ may be obtained e.g. by averaging the actual density $\varrho(r,\Omega)$ along the topographical column of height H, i.e.,

$$\varrho(\Omega) = \frac{1}{H}\int_{r=R}^{R+H} \varrho(r,\Omega) r^2 dr \ . \tag{2.6}$$

Under the assumptions (2.4) and (2.5), the topographical potential V^t, eqn.(2.1), and the condensation potential V^c, eqn.(2.3), read

$$V^t(r,\Omega) = G\int_{\Omega'} \varrho(\Omega') \int_{r'=R}^{R+H'} N(r,\psi,r') r'^2 dr' d\Omega' \ , \tag{2.7}$$

and

$$V^c(r,\Omega) = GR^2 \int_{\Omega'} \sigma(\Omega')\, N(r,\psi,R) d\Omega' \ , \tag{2.8}$$

where the Newton kernel $N(r,\psi,r')$ is given by eqn.(2.2).

2.2 A weak singularity of the Newton kernel

The definition (2.2) of the Newton kernel shows that it grows infinity when a dummy point of integration moves towards the computation point, i.e.,

$$\lim_{\psi\to 0} N(r,\psi,r')\Big|_{r'\to r} \to \infty \ . \tag{2.9}$$

Nevertheless, the Newton kernel is only **weakly** singular which means that the surface integral of it is bounded (Kellog, 1929, Chapter VI),

$$\int_{\Omega'} N(r,\psi,r') d\Omega' < \infty \ , \qquad r \neq 0 \ . \tag{2.10}$$

Writing the element of the full solid angle in polar coordinates (ψ,α) as $d\Omega' = \sin\psi d\psi d\alpha$, the weak singularity property (2.9) may also be expressed in the form

$$\lim_{\psi\to 0} \sin\psi\, N(r,\psi,r')\Big|_{r'\to r} < \infty \ , \tag{2.11}$$

which is valid for all non-zero radii r and r'.

The property (2.10) may be utilized for removing the singularity of the Newton integral (2.7). Subtracting and adding the term

$$V^B(r,\Omega) = G\,\varrho(\Omega) \int_{\Omega'} \int_{r'=R}^{R+H} N(r,\psi,r') r'^2 dr' d\Omega' \tag{2.12}$$

to the potential $V^t(r,\Omega)$, we get

$$V^t(r,\Omega) = V^B(r,\Omega) +$$

$$+ G \int_{\Omega'} \left[\varrho(\Omega') \int_{r'=R}^{R+H'} N(r,\psi,r') r'^2 dr' - \varrho(\Omega) \int_{r'=R}^{R+H} N(r,\psi,r') r'^2 dr' \right] d\Omega' \ . \tag{2.13}$$

The quantity V^B is the potential of a spherical Bouguer shell of the density $\varrho(\Omega)$ and thickness H. This potential is finite due to inequality (2.10) and is equal to (Wichiencharoen, 1982),

$$V^B(r,\Omega) = \begin{cases} 4\pi G \varrho(\Omega) \frac{1}{r} \left[R^2 H + R H^2 + \frac{1}{3} H^3 \right] \ , & r \geq R + H \ , \\ 2\pi G \varrho(\Omega) \left[(R+H)^2 - \frac{2}{3} \frac{R^3}{r} - \frac{1}{3} r^2 \right] \ , & R \leq r \leq R + H \ , \\ 4\pi G \varrho(\Omega) \left[RH + \frac{1}{2} H^2 \right] \ , & r \leq R \ . \end{cases} \tag{2.14}$$

The singularity of the Newton kernel in the integral on the right-hand side of eqn.(2.13) is now removed. Namely, if $\psi \to 0$ then $\varrho(\Omega') \to \varrho(\Omega)$ and $H' \to H$. Moreover, considering the property (2.10), the function in square brackets in eqn.(2.13) vanishes at the point $\psi = 0$. It means that the point $\psi = 0$ may be left out from integration domain for Ω', and hence the singularity of the Newton kernel at the point $\psi = 0$ is removed. This fact is important for numerical computation of the topographical potential $V^t(r,\Omega)$ because the modified formula (2.13) ensures that the numerical algorithm is not forced to evaluate the undefined expression of type 0/0 occuring in the original Newton integral (2.7).

To abbreviate notations, let us denote an indefinite integral over r' of the Newton kernel $N(r,\psi,r')$ by

$$\widetilde{N}(r,\psi,r') = \int_{r'} N(r,\psi,r') r'^2 dr' \ . \tag{2.15}$$

Using the primitive function $\widetilde{N}(r,\psi,r')$, the topographical potential V^t becomes

$$V^t(r,\Omega) = V^B(r,\Omega) +$$
$$+ G \int_{\Omega'} \left[\varrho(\Omega') \, \widetilde{N}(r,\psi,r') \Big|_{r'=R}^{R+H'} - \varrho(\Omega) \, \widetilde{N}(r,\psi,r') \Big|_{r'=R}^{R+H} \right] d\Omega' \ . \tag{2.16}$$

To remove the singularity from the condensation potential V^c at the point $r = R$, we may proceed by an analogous way as in the case of potential V^t.

Rewriting eqn.(2.8) as

$$V^c(r,\Omega) = V^\ell(r,\Omega) + GR^2 \int_{\Omega'} [\sigma(\Omega') - \sigma(\Omega)]\, N(r,\psi,R) d\Omega' \,, \qquad (2.17)$$

where $V^\ell(r,\Omega)$ is the potential of a spherical material single layer with density $\sigma(\Omega)$,

$$V^\ell(r,\Omega) = G\sigma(\Omega)R^2 \int_{\Omega'} N(r,\psi,R) d\Omega' \,, \qquad (2.18)$$

the singularity of the Newton kernel in integral (2.17) is removed. As follows from (2.10), the potential $V^\ell(r,\Omega)$ is finite and may be readily evaluated as

$$V^\ell(r,\Omega) = \begin{cases} 4\pi G\sigma(\Omega)\frac{R^2}{r} \,, & r > R \,, \\ 4\pi G\sigma(\Omega)R \,, & r \le R \,. \end{cases} \qquad (2.19)$$

2.3 Analytical expressions for integration kernels of Newton's type

Now, let us derive analytical expressions for the integration kernels appearing in the Newton integral.

The integration kernel $\widetilde{N}(r,\psi,r')$ defined by an indefinite integral (2.15) may be evaluated analytically (Gradshteyn and Ryzhik, 1980, pars. 2.261, 2.264) as:

$$\widetilde{N}(r,\psi,r') = \frac{r' + 3r\cos\psi}{2N(r,\psi,r')} + \frac{r^2}{2}(3\cos^2\psi - 1)\,\ln\left|r' - r\cos\psi + \frac{1}{N(r,\psi,r')}\right| \,, \qquad (2.20)$$

Let us remind our notations: r is the radius of the computation point, r' is the radius on an integration point, and ψ is the angular distance between the directions Ω and Ω'.

For computing the direct topographical effect on gravity δA, cf.eqn.(1.24), we need to compute the radial derivative of the Newton surface and volume integrals. The integration kernels of these integrals are formed by the radial derivative of the Newton kernel and the radial derivative of the kernel (2.15).

To find the radial derivative of the Newton kernel $N(r,\psi,r')$ is straightforward; taking the radial derivative of eqn.(2.2), we get

$$\frac{\partial N(r,\psi,r')}{\partial r} = -\frac{r - r'\cos\psi}{\left(r^2 + r'^2 - 2rr'\cos\psi\right)^{3/2}} . \tag{2.21}$$

Using eqn.(2.20), we can find an analytical formula for the radial derivative of the kernel $\widetilde{N}(r,\psi,r')$. After some algebra, we get

$$\frac{\partial \widetilde{N}(r,\psi,r')}{\partial r} = \int_{r'} \frac{\partial N(r,\psi,r')}{\partial r} r'^2 dr' =$$

$$= \left[(r'^2 + 3r^2)\cos\psi + (1 - 6\cos^2\psi)rr'\right] N(r,\psi,r') +$$

$$+ r(3\cos^2\psi - 1)\,\ln\left|r' - r\cos\psi + \frac{1}{N(r,\psi,r')}\right| . \tag{2.22}$$

The computational programs for evaluating the integration kernels (2.20) and (2.22) are introduced in Appendices attached to this report.

Chapter 3

The density of the condensation layer

In this section we will deal with a question how to choose surface density $\sigma(\Omega)$ of the Helmert condensation layer. The condensation density $\sigma(\Omega)$ should be chosen in such a way that the condensation potential V^c fits the actual topographical potential V^t as close as possible. Nevertheless, this criterium is ambiguous and allows us to choice density $\sigma(\Omega)$ by different ways. The problem is that the potentials V^t and V^c behave differently when the computation point is near to topographical masses.

Therefore a criterium for choice of $\sigma(\Omega)$ is based on similarities of potentials V^t and V^c in far distances from the topographical masses. It is possible to show (e.g. Martinec and Vaníček, 1993a) that the topographical potential V^t behaves like a potential of a thin layer with the surface density equal to the product of orthometric height H and topographical density ϱ when it is 'observed' from larger distances. We will follow this idea and assume that the condensation density is chosen in such a way that the mass of condensation layer is equal to the topographical masses. This requirement still ensures that the potential V^t and V^c behave similarly in a far zone but it further implies that the Helmert anomalous potential T^h does not contain the spherical harmonic of degree zero. In summary, we will adopt the following principle.

The principle of mass conservation: The mass M^c of the condensation layer is equal to the actual topographical masses M^t, i.e.

$$M^t = M^c \ . \tag{3.1}$$

The integral representation of this condition is readily to express:

$$\int_{\Omega} \varrho(\Omega) \int_{r=R}^{R+H} r^2 dr d\Omega = R^2 \int_{\Omega} \sigma(\Omega) d\Omega \ , \tag{3.2}$$

where the density $\varrho(\Omega)$ of the topographical masses is assumed to be laterally varying only, cf.eqn.(2.5), and the geoid is modelled by a sphere of the mean earth's radius R, cf.eqn.(2.4). The constrain (3.2) is identically satisfied putting

$$\sigma(\Omega) = \frac{\varrho(\Omega)}{R^2} \int_{r=R}^{R+H} r^2 dr \ . \tag{3.3}$$

for all directions Ω. Performing the integration over r, we get

$$\sigma(\Omega) = \varrho(\Omega) H \left(1 + \frac{H}{R} + \frac{H^2}{3R^2} \right) \ . \tag{3.4}$$

If the density of the condensation layer is chosen according to eqn.(3.4), the Helmert disturbing potential T^h has no spherical harmonic of degree zero, but it contains the spherical harmonics of the first degree. It means that the center of mass of the Helmert body is shifted from the origin of the coordinate system. Let us compute the magnitude of this shift.

Cartesian coordinates of the center of mass of the actual earth's masses M, $M = M^g + M^t$, are given by formula:

$$\mathbf{x}_T = \frac{1}{M} \int_{\Omega'} \int_{r'=0}^{r_g(\Omega')+H'} \varrho(r', \Omega') \mathbf{e}_r(\Omega') r'^3 dr' d\Omega' \ , \tag{3.5}$$

where $\mathbf{e}_r(\Omega')$ is the unit position vector in the direction Ω',

$$\mathbf{e}_r(\Omega) = \sin\vartheta \cos\lambda \, \mathbf{e}_x + \sin\vartheta \sin\lambda \, \mathbf{e}_y + \cos\vartheta \, \mathbf{e}_z \ . \tag{3.6}$$

The set of unit vectors $\mathbf{e}_x$, $\mathbf{e}_y$, and $\mathbf{e}_z$ forms the Cartesian base vectors, and the direction Ω is characterized by co-latitude ϑ and longitude λ.

The center of mass of the earth's body is usually located at the origin of the coordinate system (Heiskanen and Moritz, 1967, Chapter 2-6.), i.e.,

$$\mathbf{x}_T = \mathbf{0} \ , \tag{3.7}$$

which means that

$$\int_{\Omega'} \int_{r'=0}^{r_g(\Omega')} \varrho(r', \Omega') \mathbf{e}_r(\Omega') r'^3 dr' d\Omega' = - \int_{\Omega'} \int_{r'=r_g(\Omega')}^{r_g(\Omega')+H'} \varrho(r', \Omega') \mathbf{e}_r(\Omega') r'^3 dr' d\Omega' \ . \tag{3.8}$$

Under the assumption that the condensation of the topographical masses conserves the topographical masses, Cartesian coordinates of the Helmert body of the mass $M^h = M = M^g + M^c$ are

$$\mathbf{x}_T^h = \frac{1}{M}\left[\int_{\Omega'}\int_{r'=0}^{r_g(\Omega')} \varrho(r',\Omega')\mathbf{e}_r(\Omega')r'^3 dr' d\Omega' + \int_{\Omega'} \sigma(\Omega')\mathbf{e}_r(\Omega')r_g^3(\Omega')d\Omega'\right] . \tag{3.9}$$

Substituting for the first integral from eqn.(3.8), we get

$$\mathbf{x}_T^h = \frac{1}{M}\left[-\int_{\Omega'}\int_{r'=r_g(\Omega')}^{r_g(\Omega')+H'} \varrho(r',\Omega')\mathbf{e}_r(\Omega')r'^3 dr' d\Omega' + \right.$$

$$\left. + \int_{\Omega'} \sigma(\Omega')\mathbf{e}_r(\Omega')r_g^3(\Omega')d\Omega'\right] . \tag{3.10}$$

Approximating the radius of the geoid $r_g(\Omega)$ by a mean radius of the earth R, $r_g(\Omega) = R$, and the topographical density $\varrho(r,\Omega)$ by an column averaged value $\varrho(\Omega)$ (see section 2.1), the last equation becomes

$$\mathbf{x}_T^h = \frac{1}{M}\left[-\int_{\Omega'} \varrho(\Omega')\mathbf{e}_r(\Omega')\int_{r'=R}^{R+H'} r'^3 dr' d\Omega' + R^3\int_{\Omega'} \sigma(\Omega')\mathbf{e}_r(\Omega')d\Omega'\right] . \tag{3.11}$$

Performing the integration over r' and inserting for $\sigma(\Omega')$ from eqn.(3.4), we get

$$\mathbf{x}_T^h = -\frac{R^2}{2M}\int_{\Omega'} \varrho(\Omega')\mathbf{e}_r(\Omega')H'^2\left(1 + \frac{4}{3}\frac{H'}{R} + \frac{1}{2}\frac{H'^2}{R^2}\right)d\Omega' . \tag{3.12}$$

To estimate the magnitude of the vector $\mathbf{x}_T^h$, we put $\varrho(\Omega) = \varrho_0 = 2.67$ g/cm^3, and take only the first term within the brackets which is of three orders larger then the rest. The approximation of eqn.(3.12) then reads

$$\mathbf{x}_T^h \doteq -K\int_{\Omega'} H'^2\mathbf{e}_r(\Omega')d\Omega' , \tag{3.13}$$

where

$$K = \frac{R^2\varrho_0}{2M} \doteq 10^{-8}\,\mathrm{m}^{-1} \tag{3.14}$$

for $M = 5.97 \times 10^{24}$ kg, $R = 6371$ km, and $\varrho_0 = 2.67$ g/cm^3.

Realizing that

$$\sin\vartheta\cos\lambda = -\sqrt{\frac{2\pi}{3}}\left[Y_{11}(\Omega) + Y_{11}^{*}(\Omega)\right] ,$$

$$\sin\vartheta\sin\lambda = \mathrm{i}\sqrt{\frac{2\pi}{3}}\left[Y_{11}(\Omega) - Y_{11}^{*}(\Omega)\right] , \tag{3.15}$$

$$\cos\vartheta = \sqrt{\frac{4\pi}{3}}Y_{10}(\Omega) ,$$

where $Y_{1m}(\Omega)$ are spherical harmonics normalized according to Varshalovich et al. (1976), and asterisk denotes complex conjugation, the unit position vector $\mathbf{e}_r(\Omega)$ takes the form

$$\mathbf{e}_r(\Omega) = -\sqrt{\frac{2\pi}{3}}\left[Y_{11}(\Omega) + Y_{11}^{*}(\Omega)\right]\mathbf{e}_x + \mathrm{i}\sqrt{\frac{2\pi}{3}}\left[Y_{11}(\Omega) - Y_{11}^{*}(\Omega)\right]\mathbf{e}_y +$$

$$+\sqrt{\frac{4\pi}{3}}Y_{10}(\Omega)\,\mathbf{e}_z . \tag{3.16}$$

Substituting eqn.(3.16) into (3.13), and introducing spherical harmonic coefficients $(H^2)_{1m}$ as

$$\left(H^2\right)_{1m} = \int_{\Omega'} H'^2 Y_{1m}^{*}(\Omega')d\Omega' , \tag{3.17}$$

the Cartesian coordinates (x_T^h, y_T^h, z_T^h) of the vextor $\mathbf{x}_T^h$ are

$$x_T^h = K\sqrt{\frac{2\pi}{3}}\left[\left(H^2\right)_{11} + \left(H^2\right)_{11}^{*}\right] = 2K\sqrt{\frac{2\pi}{3}}Re\left(H^2\right)_{11} ,$$

$$y_T^h = -K\sqrt{\frac{2\pi}{3}}\mathrm{i}\left[-\left(H^2\right)_{11} + \left(H^2\right)_{11}^{*}\right] = -2K\sqrt{\frac{2\pi}{3}}Im\left(H^2\right)_{11} , \tag{3.18}$$

$$z_T^h = -K\sqrt{\frac{4\pi}{3}}\left(H^2\right)_{10} ,$$

where Re and Im stand for the real and imaginary part of a complex number.

The numerical values of the coefficients $(H^2)_{1m}$ were found for the earth topography described by the TUG87 global digital terrain model (Wieser, 1987) complete to degree and order 180. We have obtained

$$\left(H^2\right)_{10} = -0.847 \times 10^5 \,\mathrm{m}^2$$

$$\left(H^2\right)_{11} = (-0.207 \times 10^6;\, 0.509 \times 10^6)\,\mathrm{m}^2 \,. \tag{3.19}$$

Then

$$\mathrm{x}_T^h = (-6;\, -15;\, 2) \times 10^{-3}\,\mathrm{m}\,, \tag{3.20}$$

and its magnitude is equal to

$$|\mathrm{x}_T^h| = 16 \times 10^{-3}\,\mathrm{m}\,. \tag{3.21}$$

We can conclude that the center of mass of the Helmert body is shifted about 16 mm from the center of mass of the actual earth body in the case that the Helmert condensation is performed according to principle of conservation of topographical masses.

When the condensation of the topographical masses is performed according to the above principle, i.e., when the condensation density σ is taken according to eqn.(3.4), the Helmert anomalous potential T^h does not contain the spherical harmonics of degree zero but it contains the spherical harmonics of degree one (and higher, of course):

$$T^h(r,\Omega) = \sum_{j=1}^{\infty} \left(\frac{R}{r}\right)^{j+1} \sum_{m=-j}^{j} T_{jm}^h Y_{jm}(\Omega)\,. \tag{3.22}$$

The first degree harmonics T_{1m}^h are completely unresolved in the boundary condition (1.29). The left-hand side of this equation for degree $j = 1$ is always equal to zero because the matrix element is proportional to factor $j - 1$. The right-hand side of eqn.(1.29) consists of the free-air gravity anomaly, the direct topographical effect on gravity, the secondary indirect effect on gravity, and other terms. Neither the free-air gravity anomaly, nor the sum of the topographical terms contain the spherical harmonics of degree one. Therefore, equations for $j = 1$ may be left out from the system of equations (1.29). The spherical harmonics T_{1m}^h of the anomalous potential T^h will be evaluated separately according to the procedure described above, and then

will be added to the Stokes's solution of the boundary condition (1.29). Hence the Stokes function for integration of eqn.(1.29) starts from the spherical harmonics of degree two, i.e., it has the standard form (Heiskanen and Moritz, 1967, eqn.(2-164)):

$$S(\psi) = \sum_{j=2}^{\infty} \frac{2j+1}{j-1} P_j(\cos\psi) \ . \tag{3.23}$$

Chapter 4

Topographical effects on geoidal heights

As shown in Chapter 1, the effect of topographical masses on geoid determination is described by three terms: the direct topographical effect on gravity,

$$\delta A(\Omega) = \left.\frac{\partial\, \delta V(r,\Omega)}{\partial r}\right|_{r=R+H} , \tag{4.1}$$

the primary indirect topographical effect on potential,

$$\delta P^{(1)}(\Omega) = \delta V(R,\Omega) , \tag{4.2}$$

and the secondary indirect topographical effect on gravity,

$$\delta P^{(2)}(\Omega) = \frac{2}{R}\delta V(R,\Omega) . \tag{4.3}$$

The boundary condition (1.29) for determining the anomalous gravitational potential T shows that the first and last term contributes to the anomalous gravitation. To express their effects on the anomalous potential T, Stokes' integration has to be applied to them. The total topographical effect on geoidal height, δN_{top}, is then given as

$$\delta N_{top} = N_{dir} + N_{pri} + N_{sec} , \tag{4.4}$$

where the term N_{dir} is due to the direct topographical effect on gravity,

$$N_{dir}(\Omega) = \frac{R}{4\pi\gamma}\int_{\Omega'} \delta A(\Omega') S(\psi) d\Omega' , \tag{4.5}$$

the term N_{pri} is due to the primary indirect topographical effect on potential,

$$N_{pri}(\Omega) = \frac{1}{\gamma}\delta P^{(1)}(\Omega) \ , \tag{4.6}$$

and the term N_{sec} is due to the secondary indirect topographical effect on gravity,

$$N_{sec}(\Omega) = \frac{R}{4\pi\gamma}\int_{\Omega'}\delta P^{(2)}(\Omega')S(\psi)d\Omega' \ . \tag{4.7}$$

Here we have used the standard notation: $S(\psi)$ is the Stokes's function, cf. eqn.(3.23), and γ is the normal gravity on the reference ellipsoid (To abbreviate notations, we have dropped subscript Q for γ_Q).

Substituting for δA and $\delta P^{(2)}$ from eqns.(4.1) and (4.3), and then for the residual potential δV from Helmert's decomposition (1.5), each of terms N_{dir}, N_{pri} and N_{sec} may be split into two constituents:

$$N_{dir,pri,sec} = N^{t}_{dir,pri,sec} - N^{c}_{dir,pri,sec} \ , \tag{4.8}$$

where geoidal heights N with superscripts 't' are induced by the topographical potential V^t and with superscripts 'c' are induced by the condensation potential V^c. Explicitly,

$$N^{t,c}_{dir}(\Omega) = \frac{R}{4\pi\gamma}\int_{\Omega'}\left.\frac{\partial V^{t,c}(r,\Omega')}{\partial r}\right|_{r=R+H'} S(\psi)d\Omega' \ , \tag{4.9}$$

$$N^{t,c}_{pri}(\Omega) = \frac{1}{\gamma}V^{t,c}(R,\Omega) \ , \tag{4.10}$$

and

$$N^{t,c}_{sec}(\Omega) = \frac{1}{2\pi\gamma}\int_{\Omega'}V^{t,c}(R,\Omega')S(\psi)d\Omega' \ . \tag{4.11}$$

4.1 The direct topographical effect on gravity

The direct topographical effect on gravity, $\delta A(\Omega)$, is defined as the radial derivatives of the residual potential δV taken at a point on the topography,

cf. eqn.(4.1). Substituting for the residual potential δV from the Helmert's decomposition (1.5) into eqn.(4.1), we can write

$$\delta A(\Omega) = A^t(\Omega) - A^c(\Omega) \ , \tag{4.12}$$

where

$$A^t(\Omega) = \left.\frac{\partial V^t(r,\Omega)}{\partial r}\right|_{r=R+H} \ , \qquad A^c(\Omega) = \left.\frac{\partial V^c(r,\Omega)}{\partial r}\right|_{r=R+H} \ , \tag{4.13}$$

are the gravitational attractions induced by the topographical and condensed masses at a point on the topography.

Taking the radial derivative of eqn.(2.16) and then putting $r = R + H$, we obtain

$$A^t(\Omega) = A^B(\Omega) +$$
$$+ G \int_{\Omega'} \left[\varrho(\Omega') \left.\frac{\partial \widetilde{N}(r,\psi,r')}{\partial r}\right|_{r'=R}^{R+H'} - \varrho(\Omega) \left.\frac{\partial \widetilde{N}(r,\psi,r')}{\partial r}\right|_{r'=R}^{R+H} \right]_{r=R+H} d\Omega' \ , \tag{4.14}$$

where $A^B(\Omega)$ is the attraction of the Bouguer shell at the point on the topography, i.e.,

$$A^B(\Omega) = \left.\frac{\partial V^B(r,\Omega)}{\partial r}\right|_{r=R+H} \ . \tag{4.15}$$

Considering eqn.$(2.14)_1$, $A^B(\Omega)$ reads

$$A^B(\Omega) = -4\pi G \varrho(\Omega) H \frac{R^2}{(R+H)^2} \left(1 + \frac{H}{R} + \frac{H^2}{3R^2}\right) \ . \tag{4.16}$$

Similarly, we can derive the attraction $A^c(\Omega)$ of the condensed masses at the point on the topography. Taking the radial derivative of eqn.(2.17), we get

$$A^c(\Omega) = A^\ell(\Omega) + GR^2 \int_{\Omega'} [\sigma(\Omega') - \sigma(\Omega)] \left.\frac{\partial N(r,\psi,R)}{\partial r}\right|_{r=R+H} d\Omega' \ , \tag{4.17}$$

where $A^\ell(\Omega)$ is the attraction of a spherical single layer with the density $\sigma(\Omega)$:

$$A^\ell(\Omega) = \left.\frac{\partial V^\ell(r,\Omega)}{\partial r}\right|_{r=R+H} \ . \tag{4.18}$$

Considering eqn.$(2.19)_1$, $A^{\ell}(\Omega)$ reads

$$A^{\ell}(\Omega) = -4\pi G\sigma(\Omega)\frac{R^2}{(R+H)^2} \,. \tag{4.19}$$

Substituting eqns.(4.14) and (4.17) into (4.12), the direct topographical effect on gravity may be expressed in the form:

$$\delta A(\Omega) = A^{B}(\Omega) - A^{\ell}(\Omega) +$$

$$+G\int_{\Omega'}\left[\varrho(\Omega')\,\frac{\partial\widetilde{N}(r,\psi,r')}{\partial r}\bigg|_{r'=R}^{R+H'} - R^2\sigma(\Omega')\frac{\partial N(r,\psi,R)}{\partial r} -\right.$$

$$\left.-\varrho(\Omega)\,\frac{\partial\widetilde{N}(r,\psi,r')}{\partial r}\bigg|_{r'=R}^{R+H} + R^2\sigma(\Omega)\frac{\partial N(r,\psi,R)}{\partial r}\right]_{r=R+H} d\Omega' \,. \tag{4.20}$$

Moreover, provided that the condensation of the topographical masses is performed according to the principle of mass conservation, i.e., when the condensation density $\sigma(\Omega)$ is considered in form (3.4), then eqns.(4.16) and (4.19) readily show that

$$A^{B}(\Omega) = A^{\ell}(\Omega) \,. \tag{4.21}$$

This means that the attraction of the Bouguer shell is equal to the attraction of a single layer at a point on the topography. As a consequence, the first two terms in eqn.(4.10) cancel each other and the direct topographical effect on gravity reads

$$\delta A(\Omega) = G\int_{\Omega'}\left[\varrho(\Omega')\,\frac{\partial\widetilde{N}(r,\psi,r')}{\partial r}\bigg|_{r'=R}^{R+H'} - R^2\sigma(\Omega')\frac{\partial N(r,\psi,R)}{\partial r} -\right.$$

$$\left.-\varrho(\Omega)\,\frac{\partial\widetilde{N}(r,\psi,r')}{\partial r}\bigg|_{r'=R}^{R+H} + R^2\sigma(\Omega)\frac{\partial N(r,\psi,R)}{\partial r}\right]_{r=R+H} d\Omega' \,. \tag{4.22}$$

4.2 The primary indirect topographical effect on potential

The formulae (2.16) and (2.17) may be immediately utilized for determining the geoidal heights $N^{t,c}_{pri}(\Omega)$ which come from the primary indirect topographical effect on potential. Putting $r = R$ in eqns.(2.16) and (2.17) and dividing

them by normal gravity γ, as eqn.(4.10) requires, we have

$$N^t_{pri}(\Omega) = \frac{4\pi G}{\gamma}\varrho(\Omega)\left(RH + \frac{1}{2}H^2\right) +$$

$$+ \frac{G}{\gamma}\int_{\Omega'}\left[\varrho(\Omega')\,\widetilde{N}(R,\psi,r')\Big|_{r'=R}^{R+H'} - \varrho(\Omega)\,\widetilde{N}(R,\psi,r')\Big|_{r'=R}^{R+H}\right]d\Omega' \,, \qquad (4.23)$$

and

$$N^c_{pri}(\Omega) = \frac{4\pi GR}{\gamma}\sigma(\Omega) + \frac{GR^2}{\gamma}\int_{\Omega'}[\sigma(\Omega') - \sigma(\Omega)]\,N(R,\psi,R)d\Omega' \,, \qquad (4.24)$$

where for the gravitational potential of Bouguer shell we have substituted from the last relation of eqn.(2.14), and for the potential of spherical material layer from the last relation of eqn.(2.19). Taking the condensation density $\sigma(\Omega)$ according to eqn.(3.4), the geoidal height due to the primary indirect topographical effect of the residual potential δV is of the form

$$N_{pri}(\Omega) = N^t_{pri}(\Omega) - N^c_{pri}(\Omega) = -\frac{2\pi G}{\gamma}\varrho(\Omega)H^2\left(1 + \frac{2}{3}\frac{H}{R}\right) +$$

$$+\frac{G}{\gamma}\int_{\Omega'}\left[\varrho(\Omega')\,\widetilde{N}(R,\psi,r')\Big|_{r'=R}^{R+H'} - R^2\sigma(\Omega')N(R,\psi,R) -\right.$$

$$\left. -\varrho(\Omega)\,\widetilde{N}(R,\psi,r')\Big|_{r'=R}^{R+H} + R^2\sigma(\Omega)N(R,\psi,R)\right]d\Omega' \,. \qquad (4.25)$$

4.3 The secondary indirect topographical effect on gravity

Now, let us turn our attention to evaluate the geoidal height $N^{t,c}_{sec}$, cf. eqn.(4.11), which comes from the secondary indirect topographical effect on gravity. For doing this, the gravitational potential $V^t(r,\Omega)$ must be evaluated at a point on the geoid ($r = R$), and then the Stokes integral must be applied to the potential $V^t(R,\Omega)$.

For evaluating the potential $V^t(R,\Omega)$, the Newton kernel will be expanded as

$$N(R,\psi,r') = \frac{1}{r'}\sum_{j=0}^{\infty}\left(\frac{R}{r'}\right)^j P_j(\cos\psi) \,, \qquad r' \geq R \,, \qquad (4.26)$$

where $P_j(\cos\psi)$ is the Legendre polynomial of degree j. The series (4.26) is divergent at the point $\psi = 0$ and $r' = R$. This does not matter because we already known that the Newton integral may be arranged in such a way that this singularity is removed from integration domain. To perform this, we can proceed by two ways. First we could remove the singularity from the Newton integral as suggested in eqn.(2.16), and then substitute series (4.26) into (2.16). Nevertheless, to maintain understability of derivations, we will proceed by the second way. We first substitute the series (4.26) into the form (2.7) of the potential $V^t(R,\Omega)$, where the singularity is not removed. This is possible because the Newton integral (2.7) is still bounded even if the series (4.26) is divergent at the point $\psi = 0$ and $r' = R$. Then we will perform the Stokes integration and finally we will remove the singularity from the resulting integral.

Taking into consideration eqns.(2.7) and (4.26), the gravitational potential of the topographical masses on the geoid takes the form

$$V^t(R,\Omega) = G\int_{\Omega'} \varrho(\Omega') \int_{r'=R}^{R+H'} \frac{1}{r'} \sum_{j=0}^{\infty} \left(\frac{R}{r'}\right)^j P_j(\cos\psi)\, r'^2 dr' d\Omega' \ . \qquad (4.27)$$

The Stokes integral of this term (multiplied by the factor $2/R$ as eqn.(4.11) requires) then reads

$$N^t_{sec}(\Omega) = \frac{G}{2\pi\gamma}\int_{\Omega'}\int_{\Omega''} \varrho(\Omega'') \int_{r'=R}^{R+H''} \frac{1}{r'} \sum_{j=0}^{\infty} \left(\frac{R}{r'}\right)^j P_j(\cos\psi_{\Omega'\Omega''}) S(\psi_{\Omega\Omega'}) r'^2 dr' d\Omega'' d\Omega' \ , \qquad (4.28)$$

where the subscripts at ψ denote the directions between them ψ is taken; ψ without any subscripts implicitly means the angular distance is considered between the directions Ω and Ω'.

The angular integral of the product $P_j(\cos\psi_{\Omega'\Omega''})S(\psi_{\Omega\Omega'})$ may be arranged as follows:

$$\int_{\Omega'} P_j(\cos\psi_{\Omega'\Omega''}) S(\psi_{\Omega\Omega'}) d\Omega' =$$

$$= \int_{\Omega'} \frac{4\pi}{2j+1} \sum_{m=-j}^{j} Y^*_{jm}(\Omega') Y_{jm}(\Omega'') \sum_{j_1=2}^{\infty} \frac{4\pi}{j_1 - 1} \sum_{m_1=-j_1}^{j_1} Y^*_{j_1 m_1}(\Omega) Y_{j_1 m_1}(\Omega') =$$

$$= \frac{(4\pi)^2}{(2j+1)(j-1)} \sum_{m=-j}^{j} Y^*_{jm}(\Omega) Y_{jm}(\Omega'') = \frac{4\pi}{j-1} P_j(\cos\psi_{\Omega\Omega''}) \ , \qquad (4.29)$$

valid for $j > 1$; otherwise the integral is equal to zero. In the first step we have used the Laplace addition theorem for spherical harmonics, $Y_{jm}(\Omega)$ (e.g. Heiskanen and Moritz, 1967, Sec.1-15.),

$$P_j(\cos\psi) = \frac{4\pi}{2j+1} \sum_{m=-j}^{j} Y^*_{jm}(\Omega')\, Y_{jm}(\Omega) \ , \tag{4.30}$$

then we have substituted for Stokes's function from eqn.(3.23) and used the orthogonality property of spherical harmonics,

$$\int_\Omega Y_{j_1 m_1}(\Omega) Y^*_{j_2 m_2}(\Omega) d\Omega = \delta_{j_1 j_2} \delta_{m_1 m_2} \ , \tag{4.31}$$

and finally we have again evaluated the sum of products of spherical harmonics according to the addition theorem (4.30).

Substituting for the angular integral over the product $P_j(\cos\psi_{\Omega'\Omega''}) S(\psi_{\Omega\Omega'})$ from eqn.(4.29) into (4.28), we get

$$N^t_{sec}(\Omega) = 2\frac{G}{\gamma} \int_{\Omega'} \varrho(\Omega') \int_{r'=R}^{R+H'} \frac{1}{r'} \sum_{j=2}^{\infty} \frac{1}{j-1} \left(\frac{R}{r'}\right)^j P_j(\cos\psi) r'^2 dr' d\Omega' \ . \tag{4.32}$$

Introducing kernel $U(R, \psi, r')$,

$$U(R,\psi,r') = \frac{1}{r'} \sum_{j=2}^{\infty} \frac{1}{j-1} \left(\frac{R}{r'}\right)^j P_j(\cos\psi) \ , \qquad R \le r' \ , \tag{4.33}$$

and an indefinite integral of it,

$$\tilde{U}(R,\psi,r') = \int_{r'} U(R,\psi,r') r'^2 dr' \ , \tag{4.34}$$

the geoidal height N^t_{sec}, eqn.(4.32), may be written as

$$N^t_{sec}(\Omega) = 2\frac{G}{\gamma} \int_{\Omega'} \varrho(\Omega') \tilde{U}(R,\psi,r') \Big|_{r'=R}^{R+H'} d\Omega' \ . \tag{4.35}$$

The singularity of the kernel $\tilde{U}(R, \psi, r')$ for $r' = R$ and $\psi = 0$ may be removed by simple algebraic operation

$$N^t_{sec}(\Omega) = 2\frac{G}{\gamma} \int_{\Omega'} \left[\varrho(\Omega') \tilde{U}(R,\psi,r') \Big|_{r'=R}^{R+H'} - \varrho(\Omega) \tilde{U}(R,\psi,r') \Big|_{r'=R}^{R+H} \right] d\Omega' +$$

$$+2\frac{G\varrho(\Omega)}{\gamma}\int_{\Omega'}\tilde{U}(R,\psi,r')\Big|_{r'=R}^{R+H}d\Omega' \ . \tag{4.36}$$

Eqn.(4.33) shows that the angular integrals of kernels $U(R,\psi,r')$ and $\tilde{U}(R,\psi,r')$ are equal to zero because they do not contain the spherical harmonic of the degree zero, i.e.,

$$\int_{\Omega'}U(R,\psi,r')d\Omega' = \int_{\Omega'}\tilde{U}(R,\psi,r')d\Omega' = 0 \ . \tag{4.37}$$

The secondary indirect topographical effect $N^t_{sec}(\Omega)$ now becomes

$$N^t_{sec}(\Omega) = 2\frac{G}{\gamma}\int_{\Omega'}\left[\varrho(\Omega')\tilde{U}(R,\psi,r')\Big|_{r'=R}^{R+H'} - \varrho(\Omega)\tilde{U}(R,\psi,r')\Big|_{r'=R}^{R+H}\right]d\Omega' \ . \tag{4.38}$$

The geoidal heights N^c_{sec}, cf. eqn.(4.11), which comes from the secondary indirect topographical effect on gravity induced by the condensation layer may be obtain from eqn.(4.38) putting $r' = R$, $\varrho(\Omega) \equiv R^2\sigma(\Omega)$, and omitting the integration over r'. We get

$$N^c_{sec}(\Omega) = 2\frac{GR^2}{\gamma}\int_{\Omega'}(\sigma'-\sigma)\,U(R,\psi,R)d\Omega' \ . \tag{4.39}$$

Finally, the secondary indirect topographical effect on gravity induced by the residual potential δV is given by the difference of $N^t_{sec}(\Omega)$ and $N^c_{sec}(\Omega)$, i.e.,

$$N_{sec}(\Omega) = N^t_{sec}(\Omega) - N^c_{sec}(\Omega) =$$

$$= 2\frac{G}{\gamma}\int_{\Omega'}\left[\varrho(\Omega')\tilde{U}(R,\psi,r')\Big|_{r'=R}^{R+H'} - R^2\sigma(\Omega')U(R,\psi,R) - \right.$$

$$\left. -\varrho(\Omega)\tilde{U}(R,\psi,r')\Big|_{r'=R}^{R+H} + R^2\sigma(\Omega)U(R,\psi,R)\right]d\Omega' \ . \tag{4.40}$$

4.3.1 The integration kernel $U(R,\psi,r')$

Let us derive the spatial form of the integration kernel $U(R,\psi,r')$, $R \le r'$. Introducing the ratio h,

$$h = \frac{R}{r'} \ , \tag{4.41}$$

and writing the identity

$$\sum_{j=2}^{\infty} \frac{h^j}{j-1} P_j(\cos\psi) = h \sum_{\substack{j=0 \\ j\neq 1}}^{\infty} \frac{h^{j-1}}{j-1} P_j(\cos\psi) + 1 \ , \tag{4.42}$$

the kernel $U(R,\psi,r')$ may be expressed in terms of the Paul function $U_2(\cos\psi,h)$, cf. eqn.(4.58), as

$$U(R,\psi,r') = \frac{R}{r'^2} U_2\left(\cos\psi, \frac{R}{r'}\right) + \frac{1}{r'} \ . \tag{4.43}$$

4.3.2 The integration kernel $\widetilde{U}(R,\psi,r')$

The integration kernel $\tilde{U}(R,\psi,r')$ is defined by an indefinite integral over r' of the kernel $U(R,\psi,r')$, cf eqn.(4.34). Substituting from eqn.(4.33) into eqn.(4.34), and carrying out the integration over r', we get

$$\tilde{U}(R,\psi,r') = -R^2 \sum_{j=3}^{\infty} \frac{1}{(j-1)(j-2)} \left(\frac{R}{r'}\right)^{j-2} P_j(\cos\psi) + R^2 P_2(\cos\psi) \ln r' \ , \tag{4.44}$$

or using the ratio h, eqn.(4.41), we may also write

$$\tilde{U}(R,\psi,r') = R^2 \sum_{j=3}^{\infty} \left(\frac{1}{j-1} - \frac{1}{j-2}\right) h^{j-2} P_j(\cos\psi) + R^2 P_2(\cos\psi) \ln r' \ . \tag{4.45}$$

Spreading the summation over j on terms $j=0$ and $j=1$, respectively, we further have

$$\tilde{U}(R,\psi,r') = R^2 \left\{ \sum_{\substack{j=0 \\ j\neq 1}}^{\infty} \frac{h^{j-2}}{j-1} P_j(\cos\psi) + \frac{1}{h^2} - P_2(\cos\psi) - \right.$$

$$\left. - \sum_{\substack{j=0 \\ j\neq 2}}^{\infty} \frac{h^{j-2}}{j-2} P_j(\cos\psi) - \frac{1}{2h^2} - \frac{\cos\psi}{h} + P_2(\cos\psi) \ln r' \right\} \ . \tag{4.46}$$

The sums on the right-hand side of the last equation may be expressed in terms of the Paul functions $U_2(\cos\psi, h)$, and $U_3(\cos\psi, h)$, cf. section 4.3.3:

$$\tilde{U}(R,\psi,r') = R^2\left\{\frac{1}{h}U_2(\cos\psi,h) - U_3(\cos\psi,h) + \frac{1}{2h^2} - \frac{\cos\psi}{h} - P_2(\cos\psi) + \right.$$

$$\left. + P_2(\cos\psi)\ln r'\right\} \ . \tag{4.47}$$

Substituting for functions U_2 and U_3 from eqns.(4.58) and (4.59), we finally get

$$\tilde{U}(R,\psi,r') = R^2\left\{P_2(\cos\psi)\ln\left(r' - R\cos\psi + D(R,\psi,r')\right) - \right.$$

$$-\frac{r'}{R}\cos\psi\ln\left(\frac{r' - R\cos\psi + D(R,\psi,r')}{2r'}\right) +$$

$$\left. + \frac{-r' + 3R\cos\psi}{2R^2}D(R,\psi,r') - \frac{2r'}{R}\cos\psi + \frac{r'^2}{2R^2} - P_2(\cos\psi)\right\} \ , \tag{4.48}$$

where

$$D(R,\psi,r') = \sqrt{R^2 - 2Rr'\cos\psi + r'^2} \ . \tag{4.49}$$

4.3.3 Paul's functions $U_n(t,h)$ and $V_n(t,h)$

Paul (1973) introduced two sets of auxiliary functions $U_n(t,h)$ and $V_n(t,h)$, $n = 0, 1, 2, \ldots$ defined by series

$$U_n(t,h) = \sum_{\substack{k=0 \\ k\neq n-1}}^{\infty} \frac{h^{k-n+1}}{k-n+1}P_k(t) \ , \tag{4.50}$$

and

$$V_n(t,h) = \sum_{k=0}^{\infty} \frac{h^{k+n+1}}{k+n+1}P_k(t) \ , \tag{4.51}$$

where $0 < h \leq 1$, $P_k(t)$ is the Legendre polynomial of degree k, and $-1 \leq t \leq 1$. Unfortunately, Paul (ibid.) only gave the recurence relations for $U_n(t,1)$ and $V_n(t,1)$. In this report we need to evaluate the Paul functions also for $h \neq 1$. These may be computed according to the following recurence relations:

$$(n-1)U_n(t,h) - (2n-3)tU_{n-1}(t,h) + (n-2)U_{n-2}(t,h) +$$

$$+ h^{-n+1}\sqrt{1-2th+h^2} = \frac{P_{n-3}(t) - P_{n-1}(t)}{2n-3} \ , \tag{4.52}$$

and

$$nV_n(t,h) - (2n-1)tV_{n-1}(t,h) + (n-1)V_{n-2}(t,h) - h^{n-1}\sqrt{1-2th+h^2} = 0 \ . \tag{4.53}$$

The initial values for the recurence (4.52) are

$$U_0(t,h) = \ln\left(\frac{h-t+\sqrt{1-2th+h^2}}{1-t}\right) \ , \tag{4.54}$$

$$U_1(t,h) = \ln\left(\frac{2}{1-th+\sqrt{1-2th+h^2}}\right) \ , \tag{4.55}$$

and for the recurence (4.53):

$$V_0(t,h) = U_0(t,h) \ , \tag{4.56}$$

$$V_1(t,h) = tV_0(t,h) + \sqrt{1-2th+h^2} - 1 \ . \tag{4.57}$$

For evaluating the kernels $U(R,\psi,r')$, eqn.(4.43), and $\tilde{U}(R,\psi,r')$, eqn.(4.47), Paul's functions with higher indexes are needed to evaluate explicitly. Employing the recurence relations (4.52) and (4.53), we have

$$U_2(t,h) = t\,U_1(t,h) - \frac{1}{h}\sqrt{1-2th+h^2} - t \ , \tag{4.58}$$

$$U_3(t,h) = \frac{1}{2}(3t^2-1)U_1(t,h) - \frac{1}{2h^2}(1+3th)\sqrt{1-2th+h^2} - \frac{7}{4}t^2 + \frac{1}{4} \ , \tag{4.59}$$

and

$$V_2(t,h) = \frac{1}{2}(3t^2-1)V_0(t,h) + \frac{1}{2}(h+3t)\sqrt{1-2th+h^2} - \frac{3}{2}t \ . \tag{4.60}$$

Chapter 5

Anomalous density of topographical masses

For computing the geoidal heights, the density of the topographical masses is usually modelled by a constant value $\varrho_0 = 2.67$ g/cm^3 (e.g. Olliver (1980), Vaníček and Kleusberg (1987), Stewart and Hipkin (1989), Sideris (1990), Featherstone (1992), Forsberg and Sideris (1993)). Nevertheless, in a rugged mountaineous areas the actual density of the topographical masses differs from the value of 2.67 g/cm^3 due to various reasons, e.g. due to a compensation mechanism of topographical masses. Also the density of water in lakes such as the Great Lakes in the North America differs significantly from value of 2.67 g/cm^3. A question is how large are the errors of geoidal heights introduced by modelling the topographical density by value of 2.67 g/cm^3 throughout all the topographical masses without taking care of area with large density variations.

To answer this question, we will separate the laterally varying density $\varrho(\Omega)$ into two parts, the 'reference' value $\varrho_0 = 2.67$ g/cm^3 which is constant throughout all the topographical masses, and laterally varying 'anomalous' density $\delta\varrho(\Omega)$, i.e.,

$$\varrho(\Omega) = \varrho_0 + \delta\varrho(\Omega) \ . \tag{5.1}$$

Substituting the decomposition (5.1) into eqn.(3.4), the condensation density $\sigma(\Omega)$ may be split by an analogous way:

$$\sigma(\Omega) = \sigma_0(\Omega) + \delta\sigma(\Omega) \ . \tag{5.2}$$

The 'reference' value $\sigma_0(\Omega)$ corresponds to the reference density ϱ_0 according to relation

$$\sigma_0(\Omega) = \varrho_0\, \tau(\Omega) \ , \tag{5.3}$$

whereas the 'anomalous' condensation density $\delta\sigma(\Omega)$ is associated with the anomalous density $\delta\varrho(\Omega)$:

$$\delta\sigma(\Omega) = \delta\varrho(\Omega)\tau(\Omega) \ . \tag{5.4}$$

For a sake of brevity, we have introduced symbol $\tau(\Omega)$ for that part of the condensation density $\sigma(\Omega)$ which depends on the orthometric heights H only, i.e.,

$$\tau(\Omega) = H\left(1 + \frac{H}{R} + \frac{H^2}{3R^2}\right) \ . \tag{5.5}$$

Let us remind that the orthometric height H of the earth's surface is an angularly dependent function.

5.1 Topographical effects

The direct and both the indirect topographical effects on geoidal heights will be now specified for the topographical density (5.1) and the condensation density (5.2). Let us start with the direct topographical effect on gravity $\delta A(\Omega)$. Substituting for $\varrho(\Omega)$ from eqn.(5.1) and for $\sigma(\Omega)$ from eqn.(5.2) into eqn.(4.22), we get

$$\delta A(\Omega) = \delta A_0(\Omega) + \delta A_{\delta\varrho}(\Omega) \ , \tag{5.6}$$

where

$$\delta A_0(\Omega) = G\varrho_0 \int_{\Omega'} \left[\frac{\partial \widetilde{N}(r,\psi,r')}{\partial r}\bigg|_{r'=R}^{R+H'} - R^2\tau(\Omega')\frac{\partial N(r,\psi,R)}{\partial r} - \right.$$

$$\left. - \frac{\partial \widetilde{N}(r,\psi,r')}{\partial r}\bigg|_{r'=R}^{R+H} + R^2\tau(\Omega)\frac{\partial N(r,\psi,R)}{\partial r} \right]_{r=R+H} d\Omega' \ , \tag{5.7}$$

and

$$\delta A_{\delta\varrho}(\Omega) = G\int_{\Omega'} \left[\delta\varrho(\Omega') \left(\frac{\partial \widetilde{N}(r,\psi,r')}{\partial r}\bigg|_{r'=R}^{R+H'} - R^2\tau(\Omega')\frac{\partial N(r,\psi,R)}{\partial r} \right) - \right.$$

$$-\delta\varrho(\Omega)\left(\frac{\partial\widetilde{N}(r,\psi,r')}{\partial r}\bigg|_{r'=R}^{R+H}-R^2\tau(\Omega)\frac{\partial N(r,\psi,R)}{\partial r}\right)\Bigg]_{r=R+H}d\Omega' \ , \qquad (5.8)$$

The geoidal heights $N_{pri}(\Omega)$ coming from the primary indirect topographical effect on potential, cf. eqn.(4.25), may be decomposed by an analogous way to eqn.(5.6):

$$N_{pri}(\Omega)=N_{pri,0}(\Omega)+N_{pri,\delta\varrho}(\Omega) \ , \qquad (5.9)$$

where

$$N_{pri,0}(\Omega)=-\frac{2\pi G}{\gamma}\varrho_0 H^2\left(1+\frac{2}{3}\frac{H}{R}\right)+$$
$$+\frac{G\varrho_0}{\gamma}\int_{\Omega'}\Big[\widetilde{N}(R,\psi,r')\big|_{r'=R}^{R+H'}-R^2\tau(\Omega')N(R,\psi,R)-$$
$$-\widetilde{N}(R,\psi,r')\big|_{r'=R}^{R+H}+R^2\tau(\Omega)N(R,\psi,R)\Big]\,d\Omega' \ . \qquad (5.10)$$

and

$$N_{pri,\delta\varrho}(\Omega)=-\frac{2\pi G}{\gamma}\delta\varrho(\Omega)H^2\left(1+\frac{2}{3}\frac{H}{R}\right)+$$
$$+\frac{G}{\gamma}\int_{\Omega'}\Big[\delta\varrho(\Omega')\left(\widetilde{N}(R,\psi,r')\big|_{r'=R}^{R+H'}-R^2\tau(\Omega')N(R,\psi,R)\right)-$$
$$-\delta\varrho(\Omega)\left(\widetilde{N}(R,\psi,r')\big|_{r'=R}^{R+H}-R^2\tau(\Omega)N(R,\psi,R)\right)\Big]\,d\Omega' \ . \qquad (5.11)$$

Finally, the geoidal heights $N_{sec}(\Omega)$ originating from the secondary indirect topographical effect on gravity, cf. eqn.(4.40), may again be decomposed similarly to eqn.(5.6):

$$N_{sec}(\Omega)=N_{sec,0}(\Omega)+N_{sec,\delta\varrho}(\Omega) \ , \qquad (5.12)$$

where

$$N_{sec,0}(\Omega)=2\frac{G\varrho_0}{\gamma}\int_{\Omega'}\Big[\tilde{U}(R,\psi,r')\big|_{r'=R}^{R+H'}-R^2\tau(\Omega')U(R,\psi,R)-$$
$$-\tilde{U}(R,\psi,r')\big|_{r'=R}^{R+H}+R^2\tau(\Omega)U(R,\psi,R)\Big]\,d\Omega' \ , \qquad (5.13)$$

and

$$N_{sec,\delta\varrho}(\Omega) = 2\frac{G}{\gamma}\int_{\Omega'}\left[\delta\varrho(\Omega')\left(\tilde{U}(R,\psi,r')\Big|_{r'=R}^{R+H'} - R^2\tau(\Omega')U(R,\psi,R)\right) - \right.$$

$$\left. -\delta\varrho(\Omega)\left(\tilde{U}(R,\psi,r')\Big|_{r'=R}^{R+H} - R^2\tau(\Omega)U(R,\psi,R)\right)\right] d\Omega' \ . \qquad (5.14)$$

Terms $\delta A_0(\Omega)$, $N_{pri,0}(\Omega)$, and $N_{sec,0}(\Omega)$ represent the direct, primary and secondary indirect topographical effects induced by topographical masses of a constant density ϱ_0, whereas terms $\delta A_{\delta\varrho}(\Omega)$, $N_{pri,\delta\varrho}(\Omega)$, and $N_{sec,\delta\varrho}(\Omega)$ represent the gravitational effects induced by lateral changes $\delta\varrho(\Omega)$ of the topographical density. Usually, for geoid computation the former terms are considered and the latter terms are neglected. Since our interest is devoted to explore effects of lateral changes of topographical density on geoidal heights, we will further investigate terms $\delta A_{\delta\varrho}(\Omega)$, $N_{pri,\delta\varrho}(\Omega)$, and $N_{sec,\delta\varrho}(\Omega)$ separately from terms $\delta A_0(\Omega)$, $N_{pri,0}(\Omega)$, and $N_{sec,0}(\Omega)$.

5.2 A lake

A water lake whose surface has a non-zero topographical height represents an example of lateral changes of the topographical density $\varrho(\Omega)$. We will denote the density of water by ϱ_w, $\varrho_w = 1.0$ g/cm^3, and the density of surrounding topographical masses by ϱ_0 (=2.67 g/cm^3). Let the orthometric height of the surface of the lake be H and the depth of the lake be $d(\Omega)$. Approximately, we may assume that $H = H_0 = const.$ over the lake.

The laterally varying density $\varrho(\Omega)$ may be approximately evaluated from the actual 3-D density $\varrho(r,\Omega)$ by averaging the density $\varrho(r,\Omega)$ along the topographical column of height H, cf. eqn.(2.6). For our model of a lake this formula yields

$$\varrho(\Omega) = \begin{cases} \left[\varrho_w\, d(\Omega) + \varrho_0\,(H_0 - d(\Omega))\right]/H_0 \ , & d(\Omega) < H_0 \ , \\ \varrho_w \ , & d(\Omega) \geq H_0 \ . \end{cases} \qquad (5.15)$$

The anomalous density $\delta\varrho(\Omega)$, cf. eqn.(5.1), then reads

$$\delta\varrho(\Omega) = \begin{cases} (\varrho_0 - \varrho_w)d(\Omega)/H_0 \ , & d(\Omega) < H_0 \ , \\ \varrho_0 - \varrho_w \ , & d(\Omega) \geq H_0 \ . \end{cases} \qquad (5.16)$$

For the lake, term $\delta A_{\delta\varrho}(\Omega)$ of the direct topographical effect on gravity, cf. eqn.(5.8), may be further simplified. Realizing that the height H of the computation point over a lake is equal to the height H' of the surface of the lake, $H = H'$, because $H' = H_0 = const.$ over the lake, and that the anomalous density $\delta\varrho(\Omega)$ vanishes outside the lake, cf.eqn.(5.16), we can put $r' = R + H' = R + H_0$ instead of $r' = R + H$ in the third term on the right-hand side of eqn.(5.8). For the same reasons, the function $\tau(\Omega)$ may be considered as follows:

$$\tau(\Omega') = \tau(\Omega) = \tau_0 = \frac{1}{H_0}\left(1 + \frac{H_0}{R} + \frac{H_0^2}{3R^2}\right) . \tag{5.17}$$

Hence, the term $\delta A_{\delta\varrho}(\Omega)$ may be written in the form:

$$\delta A_{\delta\varrho}(\Omega) = G\int_{\Omega'}[\delta\varrho(\Omega') - \delta\varrho(\Omega)]\left[\frac{\partial\widetilde{N}(r,\psi,r')}{\partial r}\Big|_{r'=R}^{R+H_0} - R^2\tau_0\frac{\partial N(r,\psi,R)}{\partial r}\right]_{r=R+H} d\Omega' . \tag{5.18}$$

The geoidal heights $N_{pri,\delta\varrho}(\Omega)$, cf. eqn.(5.11), and $N_{sec,\delta\varrho}(\Omega)$, cf. eqn.(5.14), may be arranged by an analogous way:

$$N_{pri,\delta\varrho}(\Omega) = -\frac{2\pi G}{\gamma}\delta\varrho(\Omega)H_0^2\left(1 + \frac{2}{3}\frac{H_0}{R}\right) +$$

$$+\frac{G}{\gamma}\int_{\Omega'}[\delta\varrho(\Omega') - \delta\varrho(\Omega)]\left[\widetilde{N}(R,\psi,r')\Big|_{r'=R}^{R+H_0} - R^2\tau_0 N(R,\psi,R)\right] d\Omega' , \tag{5.19}$$

and

$$N_{sec,\delta\varrho}(\Omega) = \frac{G}{\gamma}\int_{\Omega'}[\delta\varrho(\Omega') - \delta\varrho(\Omega)]\left[\widetilde{U}(R,\psi,r')\Big|_{r'=R}^{R+H_0} - R^2\tau_0 U(R,\psi,R)\right] d\Omega' . \tag{5.20}$$

5.3 Compensation of topographical masses

As mentioned in Sect. 1.2, shape irregularities of the earth's surface generate a strong gravitational field. The undulations of the equipotential surfaces of this field are hundreds of metres and may reach even one thousand metres. But the equipotential surfaces of the observed gravity field do not vary with

such large amplitudes; the maximal undulations of the actual gravity field are 100 m at most. This fact indicates that the amplitudes of a strong gravitational field of the outer surface *must* be reduced by another source of gravitation lying beneath the topographical masses. Geodesists usually speak about the compensation of the topographical masses.

There are at least two mechanisms compensating a strong gravitation of the topographical masses. By exploration seismology it was found that there is a mass discontinuity in depths of 30-80 km where the mass density increases abruptly by about 0.3 g/cm^3. This discontinuity called the Mohorovićič discontinuity anti-correlates nearly linearly with the earth's surface and thus it generates the gravitational attraction of the opposite direction to that generated by the earth's surface. (This type of compensation is called the Airy-Heiskanen model of compensation (Heiskanen and Moritz, 1967, sect.3-4.).) Nevertheless, the compensation by undulations of the Moho discontinuity is not efficient enough to compensate all the irregularities of the earth's surface (Martinec, 1993) and another source of compensation must exist.

It was found (e.g. Tanimoto (1991), Martinec (1992b)) that the mass density laterally varies in the earth's lithosphere (i.e. up to the depths of 100-150 km) in such a way that the density is smaller beneath high mountains and is larger beneath a low terrain. This type of compensation called the Pratt-Hayford compensation model (Heiskanen and Moritz, 1967, sect. 3-4.) supplies the compensation by the Moho discontinuity.

It is still not known properly how large are the contributions of particular compensation mechanisms to the entire compensation effect. Later we will assume that the topographical masses are compensated by the Pratt-Hayford type of compensation only. Since the Pratt-Hayford compensation model is based on a laterally varying density in the lithosphere, which does not change with depth, considering this mechanism then means that the corresponding compensating laterally varying densities represent an averaged densities which could occur in the uppermost part of the earth. Magnitudes of the lateral variations of the actual density within the lithosphere could be smaller as well as larger. Especially, lateral changes of the density of topographical masses may be larger than Pratt-Hayford compensating densities, because the lateral variations of the density of the uppermost part of the earth may be 10% or even larger.

5.3.1 Pratt-Hayford compensation model

In this section we will derive the parameters of the Pratt-Hayford compensation model. This model has also been treated in the book of Heiskanen and Moritz (1967, sect. 3-4.). Unfortunately, the derivation presented there is rather misleading because it is based on the assumption of mass equality in topographical columns. Such an assumption is artifitial because no geophysical observation supports it. On contrary, our consideration will be based on two facts which follows from observations. (1) A strong gravitational field induced by the topographical masses is not observed; (2) the compensation mechanism runs into depths of 100-150 km.

Let the upper boundary of the compensation layer of the Pratt-Hayford model be the earth's surface of the radius $R + H$. Let the lower boundary of this compensation layer be a surface of the radius R_c. In agreement with geophysical observations, this lower boundary coincides with the bottom of lithosphere and R_c may be considered constant. The depth D of the lower boundary, $D = R - R_c$, will be considered as 100-150 km. The gravitational potential V^{layer} induced by the compensation layer at a point (r, Ω) is given by the Newton volume integral:

$$V^{layer}(r,\Omega) = G \int_{\Omega'} \int_{r'=R_c}^{R+H'} \varrho(r',\Omega') N(r,\psi,r') r'^2 dr' d\Omega' \ , \tag{5.21}$$

where we have used the same notations as in eqn.(2.1).

The density $\varrho(r, \Omega)$ within the compensation layer will be split into two parts:

$$\varrho(r,\Omega) = \varrho_0(r) + \delta\varrho(\Omega) \ , \tag{5.22}$$

where $\varrho_0(r)$ forms the dominant part of the actual density $\varrho(r, \Omega)$. It may be modelled e.g. by the density of the PREM model (Dziewonski and Anderson, 1981). The small density variations $\delta\varrho$ correct the reference density $\varrho_0(r)$; the Pratt-Hayford model assumes that these corrections are laterally varying only.

Substituting eqn.(5.22) into eqn.(5.21), we get

$$V^{layer}(r,\Omega) = G \int_{\Omega'} \int_{r'=R_c}^{R} \varrho_0(r') N(r,\psi,r') r'^2 dr' d\Omega' +$$

$$+G \int_{\Omega'} \int_{r'=R}^{R+H'} \varrho_0(r') N(r,\psi,r') r'^2 dr' d\Omega' +$$

$$+ G \int_{\Omega'} \delta\varrho(\Omega') \int_{r'=R_c}^{R+H'} N(r,\psi,r') r'^2 dr' d\Omega' \ . \tag{5.23}$$

The first integral yields a term which is angularly independent and contributes to potential of type $1/r$ only; this term is out of our interest. The second integral expresses the gravitational effect of the topographical masses with a radially dependent density. In this integral we may approximately put $\varrho_0(r) = \varrho_0 = 2.67$ g/cm^3. The third integral expresses the gravitational effect of laterally varying density of the compensation layer. The Pratt-Hayford compensation model assumes that the gravitational effect of the topographical masses is compensated by the effect of the laterally varying density inside the lithosphere. Mathematically, it means that the third integral cancels the second integral, i.e.,

$$\varrho_0 \int_{\Omega'} \int_{r'=R}^{R+H(\Omega')} N(r,\psi,r') r'^2 dr' d\Omega' +$$

$$+ \int_{\Omega'} \delta\varrho(\Omega') \int_{r'=R_c}^{R+H'} N(r,\psi,r') r'^2 dr' d\Omega' = 0 \tag{5.24}$$

The radial integral of the Newton kernel may be evaluated analytically. For the computation point (r,Ω) on or outside the earth's surface, i.e., when $r \geq R + H(\Omega)$, it holds

$$N(r,\psi,r') = \frac{1}{r} \sum_{j=0}^{\infty} \left(\frac{r'}{r}\right)^j P_j(\cos\psi) \ , \tag{5.25}$$

where $P_j(\cos\psi)$ is the Legendre polynomial of degree j. An indefinite radial integral of the Newton kernel then reads

$$\int_{r'} N(r,\psi,r') r'^2 dr' = \sum_{j=0}^{\infty} \frac{1}{j+3} \frac{r'^{j+3}}{r^{j+1}} P_j(\cos\psi) + C \ , \tag{5.26}$$

where C does not depend on the variable r'.

The definite radial integrals occuring in the condition (5.24) then becomes

$$\int_{r'=R}^{R+H'} N(r,\psi,r') r'^2 dr' = \sum_{j=0}^{\infty} \frac{1}{j+3} \frac{R^{j+3}}{r^{j+1}} \left[\left(1 + \frac{H'}{R}\right)^{j+3} - 1 \right] P_j(\cos\psi) \ . \tag{5.27}$$

Taking approximately

$$\left(1+\frac{H'}{R}\right)^{j+3} \doteq 1+(j+3)\frac{H'}{R}\ , \tag{5.28}$$

we have

$$\int_{r'=R}^{R+H'} N(r,\psi,r')r'^2dr' \doteq H'\sum_{j=0}^{\infty}\frac{R^{j+2}}{r^{j+1}}P_j(\cos\psi)\ . \tag{5.29}$$

Similarly

$$\int_{r'=R_c}^{R+H'} N(r,\psi,r')r'^2dr' \doteq [D+H']\sum_{j=0}^{\infty}\frac{R_c^{j+2}}{r^{j+1}}P_j(\cos\psi)\ . \tag{5.30}$$

Substituting eqns.(5.29) and (5.30) into the Pratt-Hayford condition (5.24) for compensation mechanism, we obtain

$$\varrho_0\int_{\Omega'}H'\sum_{j=0}^{\infty}\frac{R^{j+2}}{r^{j+1}}P_j(\cos\psi)d\Omega'+$$

$$+\int_{\Omega'}\delta\varrho(\Omega')\,[D+H']\sum_{j=0}^{\infty}\frac{R_c^{j+2}}{r^{j+1}}P_j(\cos\psi)d\Omega'=0\ . \tag{5.31}$$

Since the last equation is expressed in 'small' quantities, we may approximately put $R_c \approx R$. Then the equation will only be satisfied if for an arbitrary direction Ω' holds

$$\varrho_0 H' + \delta\varrho(\Omega')\,[D+H'] = 0\ . \tag{5.32}$$

This is a condition for the compensation density $\delta\varrho(\Omega)$:

$$\delta\varrho(\Omega) = -\varrho_0\frac{H(\Omega)}{D+H(\Omega)}\ , \tag{5.33}$$

where we have indicated the dependence of topographical height H on the angular coordinates Ω. Let us remind that for the density ϱ_0 we take a value of 2.67 g/cm^3, and for the compensation depth D we consider a value from interval 100-150 km.

The condition (5.33) for the compensation density $\delta\varrho(\Omega)$ was derived under assumption of vanishing the external gravitational field induced by

the topographical masses. Such a requirement is in full agreement with the observations of the surface gravity. Heiskanen and Moritz (1967, sect. 3-4) derived the same condition (ibid., eqn.(3-25)) under the assumption of equality of masses in topographical columns. Such a requirement seems to be artifitial having no correspondence with observations of the surface gravity field or other geophysical observations. But connecting their results with the derivation presented above, we can conclude that the condition for vanishing the external gravitational field induced by topographical irregularities is approximately equivalent to the condition of the conservation of masses in topographical columns.

Chapter 6

Stokes's integration

To transform gravity anomalies $\Delta g(\Omega)$ (and thus also the direct topographical effect on gravity $\delta A(\Omega)$) to geoidal heights $N(\Omega)$, the Stokes's integration is to be applied to $\Delta g(\Omega)$ (Heiskanen and Moritz, 1967, eqn.(2-163b))

$$N(\Omega) = \frac{R}{4\pi\gamma} \int_{\Omega'} \Delta g(\Omega') S(\psi) d\Omega' \,, \tag{6.1}$$

where γ is the normal gravity on the reference ellipsoid. The Stokes's function $S(\psi)$ may be represented in a spatial form (Heiskanen and Moritz, 1967, eqn.(2-164)) or in a spectral form (ibid., eqn.(2-169) or eqn.(3.23) of this report); hereafter we will use the latter representation.

Evaluating the geoidal heights according to Stokes's formula (6.1) requires knowledge of the gravity anomalies over the entire earth. This makes the problem difficult because there is a lack of gravity data in some regions of the earth or the coverage of gravity data over some areas is fairly non-homogeneous. Therefore, we will follow the idea of Vaníček and Kleusberg (1987) and separate the summation over j in the Stokes function (3.23) into a low and high degree parts:

$$S(\psi) = \sum_{j=2}^{\ell} \frac{2j+1}{j-1} P_j(\cos\psi) + S^{\ell}(\psi) \,. \tag{6.2}$$

The *spheroidal Stokes function* $S^{\ell}(\psi)$ (ibid.) is the Stokes function in which the first ℓ-th spherical harmonics are dropped, i.e.,

$$S^{\ell}(\psi) = \sum_{j=\ell+1}^{\infty} \frac{2j+1}{j-1} P_j(\cos\psi) \,. \tag{6.3}$$

Substituting for $S(\psi)$ from eqn.(6.2) into (6.1), the geoidal heights $N(\Omega)$ may be split into a low degree reference surface $N_0^\ell(\Omega)$ and a high degree contribution $N_1^\ell(\Omega)$:

$$N(\Omega) = N_0^\ell(\Omega) + N_1^\ell(\Omega) \ , \tag{6.4}$$

where

$$N_0^\ell(\Omega) = \frac{R}{4\pi\gamma} \int_{\Omega'} \Delta g(\Omega') \sum_{j=2}^{\ell} \frac{2j+1}{j-1} P_j(\cos\psi) d\Omega' \ , \tag{6.5}$$

and

$$N_1^\ell(\Omega) = \frac{R}{4\pi\gamma} \int_{\Omega'} \Delta g(\Omega') S^\ell(\psi) d\Omega' \ . \tag{6.6}$$

Vaníček and Kleusberg's (1987) approach then assumes that the low frequency part of the geoid is determined from satellite geodesy. Therefore we will chose $\ell = 20$ as Vaníček and Kleusberg's (1987) proposed, and assume that the geoidal heights $N_0^\ell(\Omega)$ are known. Stokes's integration will be employed to compute the high frequency part $N_1^\ell(\Omega)$ of geoidal heights only.

6.1 Modified spheroidal Stokes's function

The integration in eqn.(6.6) has to be still carried out over the entire earth, so that the problem with an unsufficient coverage of gravity data over some areas remains. Despite of this, let us imagine that the Stokes integration (6.6) is only taken over a spherical cap of a small radius ψ_0 around the point of interest. This shrinking of Stokes's integration is intuitively supported by the fact that the effect of local gravity coverage will be most significant due to the largest values of Stokes's kernel for small distances ψ. Shrinking the Stokes integration leads to a quantity

$$N^\ell(\Omega) = \frac{R}{4\pi\gamma} \int_{\psi=0}^{\psi_0} \int_{\alpha=0}^{2\pi} \Delta g(\psi,\alpha) S^\ell(\psi) \sin\psi d\psi d\alpha \ , \tag{6.7}$$

which somehow estimates the geoidal heights $N_1^\ell(\Omega)$. The difference between $N_1^\ell(\Omega)$ and $N^\ell(\Omega)$, i.e., the error of the estimate $N^\ell(\Omega)$ is given by so called *truncation error* (Heiskanen and Moritz, 1967, sect. 7-4); its form is given as

$$\delta N^\ell(\Omega) = N_1^\ell(\Omega) - N^\ell(\Omega) =$$

$$= \frac{R}{4\pi\gamma} \int_{\psi=\psi_0}^{\pi} \int_{\alpha=0}^{2\pi} \Delta g(\psi,\alpha) S^{\ell}(\psi) \sin\psi d\psi d\alpha \ . \tag{6.8}$$

According to Molodensky et al. (1962), Vaníček and Kleusberg's (1987) proposed to modify the spheroidal Stokes's function $S^{\ell}(\psi)$ such that truncation error $\delta N^{\ell}(\Omega)$ is minimal in a least-squares sense. A function coming from this minimization is called the *modified spheroidal Stokes's function* $S^{\ell}(\psi_0,\psi)$ (ibid.). (Let us note that we are using a different notation for the modified spheroidal Stokes function than it is introduced in Vaníček and Kleusberg's (1987) paper.)

Let us summarize the definition relations for the modified spheroidal Stokes function $S^{\ell}(\psi_0,\psi)$ as it was introduced by Vaníček and Kleusberg (1987). The function $S^{\ell}(\psi_0,\psi)$ is determined by formulae

$$S^{\ell}(\psi_0,\psi) = S^{\ell}(\psi) - \sum_{j=0}^{\ell} \frac{2j+1}{2} t_j(\psi_0) P_j(\cos\psi) \ , \tag{6.9}$$

or substituting for $S^{\ell}(\psi)$ from eqn.(6.3), we can also write

$$S^{\ell}(\psi_0,\psi) = S(\psi) - \sum_{j=2}^{\ell} \frac{2j+1}{j-1} P_j(\cos\psi) - \sum_{j=0}^{\ell} \frac{2j+1}{2} t_j(\psi_0) P_j(\cos\psi) \ . \tag{6.10}$$

The coefficients $t_j(\psi_0)$ are determined by solving the linear algebraic equations:

$$\sum_{j=0}^{\ell} \frac{2j+1}{2} R_{ij}(\psi_0) t_j(\psi_0) = Q_i^{\ell}(\psi_0) \ , \tag{6.11}$$

where $i = 0, 1, \ldots, \ell$. The matrix of the system of equations (6.11) is formed by coefficients $R_{ij}(\psi_0)$ introduced by Molodensky et al. (1962) and later investigated numerically by Paul (1973),

$$R_{ij}(\psi_0) = \int_{\psi=\psi_0}^{\pi} P_i(\cos\psi) P_j(\cos\psi) \sin\psi d\psi \ . \tag{6.12}$$

Right-hand sides of eqns.(6.11) are created by *Molodensky truncation coefficients* $Q_j^{\ell}(\psi_0)$ *for spheroidal Stokes's function* $S^{\ell}(\psi)$,

$$Q_j^{\ell}(\psi_0) = \int_{\psi=\psi_0}^{\pi} S^{\ell}(\psi) P_j(\cos\psi) \sin\psi d\psi \ . \tag{6.13}$$

Table 6.1 gives an example of a set of coefficients $t_j(\psi_0)$ for $j = 0, 1, \ldots, 20$ and $\psi_0 = 6°$.

Table 6.1: Coefficients $t_j(\psi_0)$ for $j = 0, 1, \ldots, 20$ and $\psi_0 = 6^o$.

j	$t_j(\psi_0)$	j	$t_j(\psi_0)$	j	$t_j(\psi_0)$
0	-0.113168	7	-0.109871	14	-0.101394
1	-0.113048	8	-0.108950	15	-0.099838
2	-0.112809	9	-0.107926	16	-0.098212
3	-0.112451	10	-0.106802	17	-0.096522
4	-0.111977	11	-0.105582	18	-0.094772
5	-0.111387	12	-0.104271	19	-0.092969
6	-0.110684	13	-0.102873	20	-0.091120

To get a better insight to differences between different Stokes's functions, Figure 6.1 shows the graphs of the Stokes function $S(\psi)$, the spheroidal Stokes function $S^\ell(\psi)$, and modified spheroidal Stokes function $S^\ell(\psi_0, \psi)$ for $\ell = 20$, $\psi_0 = 6^o$ and $\psi \epsilon (0, 8^o)$.

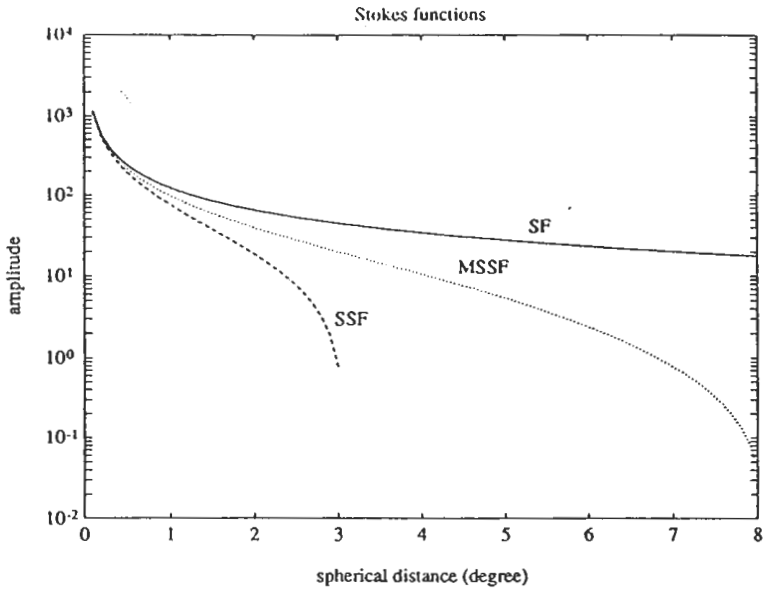

Figure 6.1: The Stokes function $S(\psi)$ (SF-curve), the spheroidal Stokes function $S^{20}(\psi)$ (SSF-curve), and the modified spheroidal Stokes function $S^{20}(\psi_0, \psi)$, $\psi_0 = 6^o$ (MSSF-curve), for $\psi = 0 - 8^o$.

6.2 Molodensky's truncation coefficients

The truncation coefficients $Q_j^\ell(\psi_0)$, cf. eqn.(6.13), have been introduced by an analogous way to the *Molodensky truncation coefficients* $Q_j(\psi_0)$ *for Stokes's function* $S(\psi)$ (Molodensky et al., 1962),

$$Q_j(\psi_0) = \int_{\psi=\psi_0}^{\pi} S(\psi) P_j(\cos\psi) \sin\psi d\psi \ . \tag{6.14}$$

The relation between the truncation coefficients $Q_j^\ell(\psi_0)$ and $Q_j(\psi_0)$ may be readily derived by substituting for $S^\ell(\psi)$ from eqn.(6.3) into eqn.(6.13). Using the definition (6.12) of Paul's functions $R_{ij}(\psi_0)$, we get

$$Q_j^\ell(\psi_0) = Q_j(\psi_0) - \sum_{k=2}^{\ell} \frac{2k+1}{k-1} R_{jk}(\psi_0) \ . \tag{6.15}$$

In the following text we will need to handle with the *Molodensky truncation coefficients* $\tilde{Q}_j^\ell(\psi_0)$ *for modified spheroidal Stokes's function* $S^\ell(\psi_0, \psi)$, i.e., with quantities

$$\tilde{Q}_j^\ell(\psi_0) = \int_{\psi=\psi_0}^{\pi} S^\ell(\psi_0, \psi) P_j(\cos\psi) \sin\psi d\psi \ . \tag{6.16}$$

The relation between the truncation coefficients $\tilde{Q}_j^\ell(\psi_0)$ and $Q_j^\ell(\psi_0)$ may be derived by substituting for $S^\ell(\psi_0, \psi)$ from eqn.(6.9) into eqn.(6.16). We get

$$\tilde{Q}_j^\ell(\psi_0) = Q_j^\ell(\psi_0) - \sum_{k=0}^{\ell} \frac{2k+1}{2} t_k(\psi_0) R_{jk}(\psi_0) \ . \tag{6.17}$$

Introducing the function

$$\tilde{S}^\ell(\psi_0, \psi) = \begin{cases} 0 \ , & 0 \le \psi < \psi_0, \\ S^\ell(\psi_0, \psi) \ , & \psi_0 \le \psi \le \pi \ , \end{cases} \tag{6.18}$$

we may also write

$$\tilde{Q}_j^\ell(\psi_0) = \int_{\psi=0}^{\pi} \tilde{S}^\ell(\psi_0, \psi) P_j(\cos\psi) \sin\psi d\psi \ . \tag{6.19}$$

Using the orthogonality property of Legendre polynomials, the last equation may be inverted obtaining

$$\tilde{S}^{\ell}(\psi_0,\psi) = \sum_{j=0}^{\infty} \frac{2j+1}{2} \tilde{Q}_j^{\ell}(\psi_0) P_j(\cos\psi) \ . \tag{6.20}$$

In the next paragraph we will prove that $\tilde{Q}_j^{\ell}(\psi_0) = 0$ for $j = 0, 1, \ldots, \ell$. Therefore the summation over j in eqn.(6.20) may start from index $j = \ell+1$, i.e.,

$$\tilde{S}^{\ell}(\psi_0,\psi) = \sum_{j=\ell+1}^{\infty} \frac{2j+1}{2} \tilde{Q}_j^{\ell}(\psi_0) P_j(\cos\psi) \ . \tag{6.21}$$

Now, let us show that truncation coefficients $\tilde{Q}_j^{\ell}(\psi_0)$, $j = 0, 1, \ldots, \ell$, are identically equal to zero. Substituting for $S^{\ell}(\psi_0,\psi)$ from eqn.(6.9) into (6.16), we have

$$\tilde{Q}_i^{\ell}(\psi_0) = \int_{\psi=\psi_0}^{\pi} \left[S^{\ell}(\psi) - \sum_{j=0}^{\ell} \frac{2j+1}{2} t_j(\psi_0) P_j(\cos\psi) \right] P_i(\cos\psi) \sin\psi d\psi =$$

$$= Q_i^{\ell}(\psi_0) - \sum_{j=0}^{\ell} \frac{2j+1}{2} t_j(\psi_0) R_{ij}(\psi_0) = 0 \tag{6.22}$$

which is valid for $i = 0, 1, \ldots, \ell$. In this derivation, we have used the definition (6.13) of truncation coefficients $Q_i^{\ell}(\psi_0)$ and relation (6.12) for Paul's incomplete integrals $R_{ij}(\psi_0)$ of the double product of Legendre polynomials. The last equality follows from system of equations (6.11) for coefficients $t_j(\psi_0)$.

The Molodensky truncation coefficients $Q_j^{\ell}(\psi_0)$ and $\tilde{Q}_j^{\ell}(\psi_0)$ for $\psi_0 = 6^{\circ}$, $\ell = 20$, and $j = 0, 1, \ldots, 180$ are plotted in Figure 6.2. As we will see later, the Molodensky truncation coefficients occur as "weights" in a spectral representation of a truncation error $\delta N^{\ell}(\Omega)$. Realizing that the spectral power of the external gravitational field of the earth decreases with increasing spherical degree (e.g., Rapp et al., 1991), Figure 6.2 shows that the truncation error of Stokes's integration which uses the modified spheroidal Stokes function is smaller than the truncation error of Stokes's integration employing the spheroidal Stokes function.

The other important finding is that when the Stokes integration is carried out with the modified spheroidal Stokes function, then the truncation error

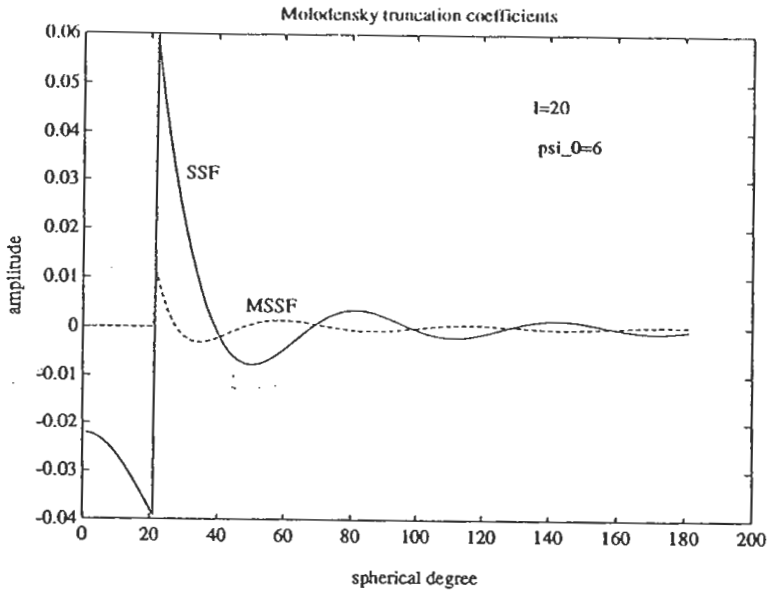

Figure 6.2: Molodensky's truncation coefficients $Q_j^\ell(\psi_0)$ and $\tilde{Q}_j^\ell(\psi_0)$ for the spheroidal Stokes function $S^{20}(\psi)$, and modified spheroidal Stokes function $S^{20}(\psi_0, \psi)$, $\psi_0 = 6°$.

$\delta\widetilde{N}^\ell(\Omega)$, see eqn.(6.28) below, does not depend on a reference field of low spherical degrees ($j = 0 - \ell$) because this function is 'blind' to spherical harmonics of these spherical degrees. This fact does not hold for integration with the spheroidal Stokes function.

6.3 Truncation error

The modified spheroidal Stokes function $S^\ell(\psi_0, \psi)$ has been chosen such that the truncation error

$$\delta\widetilde{N}^\ell(\Omega) = \frac{R}{4\pi\gamma} \int_{\psi=\psi_0}^{\pi} \int_{\alpha=0}^{2\pi} \Delta g(\psi, \alpha) S^\ell(\psi_0, \psi) \sin\psi d\psi d\alpha \qquad (6.23)$$

is minimal. Now, we ask about the magnitude of $\delta\widetilde{N}^{\ell}(\Omega)$ for a given radius ψ_0. Unfortunately, Table 2.3 in Vaníček et al. (1987) yields poor information about $\delta\widetilde{N}^{\ell}(\Omega)$. Therefore, we will investigate the truncation error $\delta\widetilde{N}^{\ell}(\Omega)$ in a detailed view.

Let us represent the disturbing potential $T(r,\Omega)$ of the external gravitational field of the earth in terms of spherical harmonics $Y_{jm}(\Omega)$ (Heiskanen and Moritz, 1967, eqn.(2-152)):

$$T(r,\Omega) = \frac{GM}{R}\sum_{j=2}^{\infty}\left(\frac{R}{r}\right)^{j+1}\sum_{m=-j}^{j} T_{jm}Y_{jm}(\Omega)\ , \tag{6.24}$$

where M is the mass of the earth, and T_{jm} are spherical coefficients of the external gravitational field of the earth. Under representation (6.24), the gravity anomaly approximately reads

$$\Delta g(\Omega) \doteq -\left[\frac{\partial T}{\partial r}+\frac{2}{R}T\right]_{r=R} = \frac{GM}{R^2}\sum_{j=2}^{\infty}\sum_{m=-j}^{j}\Delta g_{jm}Y_{jm}(\Omega)\ , \tag{6.25}$$

where

$$\Delta g_{jm} = (j-1)T_{jm}\ . \tag{6.26}$$

The truncation error $\delta\widetilde{N}^{\ell}(\Omega)$ may now be evaluated as follows:

$$\delta\widetilde{N}^{\ell}(\Omega) = \frac{R}{4\pi\gamma}\int_{\psi=0}^{\pi}\int_{\alpha=0}^{2\pi}\Delta g(\psi,\alpha)\widetilde{S}^{\ell}(\psi_0,\psi)\sin\psi d\psi d\alpha =$$

$$= \frac{R}{4\pi\gamma}\int_{\Omega'}\Delta g(\Omega')\widetilde{S}^{\ell}(\psi_0,\psi)d\Omega' =$$

$$= \frac{R}{4\pi}\int_{\Omega'}\sum_{j_1=2}^{\infty}\sum_{m_1=-j_1}^{j_1}\Delta g_{j_1m_1}Y_{j_1m_1}(\Omega')\sum_{j_2=0}^{\infty}\frac{2j_2+1}{2}\tilde{Q}^{\ell}_{j_2}(\psi_0)\times$$

$$\times\frac{4\pi}{2j_2+1}\sum_{m_2=-j_2}^{j_2}Y^{*}_{j_2m_2}(\Omega')Y^{*}_{j_2m_2}(\Omega)d\Omega' = \frac{R}{2}\sum_{j=2}^{\infty}\sum_{m=-j}^{j}\tilde{Q}^{\ell}_{j}(\psi_0)\Delta g_{jm}Y_{jm}(\Omega)\ .$$

In the first step, we have spread the integration from the interval $<\psi_0,\pi>$ onto the interval $<0,\pi>$ because of replacing the Stokes function $S^{\ell}(\psi_0,\psi)$ by the Stokes function $\widetilde{S}^{\ell}(\psi_0,\psi)$, cf. eqn.(6.18). Then we have transformed the integration over polar coordinates (ψ,α) to the spherical coordinates

$\Omega = (\vartheta, \lambda)$, then we have substituted for $\tilde{S}^{\ell}(\psi_0, \psi)$ from eqn.(6.20), and used and the addition theorem for spherical harmonics (eqn.(4.30)). Finally we have applied the orthogonality property of spherical harmonics (eqn.(4.31)). We get an important formula for the truncation error,

$$\delta\widetilde{N}^{\ell}(\Omega) = \frac{R}{2}\sum_{j=2}^{\infty}\sum_{m=-j}^{j}\tilde{Q}_j^{\ell}(\psi_0)\Delta g_{jm}Y_{jm}(\Omega) \tag{6.27}$$

showing that the Molodensky truncation coefficients $\tilde{Q}_j^{\ell}(\psi_0)$ appear as "weights" of series of spherical harmonics $\Delta g_{jm}Y_{jm}(\Omega)$. The smaller are the truncation coefficients, the smaller is the truncation error. As we have shown in eqn.(6.22), $\tilde{Q}_j^{\ell}(\psi_0) = 0$ for $j = 0, 1, \ldots, \ell$. Therefore the summation in eqn.(6.27) may start from index $j = \ell + 1$, i.e.,

$$\delta\widetilde{N}^{\ell}(\Omega) = \frac{R}{2}\sum_{j=\ell+1}^{\infty}\sum_{m=-j}^{j}\tilde{Q}_j^{\ell}(\psi_0)\Delta g_{jm}Y_{jm}(\Omega)\ . \tag{6.28}$$

Figures 6.3 and 6.4 plot the truncation errors $\delta N^{\ell}(\Omega)$ and $\delta\widetilde{N}^{\ell}(\Omega)$ over Canada. The gravitational field of the earth was described by the model OSU91A (Rapp et al., 1991); the cut of degree of spherical harmonic series (6.28) was equal to 360, the degree of reference spheroidal field was $\ell = 20$ and the radius of the integration cap was $\psi_0 = 6^{\circ}$. The values of the error $\delta N^{\ell}(\Omega)$ are within the interval (-1.9, 2.3) metres, whereas the errors $\delta\widetilde{N}^{\ell}(\Omega)$ lie in the interval (-0.24, 0.34) metres. This means that the modification of the spheroidal Stokes function significantly reduces the magnitude of the truncation error of Stokes's integration.

6.4 Removing singularity of Stokes's function

The Stokes integration with the modified spheroidal Stokes function yields a high frequency part $N^{\ell}(\Omega)$ of the geoidal heights $N(\Omega)$,

$$\widetilde{N}^{\ell}(\Omega) = \frac{R}{4\pi\gamma}\int_{\psi=0}^{\psi_0}\int_{\alpha=0}^{2\pi}\Delta g(\Omega')S^{\ell}(\psi_0, \psi)\sin\psi d\psi d\alpha\ . \tag{6.29}$$

The Stokes function $S^\ell(\psi_0, \psi)$ has a weak singularity at the point $\psi = 0$, i.e.,

$$\lim_{\psi \to 0} S^\ell(\psi_0, \psi) \to \infty \ , \tag{6.30}$$

and

$$\lim_{\psi \to 0} S^\ell(\psi_0, \psi) \sin\psi < \infty \ . \tag{6.31}$$

The method of removing this singularity is described in Heiskanen and Moritz (1967, sect. 2.24) or in Vaníček and Kleusberg (1987). We will use another technique of eliminating the singularity of the Stokes function $S^\ell(\psi_0, \psi)$. Subtracting and adding the gravity anomaly $\Delta g(\Omega)$ at the computation point to the gravity anomaly $\Delta g(\Omega')$ at an integration point, the formula (6.29) may be formally rewritten as

$$\widetilde{N}^\ell(\Omega) = \frac{R}{4\pi\gamma} \int_{\psi=0}^{\psi_0} \int_{\alpha=0}^{2\pi} [\Delta g(\Omega') - \Delta g(\Omega)]\, S^\ell(\psi_0, \psi) \sin\psi d\psi d\alpha +$$

$$+ \frac{R}{4\pi\gamma} \Delta g(\Omega) \int_{\psi=0}^{\psi_0} \int_{\alpha=0}^{2\pi} S^\ell(\psi_0, \psi) \sin\psi d\psi d\alpha \ . \tag{6.32}$$

The singularity of the Stokes function $S^\ell(\psi_0, \psi)$ in the first term is removed. Namely, if $\psi \to 0$, then $\Delta g(\Omega') \to \Delta g(\Omega)$. Moreover, considering the property (6.31), the integrand in the first integral vanishes at the point $\psi = 0$. It means that this point may be left out from the integration domain.

It remains to evaluate analytically the second integral in eqn.(6.32). We may proceed as follows:

$$\int_{\psi=0}^{\psi_0} \int_{\alpha=0}^{2\pi} S^\ell(\psi_0, \psi) \sin\psi d\psi d\alpha = 2\pi \int_{\psi=0}^{\psi_0} S^\ell(\psi_0, \psi) \sin\psi d\psi =$$

$$= 2\pi \int_{\psi=0}^{\psi_0} \left[S(\psi) - \sum_{j=2}^{\ell} \frac{2j+1}{j-1} P_j(\cos\psi) - \sum_{j=0}^{\ell} \frac{2j+1}{2} t_j(\psi_0) P_j(\cos\psi) \right] \sin\psi d\psi \ , \tag{6.33}$$

where we have firstly carried out the integral over α and then substituted for $S^\ell(\psi_0, \psi)$ from eqn.(6.10). Using the relations

$$\int_{\psi=0}^{\psi_0} S(\psi) \sin\psi d\psi = - \int_{\psi=\psi_0}^{\pi} S(\psi) \sin\psi d\psi \ , \tag{6.34}$$

and

$$\int_{\psi=0}^{\psi_0} P_j(\cos\psi)\sin\psi d\psi = -\int_{\psi=\psi_0}^{\pi} P_j(\cos\psi)\sin\psi d\psi \qquad (6.35)$$

for $j > 0$, eqn.(6.33) becomes

$$\int_{\psi=0}^{\psi_0}\int_{\alpha=0}^{2\pi} S^{\ell}(\psi_0,\psi)\sin\psi d\psi d\alpha =$$

$$= -2\pi\int_{\psi=\psi_0}^{\pi}\left[S(\psi) - \sum_{j=2}^{\ell}\frac{2j+1}{j-1}P_j(\cos\psi) - \sum_{j=1}^{\ell}\frac{2j+1}{2}t_j(\psi_0)P_j(\cos\psi)\right]\sin\psi d\psi -$$

$$-\pi t_0(\psi_0)\int_{\psi=0}^{\psi_0}\sin\psi d\psi =$$

$$= -2\pi\left[Q_0(\psi_0) - \sum_{j=2}^{\ell}\frac{2j+1}{j-1}R_{j0}(\psi_0) - \sum_{j=1}^{\ell}\frac{2j+1}{2}t_j(\psi_0)R_{j0}(\psi_0) + \right.$$

$$\left. + \frac{1}{2}t_0(\psi_0)(1-\cos\psi_0)\right] =$$

$$= -2\pi\left[Q_0^{\ell}(\psi_0) - \sum_{j=0}^{\ell}\frac{2j+1}{2}t_j(\psi_0)R_{j0}(\psi_0) + \frac{1}{2}t_0(\psi_0)\left(R_{00}(\psi_0)+1-\cos\psi_0\right)\right] =$$

$$= -2\pi\left[\tilde{Q}_0^{\ell}(\psi_0) + t_0(\psi_0)\right] . \qquad (6.36)$$

In the above derivation we have used the definition (6.14) of the Molodensky truncation coefficient $Q_j(\psi_0)$; for $j = 0$ this coefficient reads (Heiskanen and Moritz, 1967, eqn.(7-43)):

$$Q_0(\psi_0) = -4t + 5t^2 + 6t^3 - 7t^4 + 6t^2(1-t^2)\ln(t+t^2) , \qquad (6.37)$$

where

$$t = \sin\frac{\psi_0}{2} . \qquad (6.38)$$

The Paul function $R_{j0}(\psi_0)$ employed in eqn.(6.36) takes a simple form (Paul, 1973):

$$R_{j0}(\psi_0) = \frac{P_{j+1}(\cos\psi_0) - P_{j-1}(\cos\psi_0)}{2j+1} \qquad (6.39)$$

when $j > 0$, and

$$R_{00}(\psi_0) = 1 + \cos\psi_0 . \qquad (6.40)$$

Stokes's formula (6.32) for a high frequency part of the geoid may be finally written as

$$\widetilde{N}^{\ell}(\Omega) = \frac{R}{4\pi\gamma}\int_{\psi=0}^{\psi_0}\int_{\alpha=0}^{2\pi}\left[\Delta g(\Omega') - \Delta g(\Omega)\right] S^{\ell}(\psi_0,\psi)d\Omega' - \\ - \frac{R}{2\gamma}\Delta g(\Omega)\left[\tilde{Q}_0^{\ell}(\psi_0) + t_0(\psi_0)\right] \ . \tag{6.41}$$

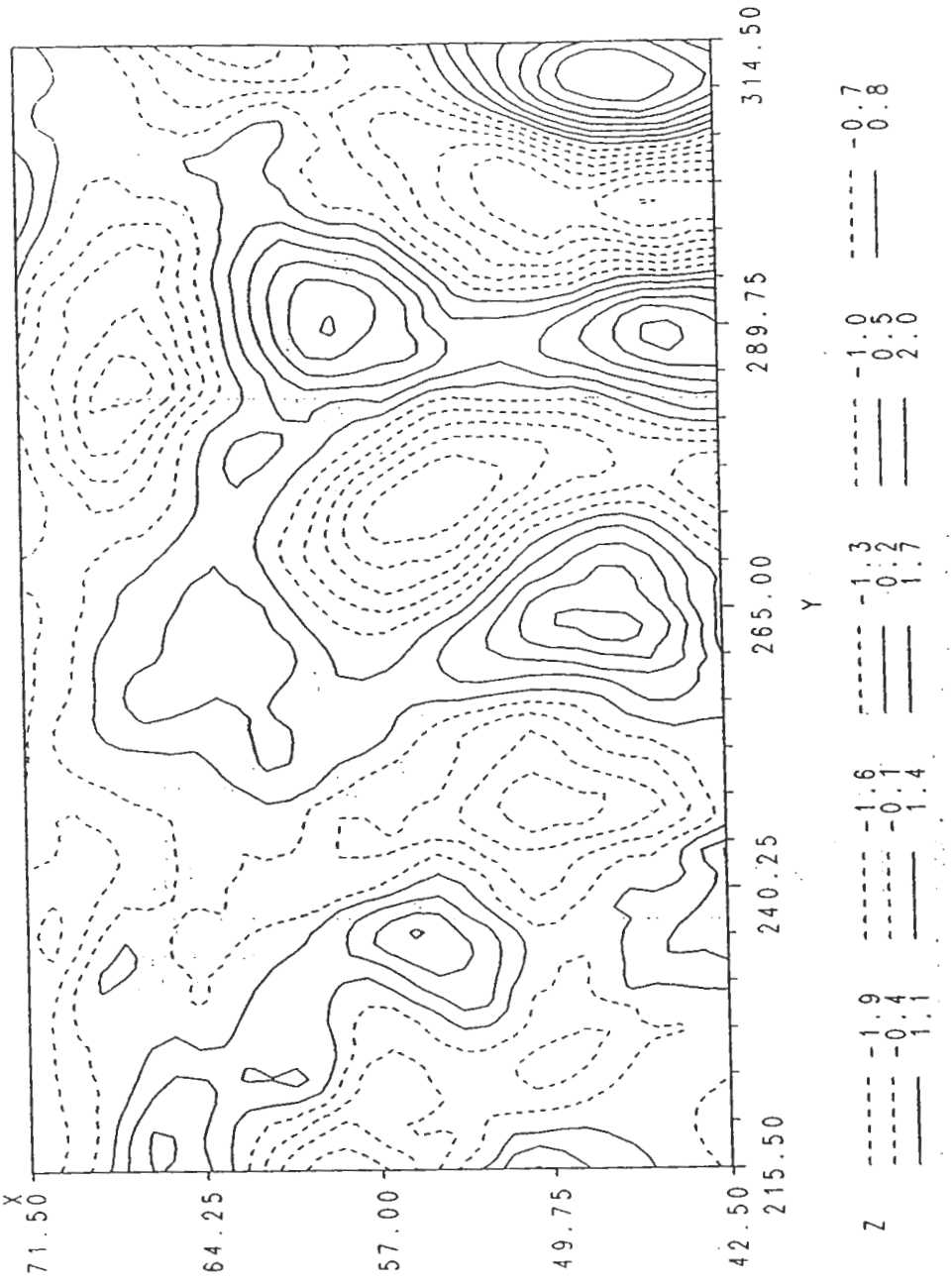

Figure 6.3: The truncation errors $\delta N^{20}(\Omega)$ (in metres), $\psi_0 = 6°$, of Stokes's integration with the spheroidal Stokes function $S^{20}(\psi)$ over Canada.

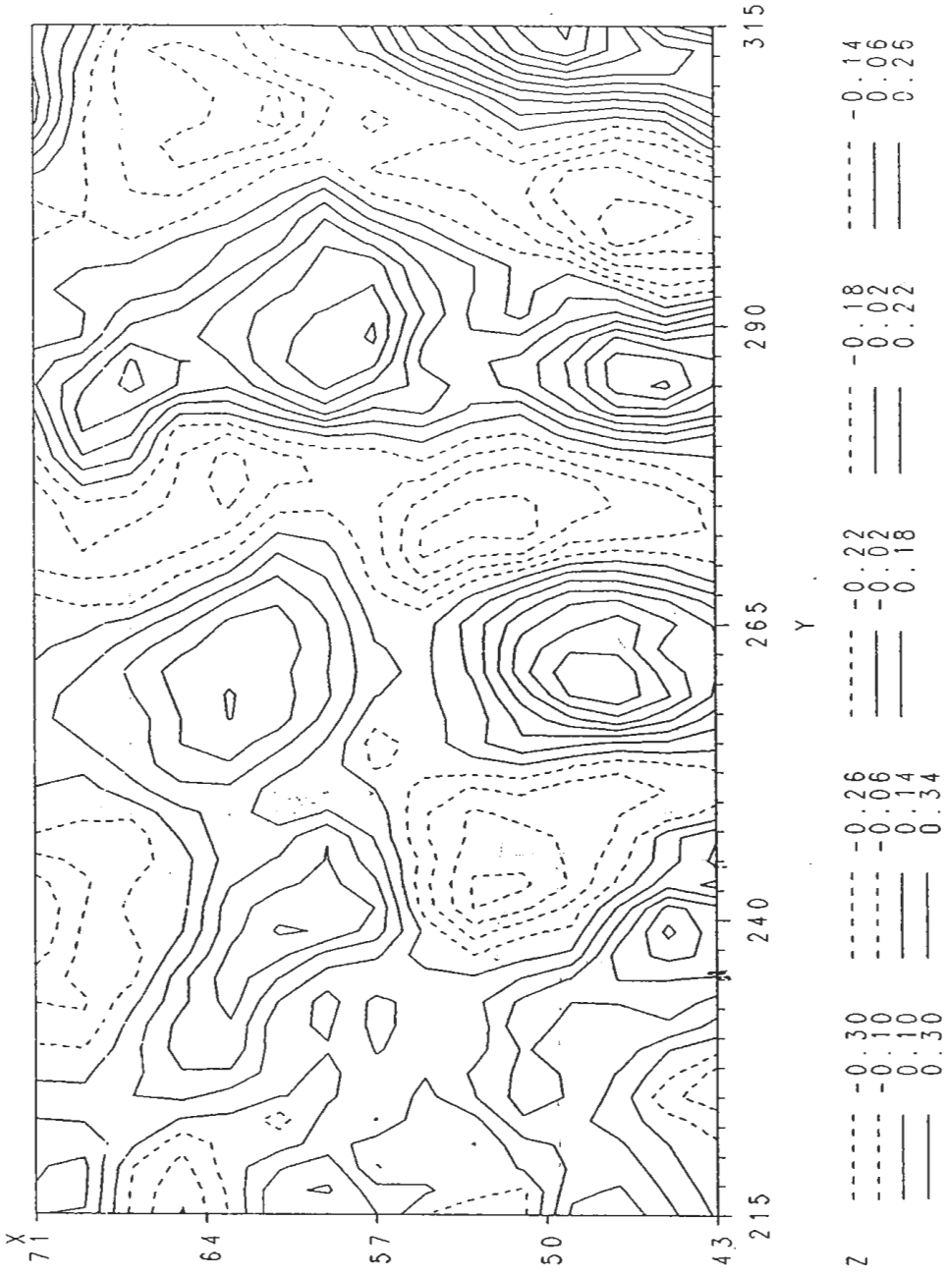

Figure 6.4: The truncation errors $\delta\widetilde{N}^{20}(\Omega)$ (in metres), $\psi_0 = 6°$, of Stokes's integration with the modified spheroidal Stokes function $S^{20}(\psi_0, \psi)$ over Canada.

Chapter 7

Numerical results

7.1 Data sets used

The orthometric heights $H(\Omega)$ of the earth's surface were described by the ETOPO5 digital terrain model which provides the topographical heights over Canada in a regular grid $5' \times 5'$. Results of numerical computations were presented over four areas, (1) **area A**: latitudes $\Phi \doteq 42^o - 72^o$N, longitudes $\lambda \doteq 218^o - 258^o$, which covers the Rocky Mountains in west Canada, (2) **area B**: $\Phi \doteq 48^o - 58^o$N, $\lambda \doteq 238^o - 248^o$, which covers the Columbia Mountains (Figures 7.1-7.3), (3) **area C**: $\Phi \doteq 49^o - 51^o$N, $\lambda \doteq 242^o - 244^o$, which covers the Purcell Mountains (Figure 7.4), and (4) the region of the lake Superior, $\Phi \doteq 46^o - 49^o$N, $\lambda \doteq 268^o - 276^o$. Figure 7.5 shows depths of the lake Superior; the maximal depth is 329 m, the orthometric heights of the lake surface is approximately 183 m.

The reference density ϱ_0 of the topographical masses was chosen equal to 2.67 g/cm^3.

The anomalous density $\varrho(\Omega)$ of the topographical masses was considered for three different cases:

(i) Density contrast of lake water. According to eqn.(5-16), we evaluated the anomalous density $\varrho(\Omega)$ due to the density contrast between water of the lake Superior and surrounding rockies.

(ii) The Pratt-Hayford density anomalies. According to eqn.(5-33), we evaluated the anomalous density $\varrho(\Omega)$ due to the Pratt-Hayford compensation mechanism of the Columbia Mountains.

(iii) Anomalous densities coming from geological information. We discretized the Geological Map of Canada (1962) and the Geological Map of British Columbia (1962) and obtained a data set of rocks and sediments in the region of the Purcell Mountains. The discretization step was $5' \times 5'$. Then we transformed the map of sediments and rocks to a map of anomalous densities $\varrho(\Omega)$ according to tables of rock and sediment densities (Telford at al., 1978). The resulting anomalous density of the geological structure beneath the Purcell Mountains is shown in Figure 7.6.

The first step of this procedure is fairly reliable because there is good knowledge of geological structure of the Rocky Mountains. On contrary, to associate mass densities to geological rocks or sediments is highly unreliable because the densities of rocks and sediments are influenced by many factors, e.g. their age, previous history, depth below surface, geological history of the region, etc. This causes that the density varies in a large range even for one type of rock or sediment.

7.2 The primary indirect topographical effect on potential

To get a better view about magnitudes of particular terms creating the corrections $N_{pri}(\Omega)$ to the geoidal heights due to the primary indirect topographical effect on potential, let us separate this term into two constituents:

$$N_{pri}(\Omega) = N^B_{pri}(\Omega) + N^R_{pri}(\Omega) \ , \tag{7.1}$$

where the Bouguer term $N^B_{pri}(\Omega)$ is equal to

$$N^B_{pri}(\Omega) = -\frac{2\pi G \varrho(\Omega)}{\gamma} H^2 \left(1 + \frac{2}{3}\frac{H}{R}\right) \ . \tag{7.2}$$

The term $N^R_{pri}(\Omega)$, an analog of the terrain correction (Heiskanen and Moritz, 1967, sect. 3-3.) for the condensation technique, is equal to

$$N^R_{pri}(\Omega) = \frac{G}{\gamma} \int_{\Omega'} \left[\varrho(\Omega') \left(\widetilde{N}(R,\psi,r') \Big|_{r'=R}^{R+H'} - R^2 \tau(\Omega') N(R,\psi,R) \right) - \right.$$

$$\left. - \varrho(\Omega) \left(\widetilde{N}(R,\psi,r') \Big|_{r'=R}^{R+H} + R^2 \tau(\Omega) N(R,\psi,R) \right) \right] d\Omega' \ , \tag{7.3}$$

where the Newton kernel $N(R,\psi,r')$ and the kernel $\widetilde{N}(R,\psi,r')$ are given by eqns.(2.2) and (2.20).

Bouguer term

In correspondence with notations introduced in sect. 5.1, $N^B_{pri,0}(\Omega)$ will denote the Bouguer term $N^B_{pri}(\Omega)$ for a constant density $\varrho_0 = 2.67\,\mathrm{g/cm^3}$and $N^B_{pri,\delta\varrho}(\Omega)$ will stand for the Bouguer term $N^B_{pri}(\Omega)$ for anomalous density $\delta\varrho(\Omega)$. Numerical computation of the term $N^B_{pri,0}(\Omega)$ is easy to carry out, because it is created by a simple algebraic expression and it does not include any integration over topographical masses as other topographical terms. The dependence of $N^B_{pri,0}(\Omega)$ on the topographical height is shown in Figure 7.7. Over Canada ($H \leq 6000\,\mathrm{m}$) the term $N^B_{pri,0}(\Omega)$ may reach -4m which is a large contribution to the geoidal heights.

The plot of the term $N^B_{pri,0}(\Omega)$ over area A is shown in Figure 7.8. Minimal value is -1.41m. Figure 7.9 plots the same term over area B; minimal value si -0.78m. We can see that the minimal values of $N^B_{pri,0}(\Omega)$ do not reach the value of -4 m as predicted in Figure 7.7 for heights of 6000 m. The reason is that the ETOPO5 topography is smoother than the actual terrain; the height of some hills in the Rocky Mountains is reduced very significantly.

Numerical tests

For computing the terrain corrections $N^R_{pri}(\Omega)$ of the primary indirect topographical effect on potential, cf. eqn.(7.3), we have created the computation subroutine NEWTC for carrying out (i) the integration kernel

$$\widetilde{N}(R,\psi,r')\Big|_{r=R}^{R+H'} \tag{7.4}$$

generating the gravitational potential $V^t(R,\Omega)$ of the topographical masses at a point on the geoid, (ii) the integration kernel

$$R^2\tau(\Omega')N(R,\psi,R) \tag{7.5}$$

generating the potential $V^c(R,\Omega)$ of the condensed masses on the geoid, and (iii) the difference

$$\widetilde{N}(R,\psi,r')\Big|_{r=R}^{R+H'} - R^2\tau(\Omega')N(R,\psi,R) \tag{7.6}$$

generating the residual potential $\delta V(R,\Omega)$ on the geoid. The condensation density $\tau(\Omega)$ is considered in the form (5.5). The subroutine NEWTC is listed in Appendix A. The input and output parameters of this program are described in comments at the beginning of the program.

We have carried out several numerical tests to explore the behaviour of the integration kernel (7.6) in dependence of varying topographical height H' and the angular distance ψ. The angular distance ψ was changed fluently from 0.0001° to 10°, i.e., the distance between the computation point and an integration point ranges approximately from 11m to 1100km. The height H' of the integration point was modelled by three values: $H' = 200$m, 1km, and 5km. The results are shown in Figures 7.10-7.13. We have plotted separately the particular parts of the integration kernel (7.6); the solid curves in Figures 7.10-7.12 show the behaviour of the kernel (7.4), the dashed lines the kernel (7.5), and the dotted curves their difference, i.e., the kernel (7.6). Observing Figures 7.10-7.13, we can see that:

(i) The computation algorithm is very stable even if a dummy point of integration is very close to the computational point. This stability of the integration kernel is caused by the logarithmic function occuring in the kernel (2.20). When a dummy point of integration is very close to the computation point such that $\psi \leq \varepsilon$ (ε is a small number), then the logaritmic function in eqn.(2.20) becomes dominant and the kernel $\widetilde{N}(R,\psi,r')\Big|_{r'=R}^{R+H'}$ behaves like a function $\ln \ell_0$, where ℓ_0 is the horizontal distance between the computation point and a dummy point of integration. Because of the limit

$$\lim_{\ell_0 \to 0} \frac{\ln \ell_0}{\frac{1}{\ell_0}} = 0 \ , \tag{7.7}$$

the kernel $\widetilde{N}(R,\psi,r')\Big|_{r'=R}^{R+H'}$ goes to infinity when ψ approaches zero even slower than a reciprocal distance $1/\ell_0$. Therefore, the numerical procedure of computing the Newton integral (7.3) based on the formula (2.20) is very stable near the point $\psi = 0$ and is not limited by a restriction that a discretization step has to be greater then the heighest topographical elevation as in the procedure based on the Taylor series expansion (Martinec et al., 1993b)

(ii) The topography used over Canada is gridded by step $5'$. If, for instance, the topographical step would be shorter, say 1km, then the integration kernel (7.6) grows up in magnitude about 3 orders for a hill of 1 km high

(Figure 7.11) and about 2 orders for a hill of 5 km high (Figure 7.12). This increase of the integration kernel causes an increase of geoidal height $N^R_{pri}(\Omega)$. Of course, not with the same magnitude as for the integration kernel because the integration in eqn.(7.3) is taken over varying topographical heights surrounding the computation point. For example, when the topographical grid is made denser from a grid of $5' \times 5'$ to 1km×1km, the maximal amplitude of the terrain corrections $N^R_{pri,0}(\Omega)$ over area B increases from 5cm to 18cm (Martinec at al., 1993). Therefore, the grid step $5'$ in a quickly varying mountaineous terrain such as in the Rocky Mountains is not able to fit feature of the terrain with a sufficient resolution and does not reveal contributions to geoidal height that are larger than 1cm.

(iii) As soon as the computation point moves away from the integration point, the integration kernel (7.4) starts to approach the integration kernel (7.5), and the kernel (7.6) goes to zero. This means that the gravitational potential of topographical shell of a finite thickness behaves like that of a thin layer when it is observed from larger distances. The integration over the full solid angle Ω' in term $N^R_{pri}(\Omega)$ may be therefore shrinked to an integration over a small area (of radius ψ_0) surrounding the computation point. A question is how large the integration radius ψ_0 should be chosen in order to retain a prescribed accuracy of geoidal heights. To answer it, we have evaluated the term $N^R_{pri,0}(\Omega)$ for various radii ψ_0; Table 7.1 summarizes result of the tests.

Table 7.1: The minimum and maximum values of the term $N^R_{pri,0}(\Omega)$ over the west Canada (area A) for different integration radii ψ_0

ψ_0 (degrees)	min (cm)	max (cm)
0.5	-2.7	4.2
1.0	-2.7	4.9
1.5	-2.6	5.2
2.0	-2.0	5.9
3.0	-2.0	6.7
4.0	-2.1	7.0

From Table 7.1 we can see that the accuracy of geoidal heights of the order of 1 cm may be maintained when the integration radius is considered equal to $\psi_0 = 3^o$.

Columbia Mountains
The plot of geoidal heights due to the terrain correction term $N^R_{pri,0}(\Omega)$ (with integration radius $\psi_0 = 3^o$) over area B is shown in Figure 7.14. We can observe that the magnitudes of this term lay within the interval (-3, 5) cm. The maximum values are linked with high hills in the Rocky Mountains. This expresses the fact that the Bouguer term $N^B_{pri,0}(\Omega)$ (Figure 7.9) subtracts too large values of geoidal heights, and therefore, the terrain corrections $N^R_{pri,0}(\Omega)$ have to correct it by adding positive values. The opposite situation is for a valley.

Figures 7.15 and 7.16 show the geoidal heights $N^B_{pri,\delta\varrho}(\Omega)$ and $N^R_{pri,\delta\varrho}(\Omega)$ induced by the Pratt-Hayford density anomalies (5.33). The values of the term $N^B_{pri,\delta\varrho}(\Omega)$ are within the interval (0, 2) cm, whereas the term $N^R_{pri,\varrho}(\Omega)$ varies in the interval (-1, 0.7) mm. The Bouguer term $N^B_{pri,\delta\varrho}(\Omega)$ is always positive because the density anomalies of the Pratt-Hayford compensation model take only the negative sign, cf.eqn.(5.33). Neglecting the compensation of topographical masses then means that the geidal heights may be biased because of the systematic contribution of the Bouguer term $N^B_{pri,\delta\varrho}(\Omega)$. Comparing Figures 7.14 and 7.15, we can see that terms $N^R_{pri,0}(\Omega)$ and $N^B_{pri,\delta\varrho}(\Omega)$ are approximately of the same magnitudes (of units of centimetres); both have to be taken into consideration for a 1-cm geoid computation. On contrary, the terrain corrections $N^R_{pri,\delta\varrho}(\Omega)$ due to lateral changes of compensation density may be omitted for geoid computations with such an accuracy.

Purcell Mountains
Figures 7.17 and 7.18 show the Bouguer term $N^B_{pri,\delta\varrho}(\Omega)$ and terrain corrections $N^R_{pri,\delta\varrho}(\Omega)$ over area of the Purcell Mountains. The laterally varying density $\delta\varrho$ was taken according to the laterally varying geological structure of this region (Figure 7.6). The values of terms $N^B_{pri,\delta\varrho}(\Omega)$ and $N^R_{pri,\delta\varrho}(\Omega)$ range between -8cm and 7cm, and -0.8cm and 0.6cm, respectively. Hence, for 1-cm geoid computations, the Bouguer term $N^B_{pri,\delta\varrho}(\Omega)$ is to be taken into considerations whereas the terrain corrections $N^R_{pri,\delta\varrho}(\Omega)$ may be ommited.

Lake Superior

Figure 7.19 shows the plot of term $N^B_{pri,\delta\varrho}(\Omega)$ over the lake Superior. We can observe that the magnitude of this term lies within the interval (-0.24, 0.0) cm, the largest negative values are linked with the deepest parts of the lake Superior.

Let us explain the reason why the minimal value of -0.24 cm has a 'plateau' over the deepest parts of the lake Superior. The orthometric height of the surface of the lake is 183 m, the depth of the lake reaches value of 329 m. This means that deeper water masses of the lake whose depths are larger than 183 m lie under the geoid. Inspecting the definition (5.16) of the anomalous density $\delta\varrho(\Omega)$ of the topographical masses, we can find out that topographical masses for these deepest parts of the lake have a constant density $\varrho_0 - \varrho_w$ (=1.67 g/cm^3). Since the height H of the observer is also constant over the lake, $H = H_0$, the first term on the right-hand side of eqn.(5.19) shows that the term $N^B_{pri,\delta\varrho}(\Omega)$ is constant over the deepest parts of the lake (i.e. parts whose depths are larger than 183 m).

Figure 7.20 plots the term $N^R_{pri,\delta\varrho}(\Omega)$ over the lake Superior. The magnitude of this term is of the order of 4×10^{-5} m. Comparing these values with the magnitude of term $N^B_{pri,\delta\varrho}(\Omega)$ (Figure 7.19), we observe that Bouguer term $N^B_{pri,\delta\varrho}(\Omega)$ is about two orders larger than the terrain correction term $N^R_{pri,\delta\varrho}(\Omega)$. This fact can be easily explained by the shape of the bottom of the lake. The slope of shores of the lake is such severe that a larger part of the lake has a depth greater than 183m. Therefore, replacing the real topographical masses by the Bouguer plate is a fairly good approximation.

7.3 The direct topographical effect on gravity

Numerical tests

For computing the direct topographical effect on gravity, see sect. 5.1, we have created the computational subroutine DNEWTC for evaluating (i) the integration kernel

$$\left.\frac{\partial \widetilde{N}(r,\psi,r')}{\partial r}\right|_{r=R}^{R+H'} \tag{7.8}$$

generating the gravitational attraction $A^t(r,\Omega)$ of the topographical masses,

(ii) the integration kernel

$$R^2\tau(\Omega')\frac{\partial N(r,\psi,R)}{\partial r} \tag{7.9}$$

generating the attraction $A^c(r,\Omega)$ of the condensed masses, and (iii) the difference

$$\frac{\partial \widetilde{N}(r,\psi,r')}{\partial r}\Big|_{r=R}^{R+H'} - R^2\tau(\Omega')\frac{\partial N(r,\psi,R)}{\partial r} \tag{7.10}$$

generating the residual attraction $\delta A(r,\Omega)$. The condensation density τ is considered in the form (5.5). The subroutine DNEWTC is listed in Appendix B. The input and output parameters of this program are described in remarks at the beginning of the program.

Figures 7.21-7.23 show the behaviour of the kernels (7.8)-(7.10) for height of the integration point $H' = 1$km. The height of the computation point was described by three values: $H = 200$m, 1km, and 5km. The angular distance ψ was fluently changed from 0.001^0 to 10°, i.e., the horizontal distance between the computation point and the integration point ranges approximately from 110m to 1100km. Observing Figures 7.21-7.23, we can drew similar results as we did for the kernel $N(r,\psi,r')|_{r=R}^{R+H'}$ in sect. 7.2:

(i) The computational algorithm for evaluating the kernels (7.8)-(7.10) is very stable even if a dummy point of integration lies very close to the computation point.

(ii) There is a large difference in magnitude of kernels (7.8) and (7.9) in an immediate neighbourhood of the computation point. The higher is the topography above the computation point, the larger is the difference between these kernels, and therefore, the stronger is the direct topographical effect on gravity.

(iii) When an integration point moves away from the computation point, the integration kernel (7.9) starts to approach the kernel (7.8), and the magnitude of the residual kernel (7.10) goes fastly to zero. This means that the gravitational attraction of a material shell of a finite thickness behaves similarly to the gravitational attraction of a thin material layer when it is observed from larger distances. The integration over the full solid angle Ω' in the term $\delta A(\Omega)$ may be therefore shrinked to an integration over a small cap of a radius ψ_0 surrounding the computation point. A question is how to choose the integration radius ψ_0 to maintain a prescribed accuracy of gravitation $\delta A(\Omega)$.

To answer it, we have evaluated the direct topographical effect on gravity $\delta A_0(\Omega)$, cf.eqn.(5.7), for several radii ψ_0 over the area A. Table 7.2 summarizes results of the test.

Table 7.2: The minimal and maximal values of the direct topographical effect on gravity $\delta A_0(\Omega)$ over west Canada (area A) for several integration radii ψ_0

ψ_0 (degrees)	min (mGals)	max (mGals)
0.5	-107.8	47.1
1.0	-117.7	47.1
1.5	-121.2	47.1
2.0	-123.0	47.1
3.0	-124.1	47.1

From Table 7.2 we can see that the accuracy of 1 mGal may be maintained when the integration radius ψ_0 is chosen equal to 3^o. Surprising is that the maximal values of $\delta A_0(\Omega)$ do not change within tenth of mGals; changes of this value appear in hundredths (10^{-2}) of mGals.

Columbia Mountains

The plot of the direct topographical effect on gravitation $\delta A_0(\Omega)$ (with integration radius $\psi_0 = 3^o$) over the area B is shown in Figure 7.24. We can see that the maximal value of $\delta A_0(\Omega)$ is 28 mGals and minimal value is -28 mGals. As expected, these values are linked with hills and valeys of the Rocky Mountains. In a flat terrain, the magnitude of $\delta A_0(\Omega)$ is small reaching at most the units of mGals.

Figure 7.25 shows the direct topographical effect on gravity $\delta A_{\delta\varrho}(\Omega)$ induced by the Pratt-Hayford compensation density $\delta\varrho$, cf. eqn.(5-33). The values of $\delta A_{\delta\varrho}(\Omega)$ range from -0.7 mGals and 0.7 mGals. The Stokes integration (4.3) of the gravitation $\delta A_{\delta\varrho}(\Omega)$ provides corrections $N_{dir,\delta\varrho}(\Omega)$ to be added to the geoidal heights. Figure 7.26 plots geoidal heights $N_{dir,\delta\varrho}(\Omega)$ due to the Pratt-Hayford compensation mechanism of area B; values are in the interval (-7, 7) cm.

Purcell Mountains

The direct topographical effect on gravity $\delta A_{\delta\varrho}(\Omega)$ generated by lateral density variations of geological structure beneath the Purcell Mountains (Figure 7.6) ranges from -6 mGals to 9 mGals (see Figure 7.27). These large contributions to gravity anomalies are significant for precise determination of the geoid and surely contribute to decimetres of geoidal heights. Unfortunately, the area plotted in Figure 7.27 is too small for applying Stokes's integration (4.3).

Lake Superior
Figure 7.28 shows the plot of term $\delta A_{\delta\varrho}(\Omega)$ over the lake Superior. We can see that the magnitudes of this term lie within the interval (-0.14, 0.18) mGals. The Stokes's integration of $\delta A_{\delta\varrho}(\Omega)$ is shown in Figure 7.29. The corrections $N_{dir,\delta\varrho}(\Omega)$ to geoidal heights are in the interval (-1.1, 1.3) cm.

7.4 The secondary indirect topographical effect on gravity

Numerical tests
For computing the Stokes integral $N_{sec}(\Omega)$ of the secondary indirect effect on gravity, cf. eqns.(5.12)-(5.14), we have created the computation subroutine UKERTC for carrying out (i) the integration kernel

$$\tilde{U}(R,\psi,r')\Big|_{r=R}^{R+H'} , \tag{7.11}$$

(ii) the integration kernel

$$R^2\tau(\Omega')U(R,\psi,R) , \tag{7.12}$$

and (iii) their difference

$$\tilde{U}(R,\psi,r')\Big|_{r=R}^{R+H'} - R^2\tau(\Omega')U(R,\psi,R) . \tag{7.13}$$

The condensation density $\tau(\Omega)$ is considered in the form (5.5). The subroutine UKERTC is listed in Appendix C. The input and output parameters of this program are described in comments at the beginning of the program.

We have performed several numerical computations to explore the behaviour of the integration kernel (7.13) with respect to varying topographical height H' and the angular distance ψ. These parameters were changed within the same ranges as for testing the subroutine NEWTC (sect. 7.2). The results are shown in Figures 7.30-7.32. Observing these figures, we can drew the similar conclusions as we did for the kernel (7.6) (sect. 7.2):

(i) The computational algorithm for evaluating the kernel (7.13) is very stable even if a dummy point of integration lies very close to the computational point.

(ii) The magnitude of the kernel (7.13) decreases very rapidly to zero when an integration point moves away from the computational point.

Figures 7.33-7.35 compare the kernel (7.6) (curves 'N') and the kernel (7.13) (curves 'U') for various heights of the integration point. We can observe that the magnitude of the kernel 'N' is significantly larger then the magnitude of the kernel 'U' in an immediate vicinity of the computation point. The higher is the topography above geoid, the larger is the difference between the kernel 'N' and 'U'.

On contrary, the magnitude of kernel 'U' becomes comparable with that of kernel 'N' when the distance between the computation point and an integration point starts to enlarge. For instance, the kernel 'U' is approximately the same as that of the kernel 'N' in distances of about 20 km from computation point for topographical height of 200m (Figure 7.33), or in distances of about 90 km for topographical height 5km (Figure 7.35). The kernel 'U' is even larger in farther distances. This indicates that if the kernel 'N' for the primary indirect effect is taken into consideration for geoid computation, then the kernel 'U' cannot be left out because it contributes to geoidal heights by terms of comparable magnitudes as the kernel 'N'.

Figure 7.36 showing the geoidal heights generated by the secondary indirect term $N_{sec,0}(\Omega)$ over areas B prove the above statement. The magnitude of $N_{sec,0}(\Omega)$ ranges from -1.5 cm to +3 cm that is comparable with magnitude of the term $N^R_{pri,0}(\Omega)$ plotted in Figure 7.14.

7.5 Discussion

The above numerical computations aimed to estimate the effect of laterally varying anomalous density $\varrho(\Omega)$ of topographical masses on the geoidal

heights. For comparison, we also carried out numerical values of topographical terms for the constant reference density ϱ_0. Let us summarize the basic facts which follow from numerical analysis.

The topographical terms can be sorted into three groups according to their magnitudes.

(1) The largest contributions to the geoidal heights are induced by the Bouguer term $N^B_{pri,0}(\Omega)$ of the primary indirect topographical effect on potential and the direct topographical effect on gravity $\delta A_0(\Omega)$. The magnitude of the former term may reach values of -4m in a rugged mountaineous terrain such as the Rocky Mountains (see Figures 7.8 and 7.9), the latter term may contribute to gravity anomalies by values of tens and even hundred of mGals (see Table 7.2). Since these two terms are evaluated for the constant density ϱ_0 of topographical masses, the only errors of these terms are caused by inaccuracies of topographical heights and/or a poor resolution of a topographical grid. Namely, if the topographical heights are discretized by a very large step, the DTM is not able to fit rough irregularities of a terrain, and consequently, topographical terms are distored by large errors. For example, the grid $5' \times 5'$ for description of the terrain shape of the Rocky Mountains is of such a poor resolution that it causes errors in geoidal heights of the order of metre (compare Figure 7.7 with Figure 7.8).

(2) The second group is formed by terms $N^R_{pri,0}(\Omega)$, $N^B_{pri,\delta\varrho}(\Omega)$, $\delta A_{\delta\varrho}(\Omega)$, and $N_{sec,0}(\Omega)$. All these terms contribute to the geoidal heights by decimetres at most in a rugged mountaineous terrain and by a few milimetres in a flat region (see Figures 7.14, 7.15, 7.17, 7.25-7.27, 7.36). Even if the magnitude of these terms is about one order smaller than that of terms of the first group, a sparse discretization of topographical elevations may still cause large errors of geoidal height. For instance, topographical terms of this group carried out for the topographical grid $5' \times 5'$ in area of the Rocky Mountains do not possess a desired accuracy of 1 cm; errors of geoidal heights due to a sparse disretization may reach decimetres (Martinec et al., 1993c).

Poor knowledge of lateral variations of the density of topographical masses is other source of errors of the geoidal heights. For instance, for area of the Rocky Mountains the topographical density has to be known with a relative accuracy of 1% or better to be able to evaluate the topographical terms of this group with 1-cm accuracy (compare Figure 7.15 with 7.17, or Figure 7.25 with 7.27).

(3) Terms $N^R_{pri,\delta\varrho}(\Omega)$ and $N_{sec,\delta\varrho}(\Omega)$ induce geoidal heights of magnitudes smaller than 1 cm (Figures 7.16 and 7.18), and may be therefore neglected in 1-cm geoid determination.

In summary, for a **1-cm geoid** the terms of the first group have to be taken into consideration in all cases, for a rugged terrain as well as for a flat area. The topographical terms of the second group may be left out from geoid computation over a flat terrain but they have to be considered over a rugged mountaineous region. For the Rocky Mountains, the topographical heights have to be gridded by step of 1km or denser, and the density of topographical masses must be known with a relative accuracy of 1% or better. The topographical terms of the third group may be omitted.

A density contrast between lake water and rockies and sediments represents another source of lateral changes of the topographical densities. Numerical computations carried out for the lake Superior showed that this anomalous density effects the geoidal heights in a few centimetres at most. Therefore, the "water" effect of large lakes is to be considered only for a very accurate modeling of the geoid.

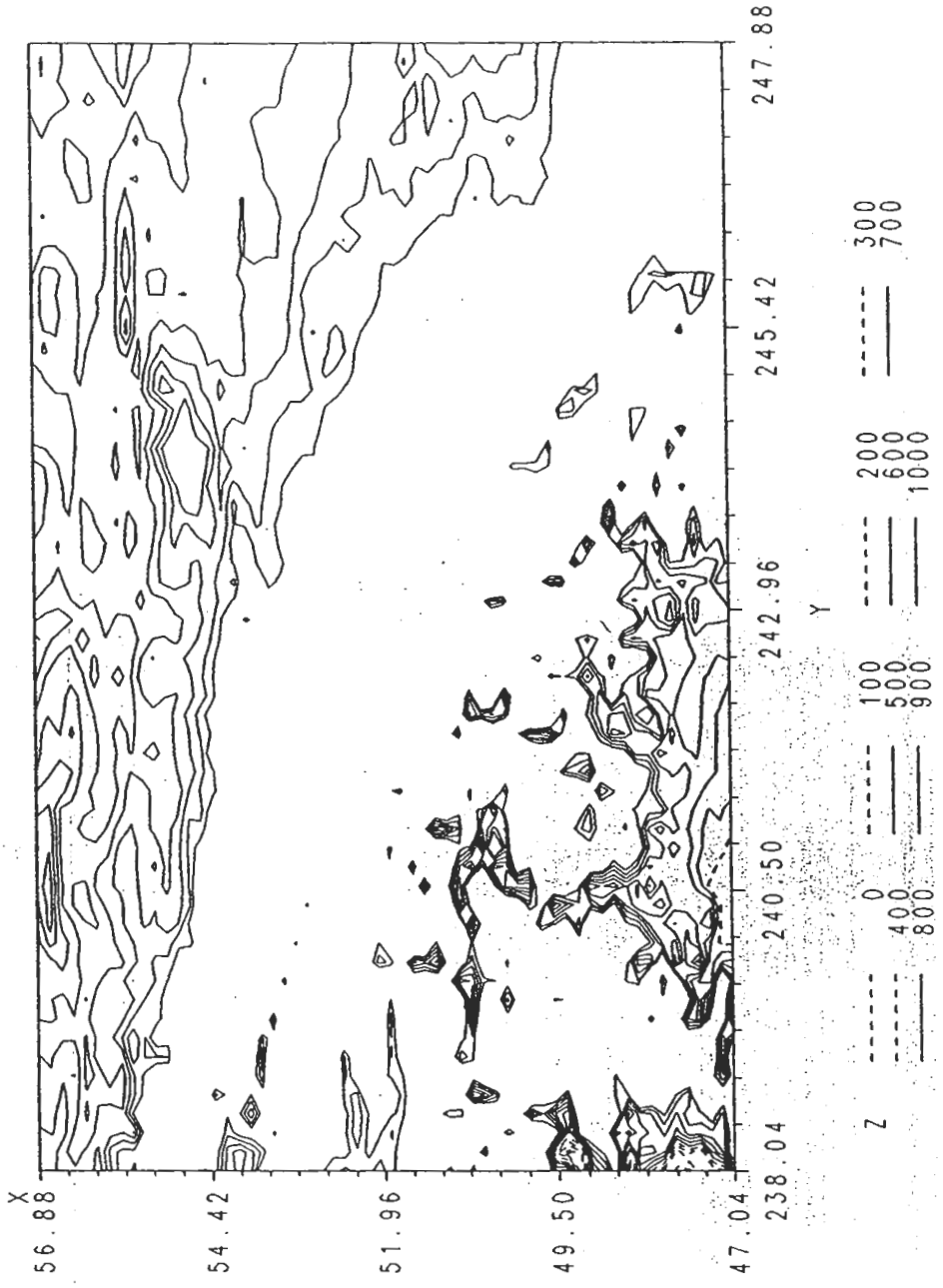

Figure 7.1: ETOPO5 topographical heights over area B ($\Phi \doteq 48^o - 58^o$N, $\lambda \doteq 238^o - 248^o$), range: 0-1000m.

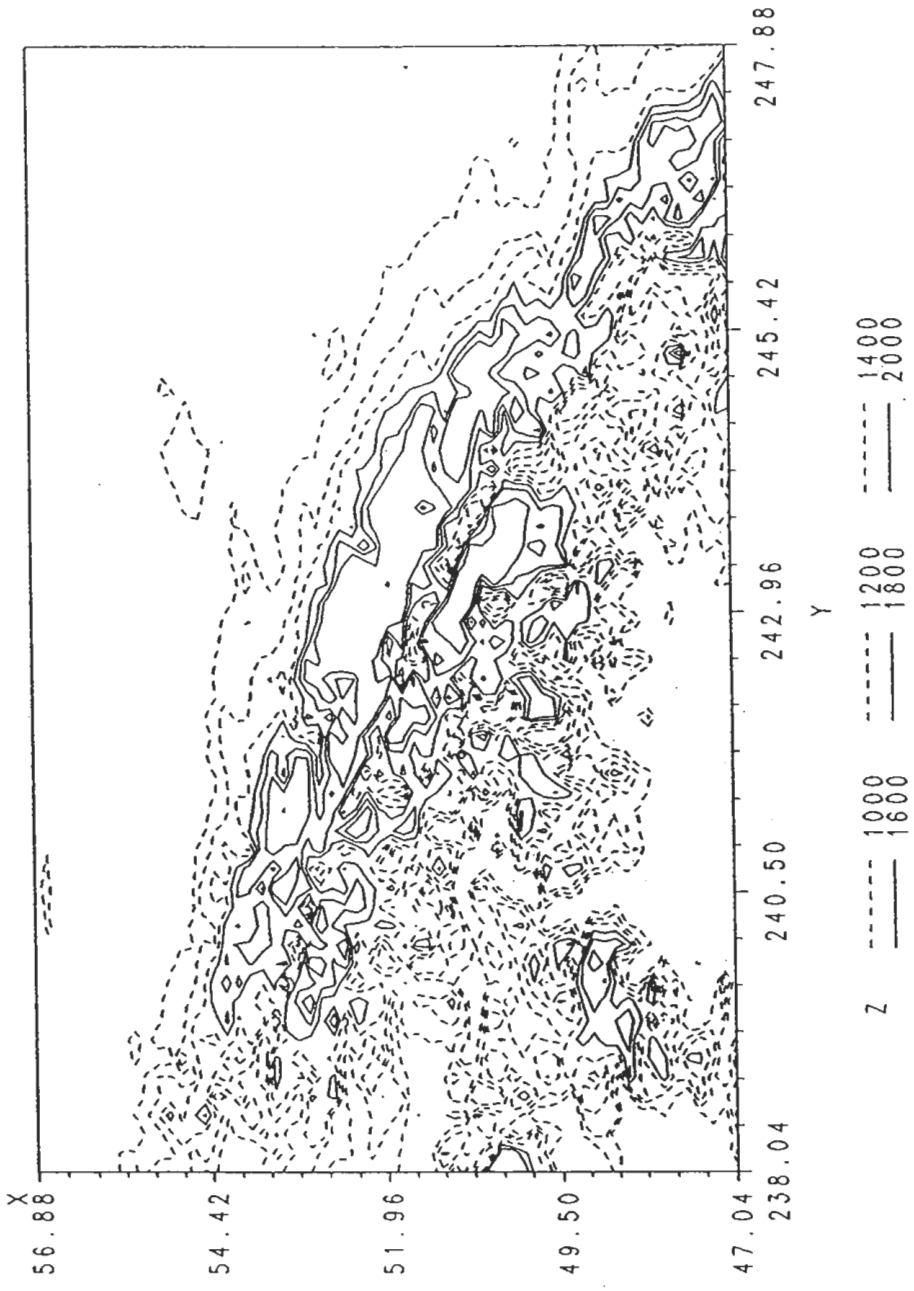

Figure 7.2: ETOPO5 heights in area B for range 1000-2000m.

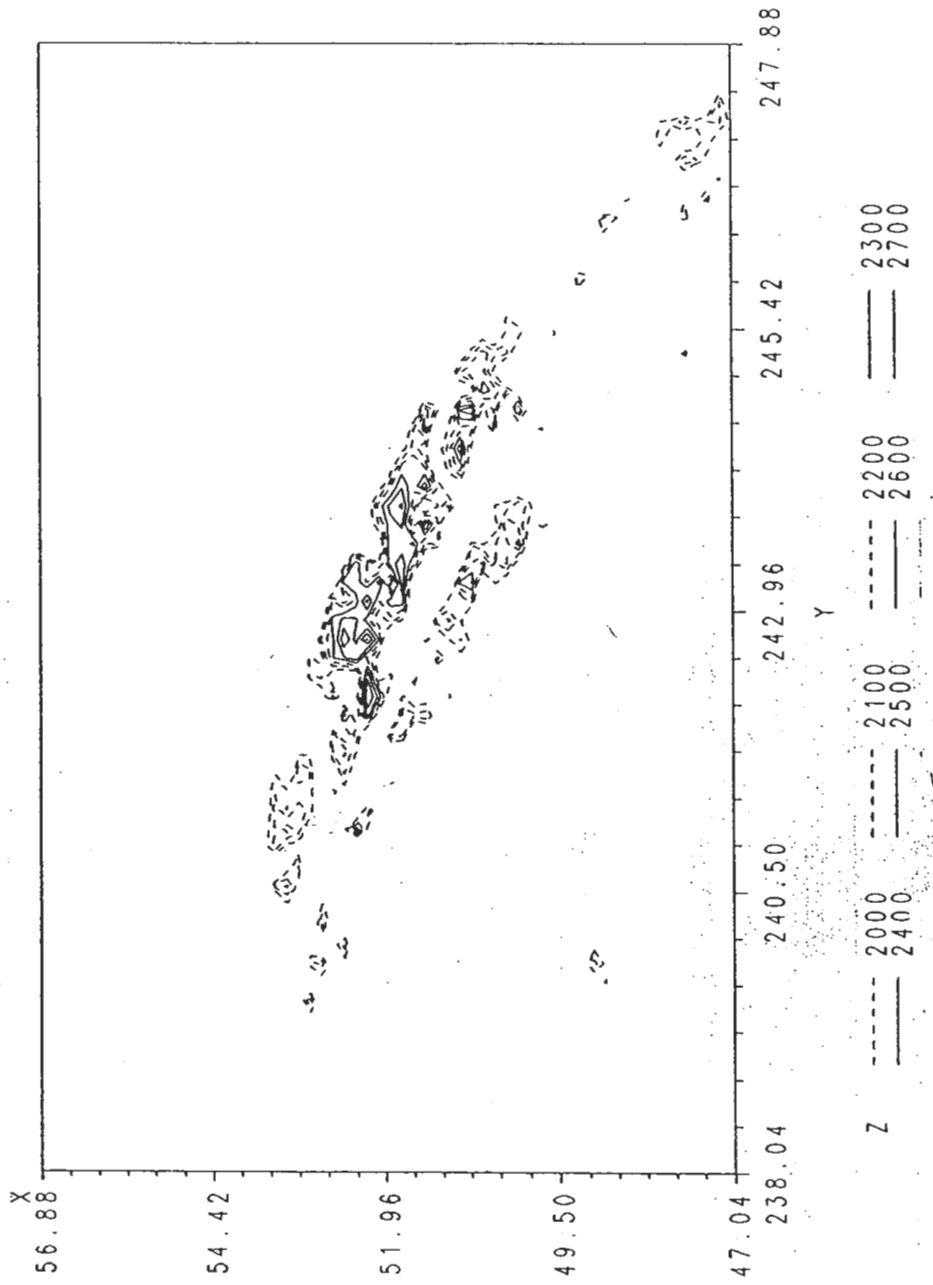

Figure 7.3: ETOPO5 heights in area B for range 2000-2700m.

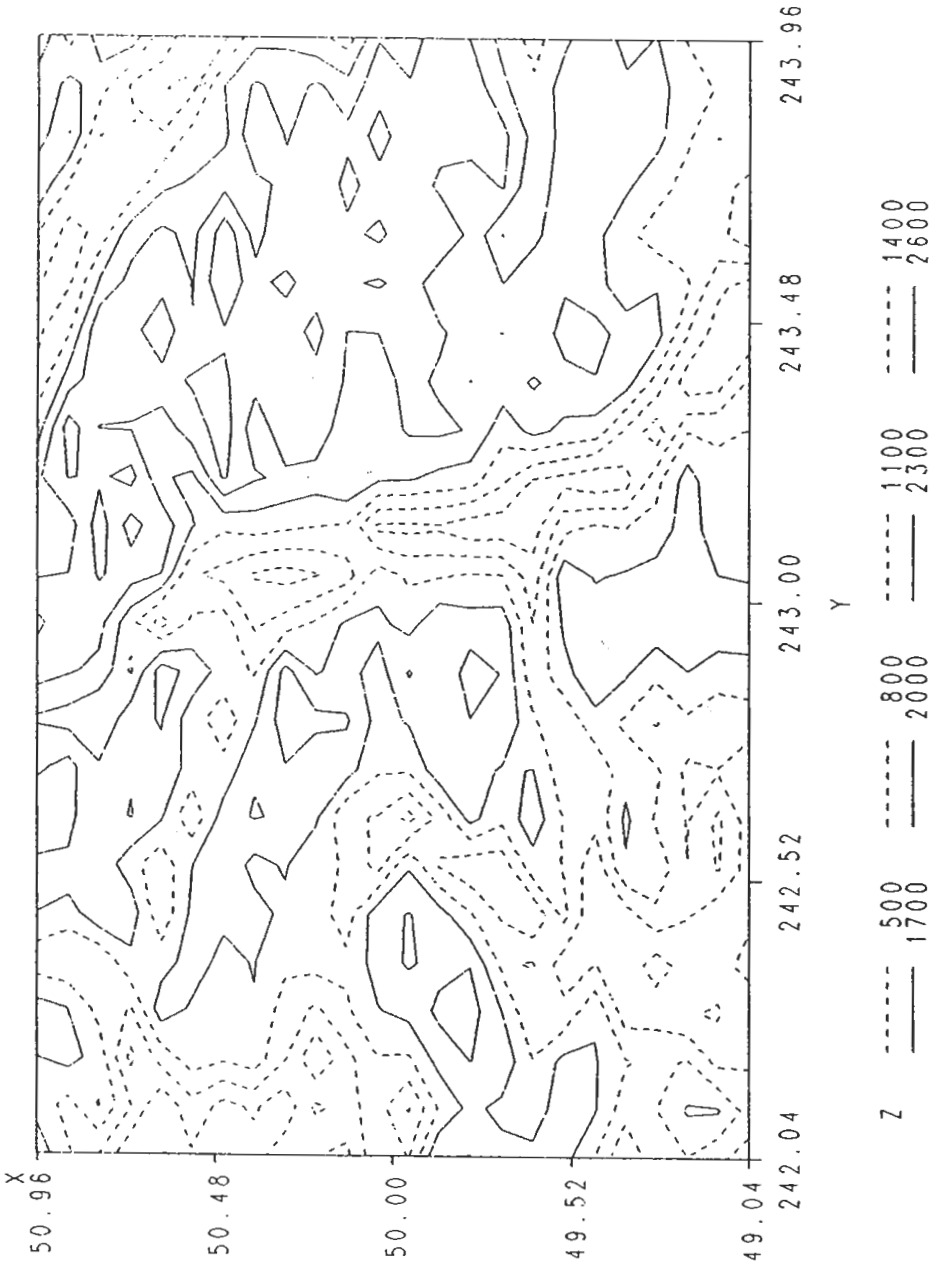

Figure 7.4: ETOPO5 heights (in metres) over area C ($\Phi \doteq 49° - 51°$N, $\lambda \doteq 242° - 244°$).

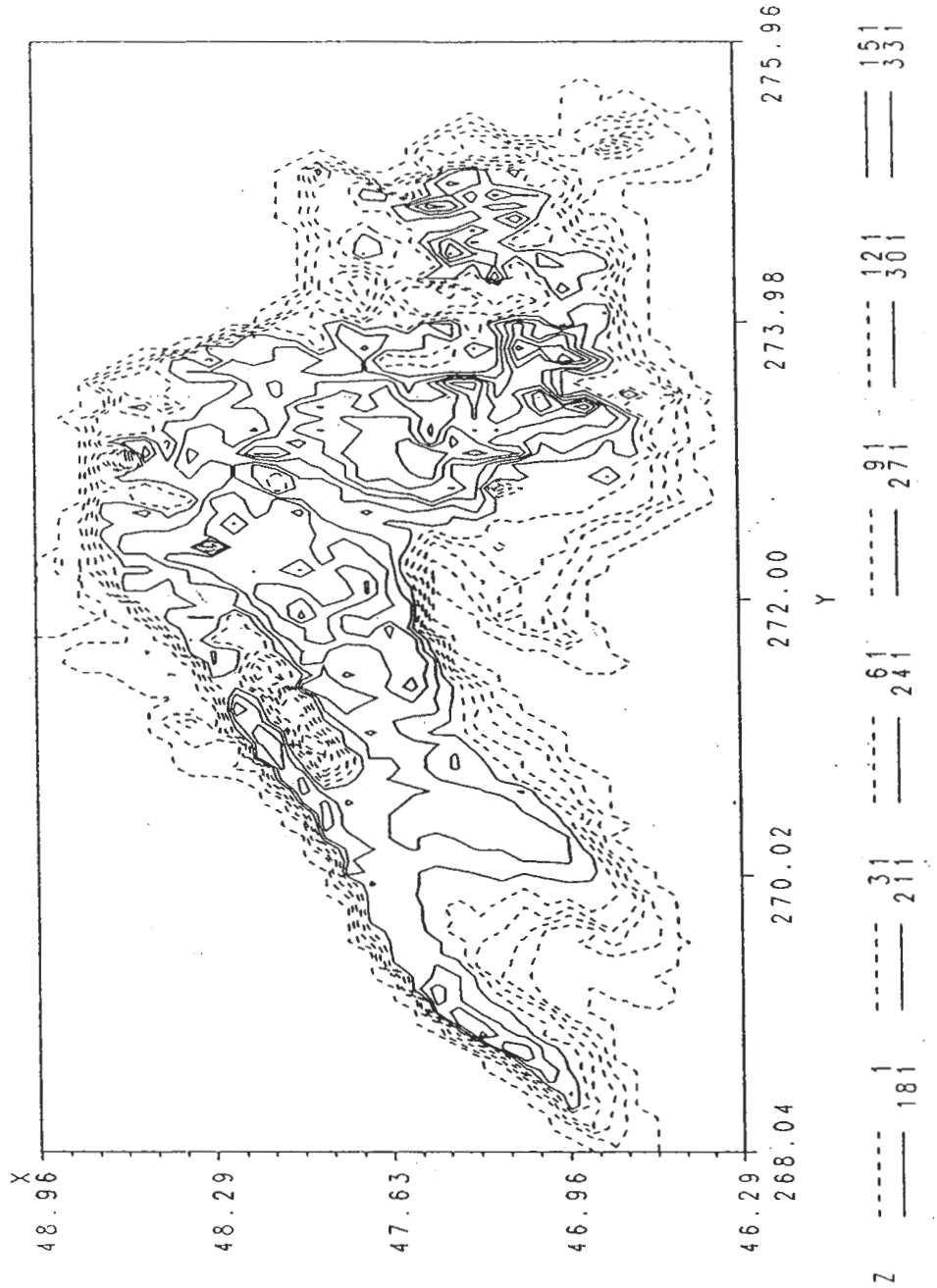

Figure 7.5: Depths of the lake Superior (in metres).

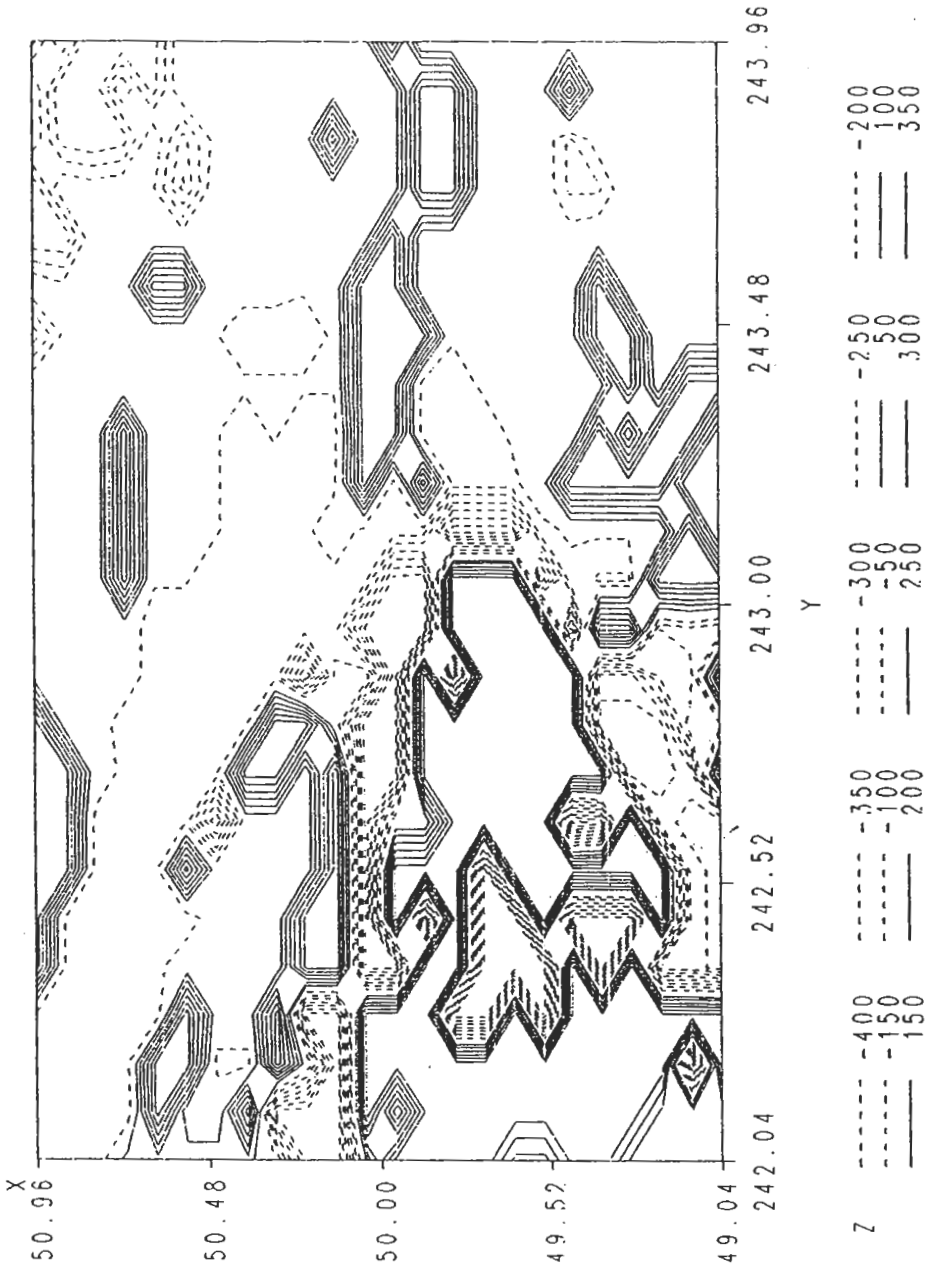

Figure 7.6: The anomalous density $\varrho(\Omega)$ (in kg/m^3) of the laterally varying geological structure beneath the Purcell Mountains.

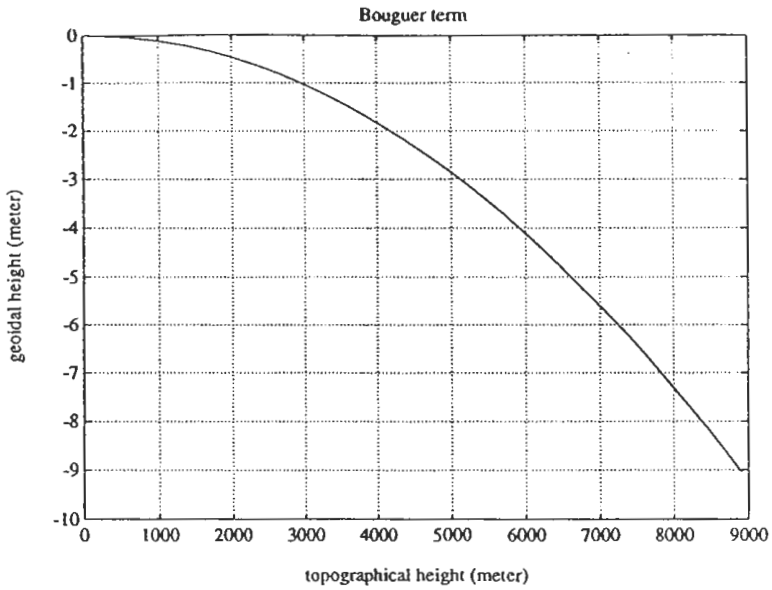

Figure 7.7: The dependence of the Bouguer term $N^{B}_{pri,0}(\Omega)$ on the topographical height H.

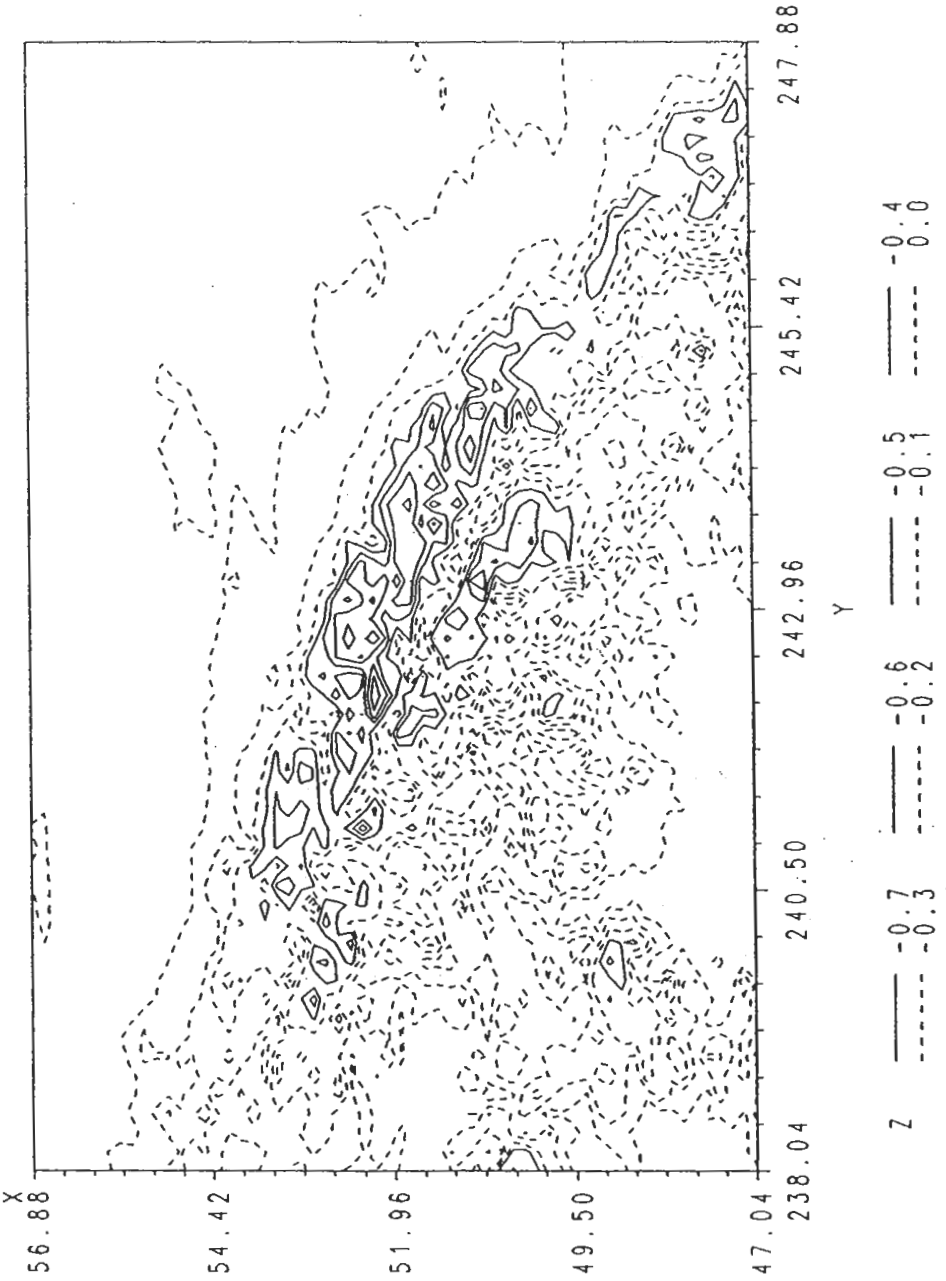

Figure 7.9: The geoidal heights (in metres) induced by term $N^{B}_{pri,0}(\Omega)$ over area B.

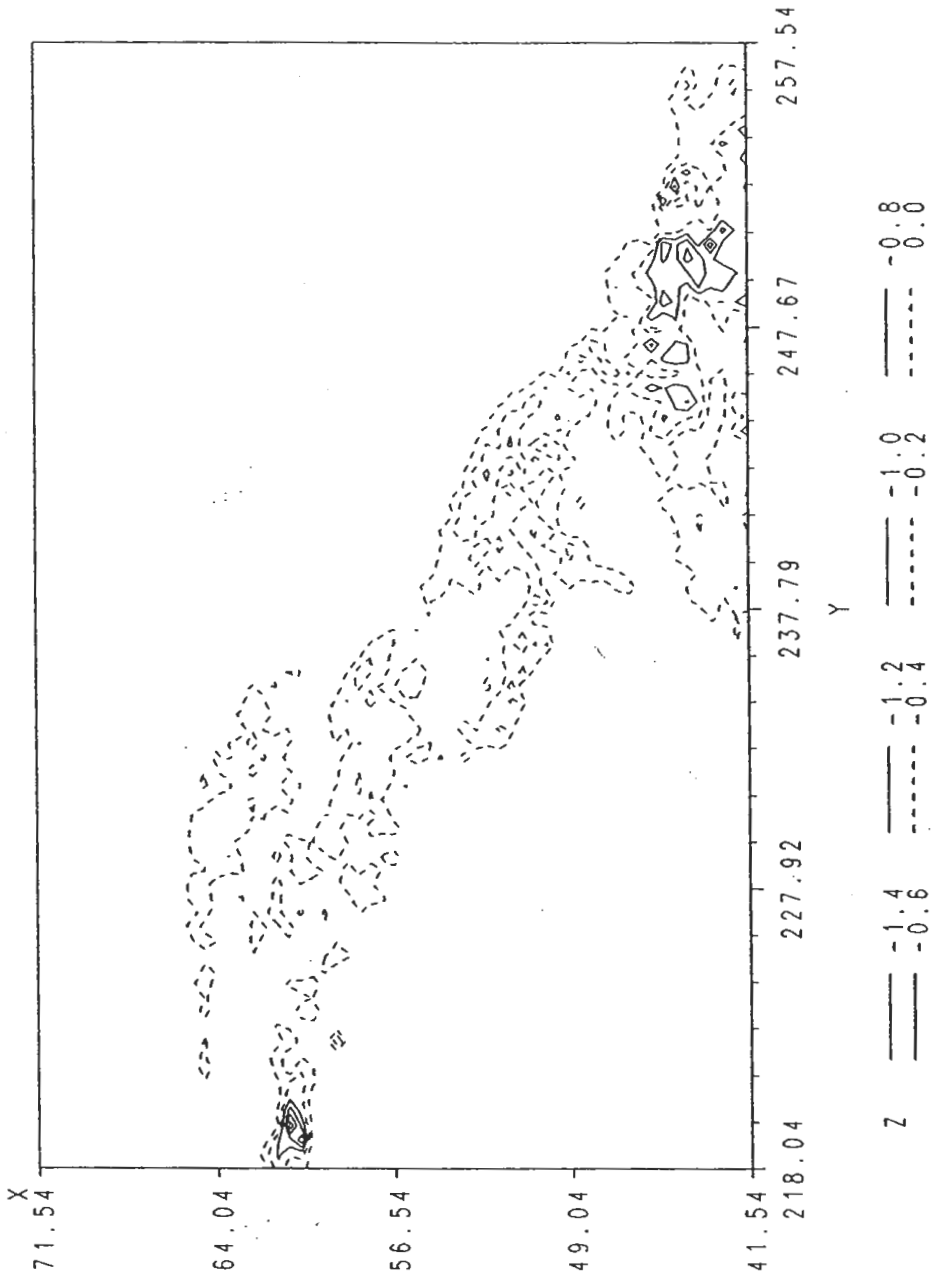

Figure 7.8: The geoidal heights (in metres) induced by term $N^B_{pri,0}(\Omega)$ over area A.

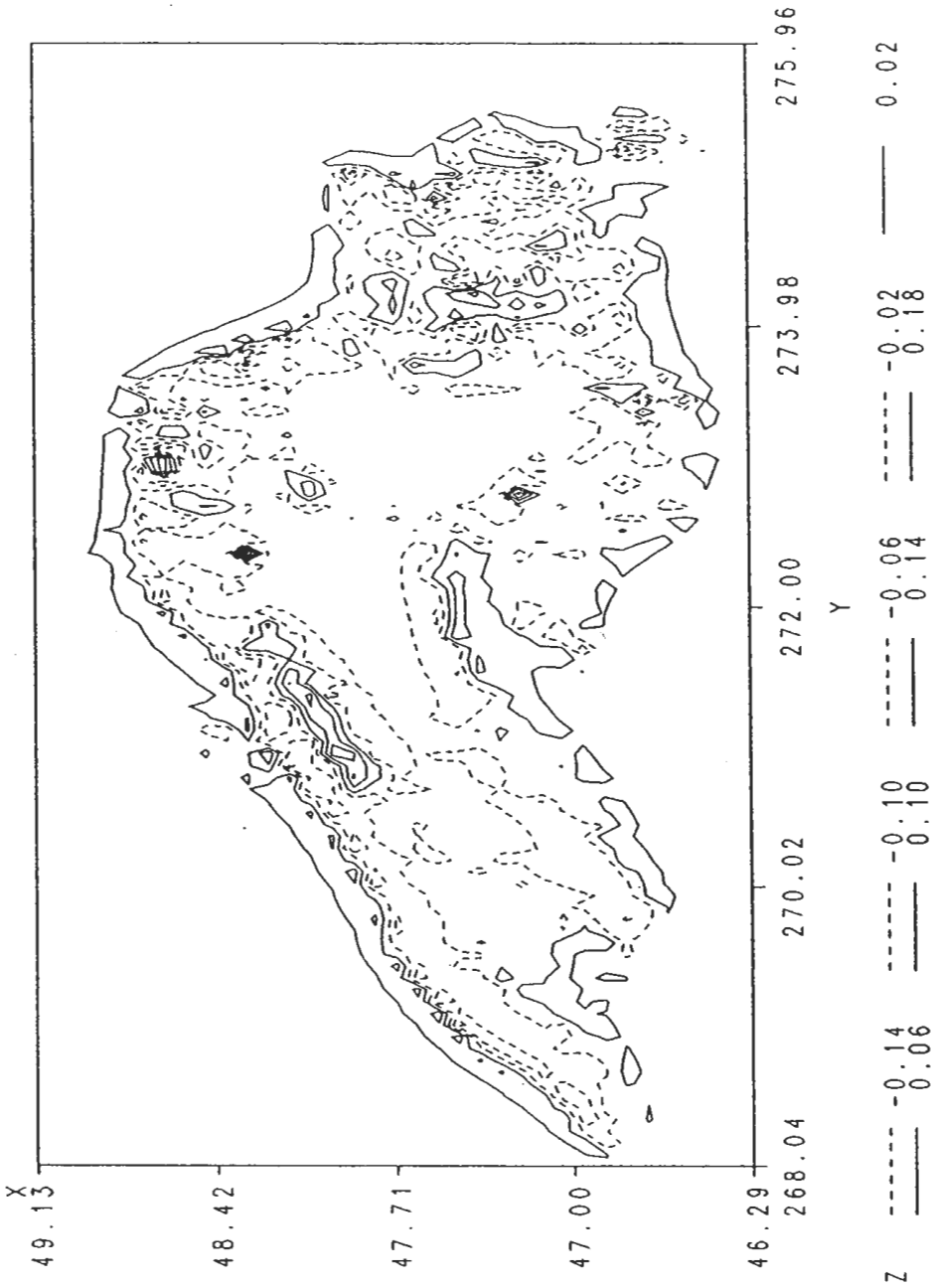

Figure 7.28: The direct topographical effect on gravity $\delta A_{\delta\varrho}(\Omega)$ (in mGals) over the lake Superior.

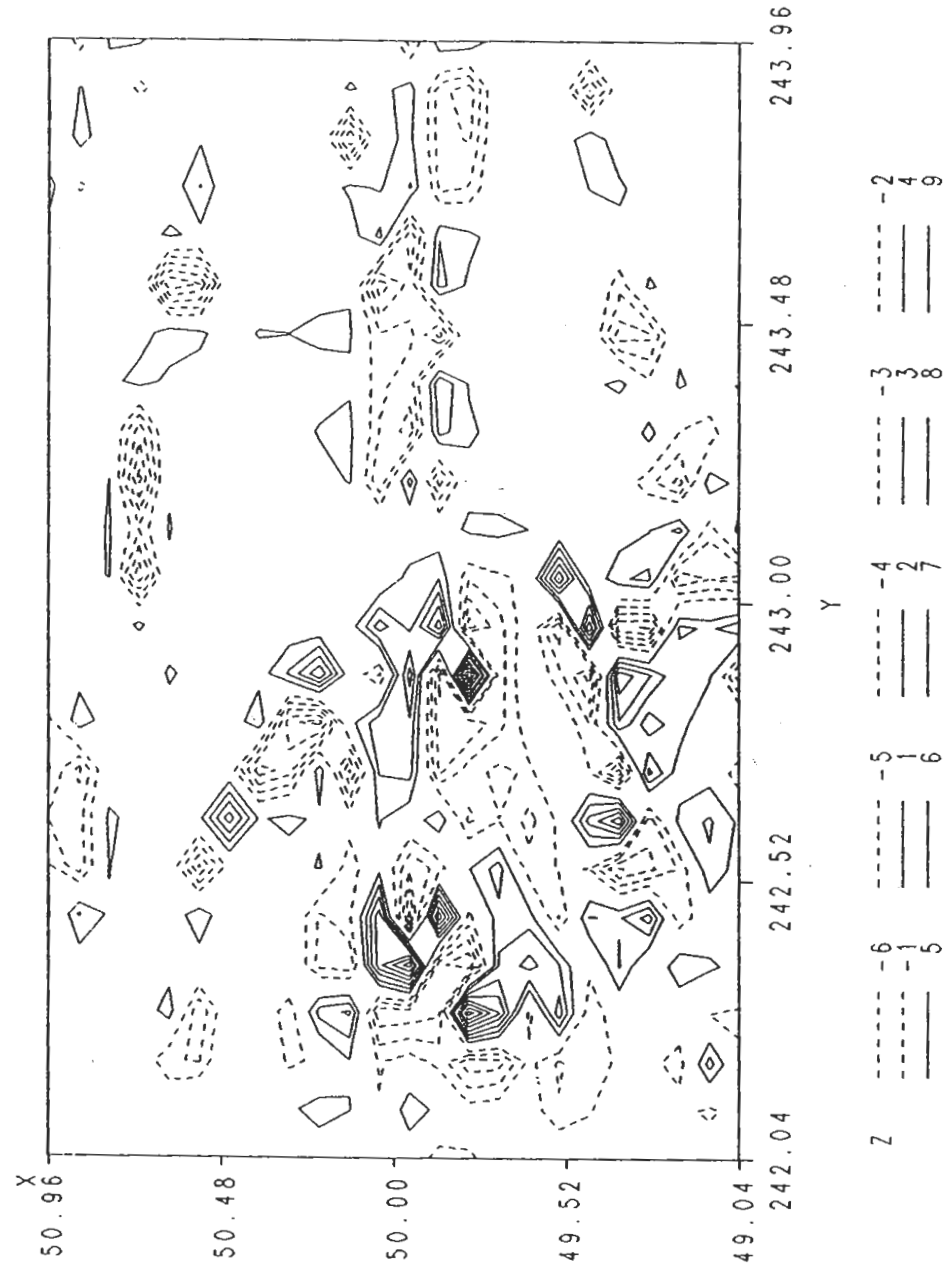

Figure 7.27: The direct topographical effect on gravity $\delta A_{\delta\varrho}(\Omega)$ (in mGals) induced by the laterally varying geological structure beneath the Purcell Mountains.

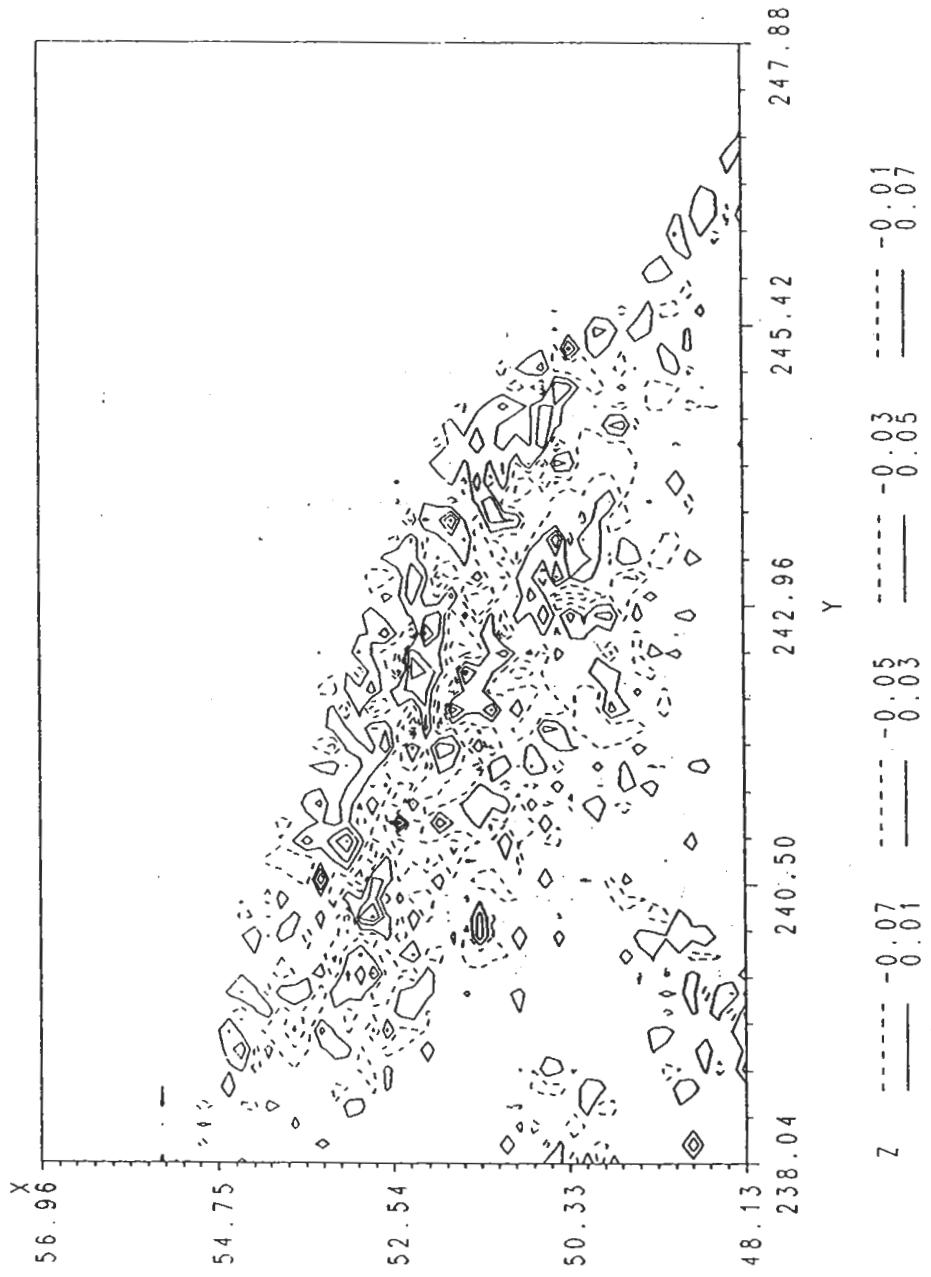

Figure 7.26: The geoidal heights $N_{dir,\delta\varrho}(\Omega)$ (in metres) due to the Pratt-Hayford compensation mechanism of area B.

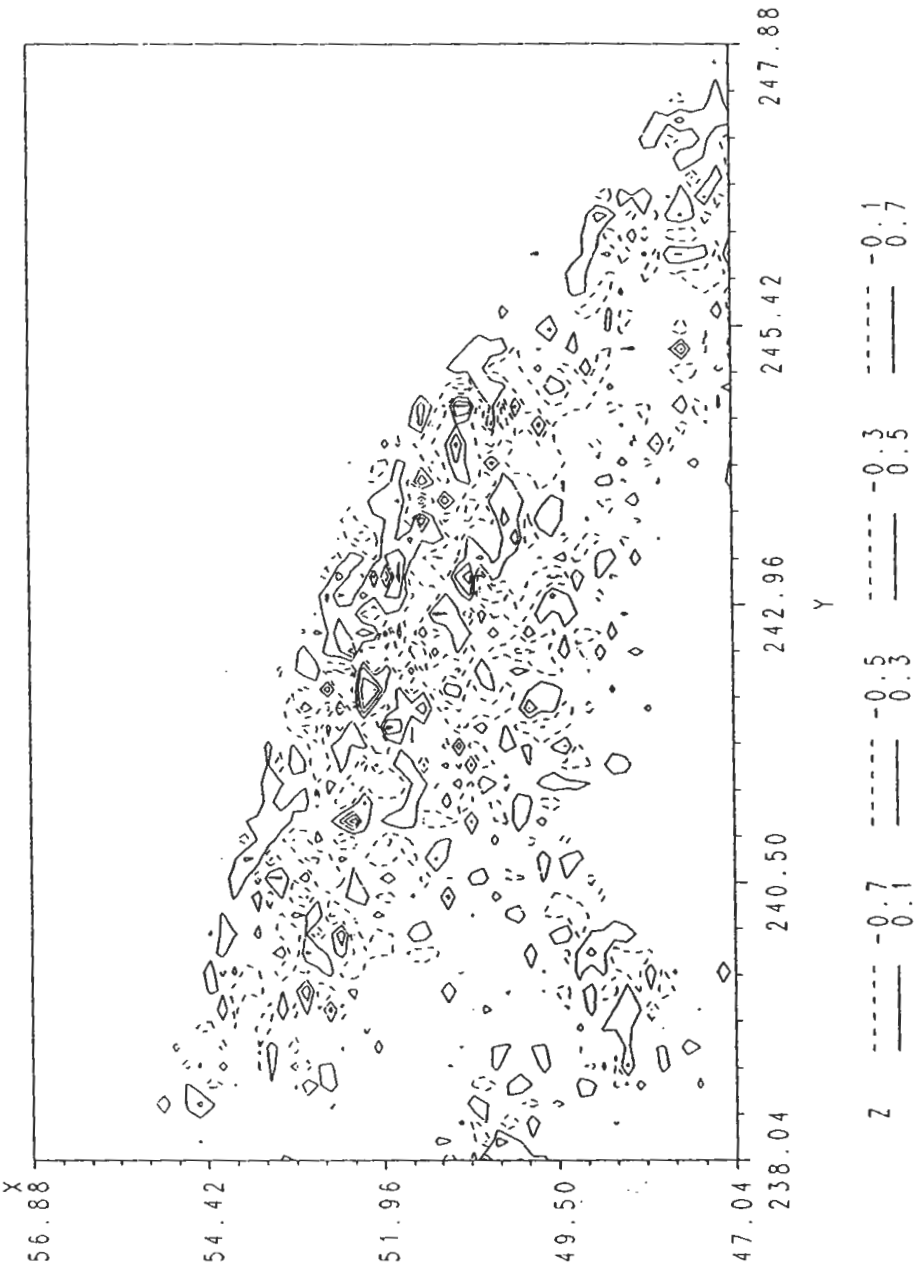

Figure 7.25: The direct topographical effect on gravity $\delta A_{\delta\varrho}(\Omega)$ (in mGals) induced by the Pratt-Hayford compensation density (5.33) over area B.

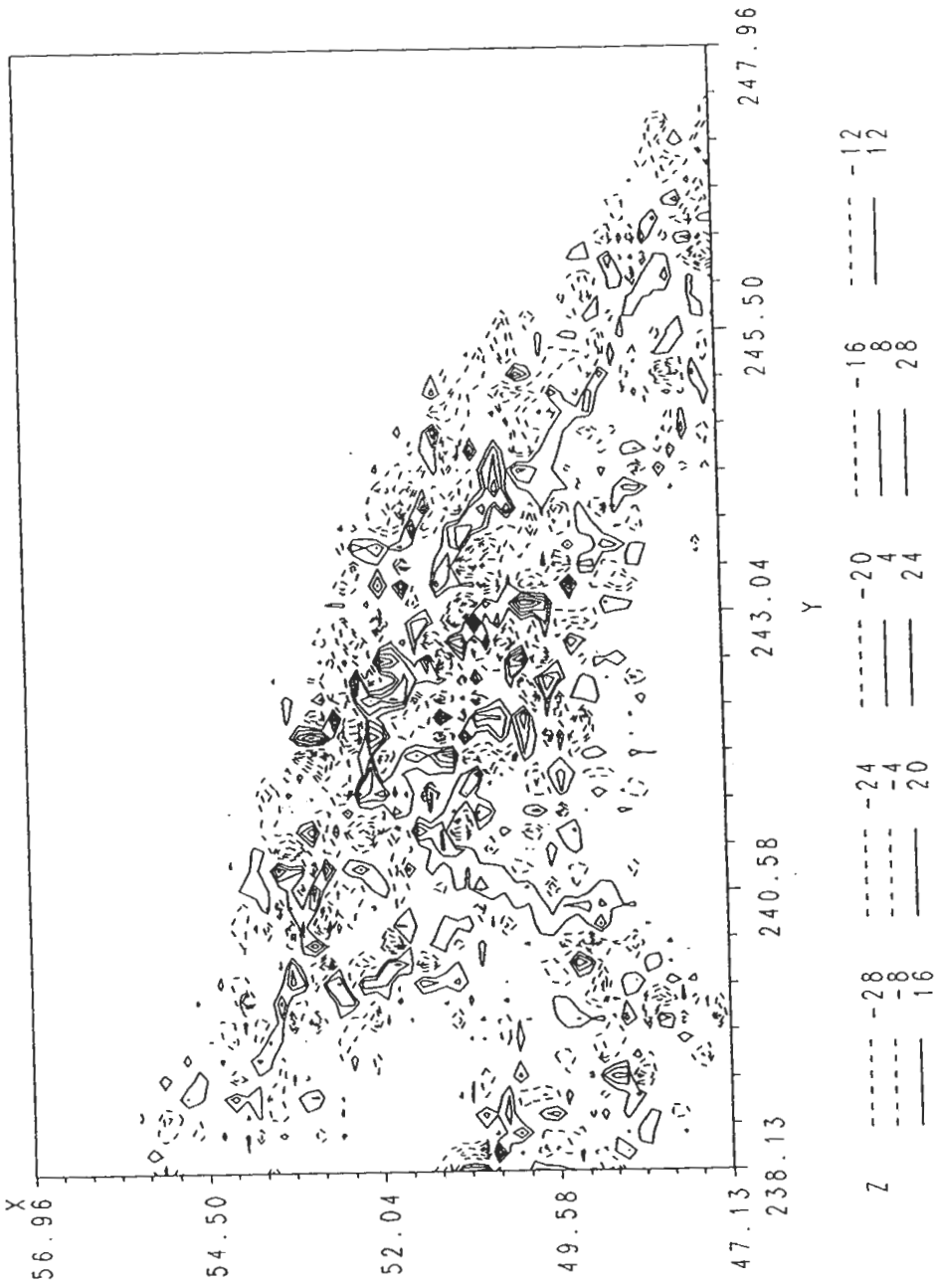

Figure 7.24: The direct topographical effect on gravity $\delta A_0(\Omega)$ (in mGals) over the area B.

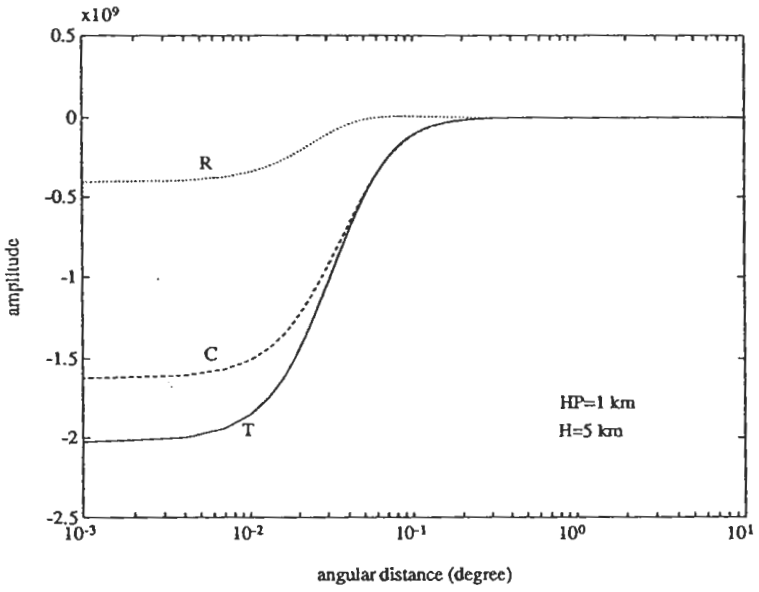

Figure 7.23: The same as Figure 7.21 for $H = 5$km.

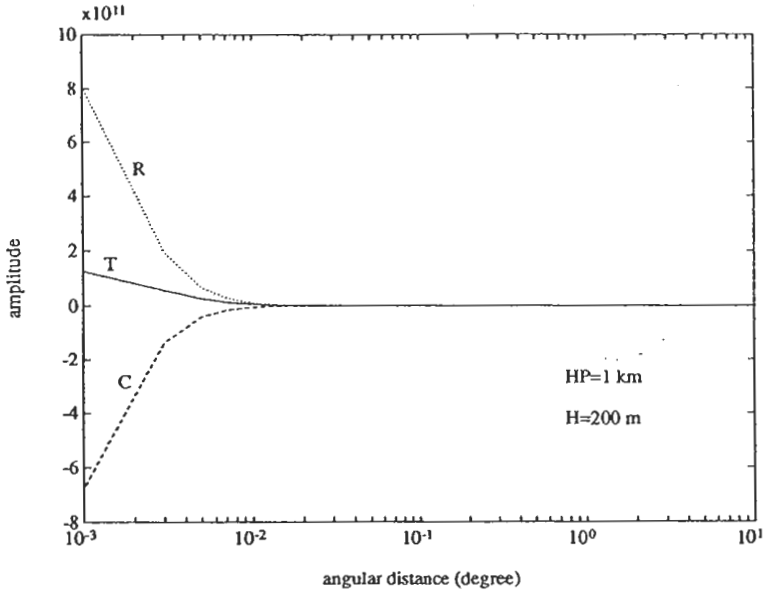

Figure 7.21: Integration kernels $\partial\widetilde{N}(R,\psi,r')/\partial r\big|_{r'=R}^{R+H'}$ (T-curve), $R^2\tau(\Omega')\partial N(r,\psi,R)/\partial r$ (C-curve), and their difference (R-curve) for $H' = 1$km and $H = 200$m.

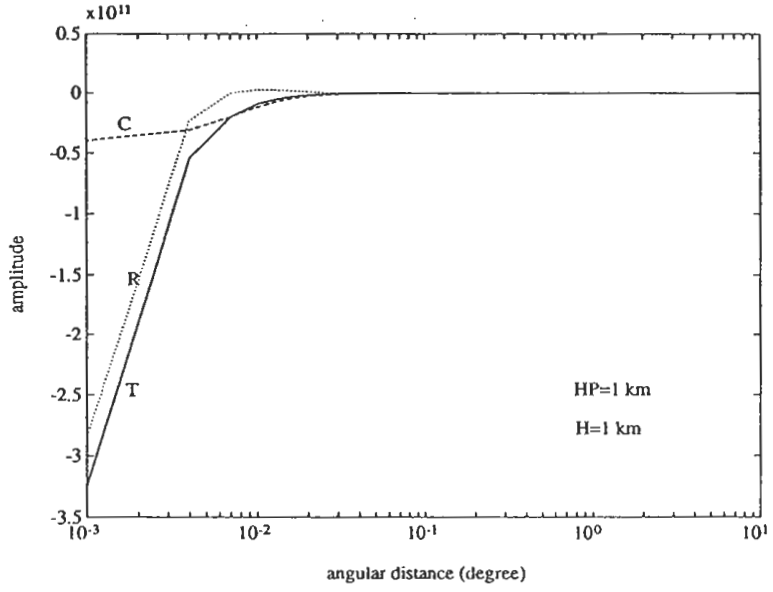

Figure 7.22: The same as Figure 7.21 for $H = 1$km.

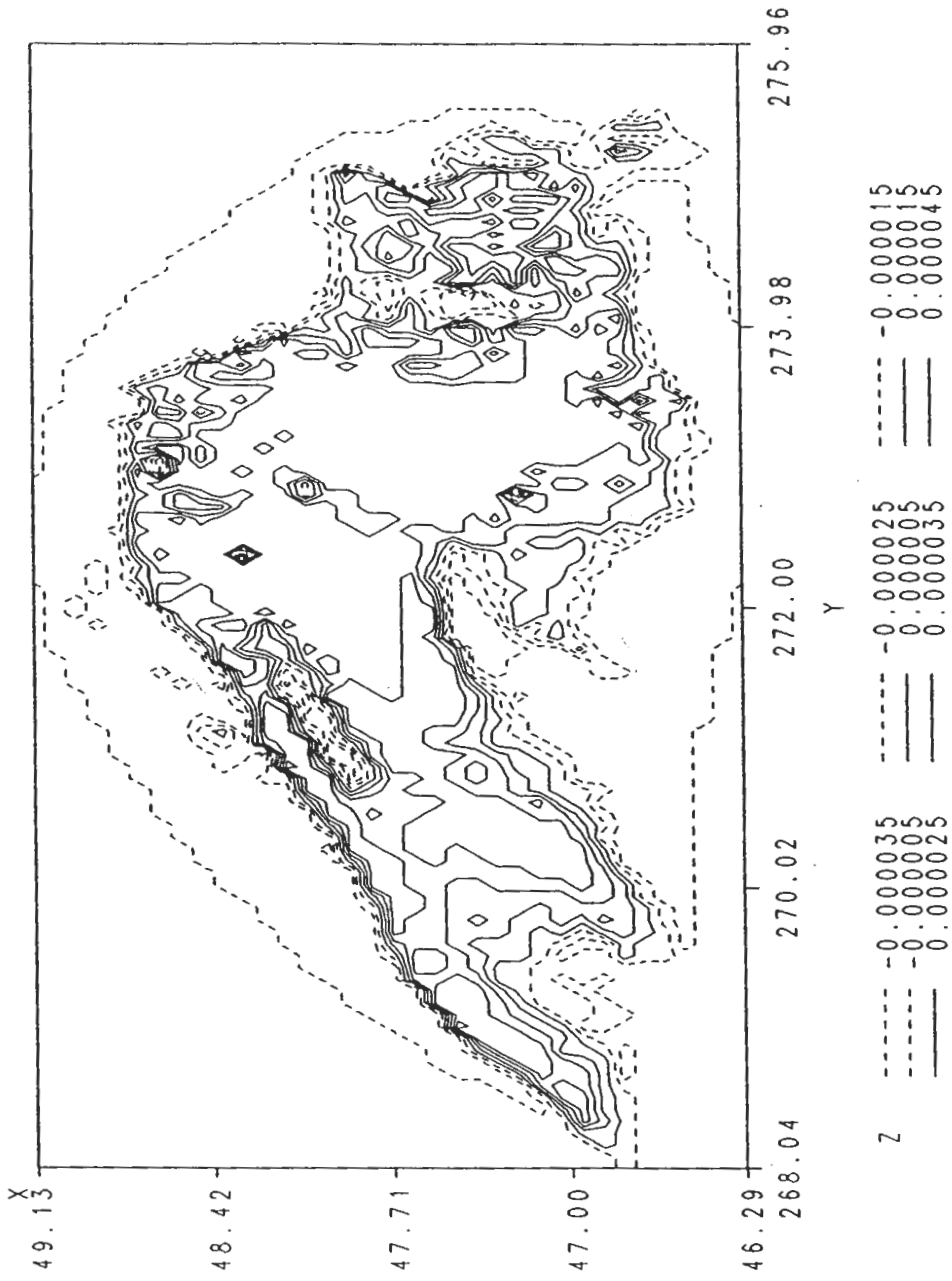

Figure 7.20: The geoidal heights $N^R_{pri,\delta\varrho}(\Omega)$ (in metres) over the lake Superior.

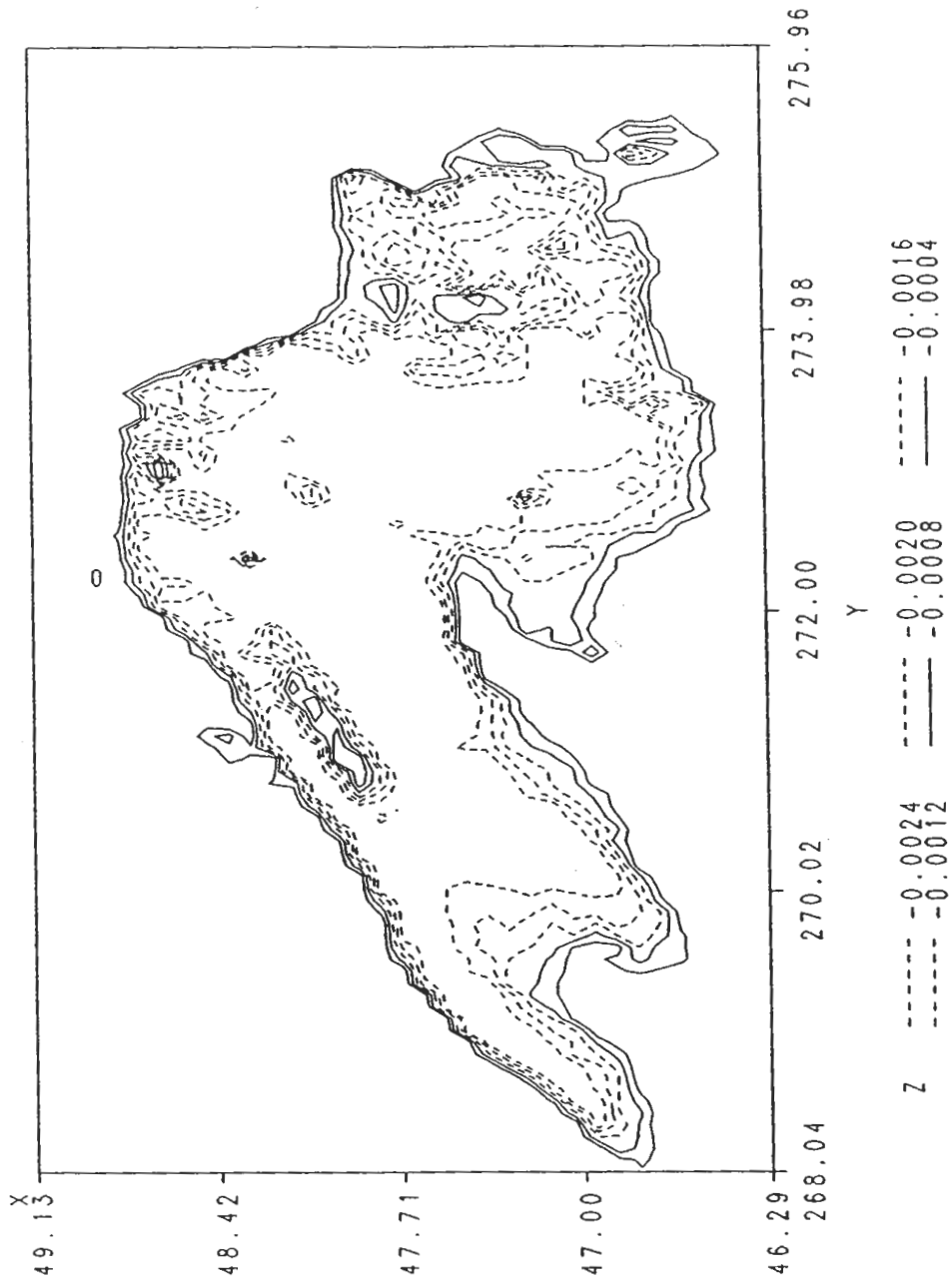

Figure 7.19: The geoidal heights $N^B_{pri,\delta\varrho}(\Omega)$ (in metres) over the lake Superior.

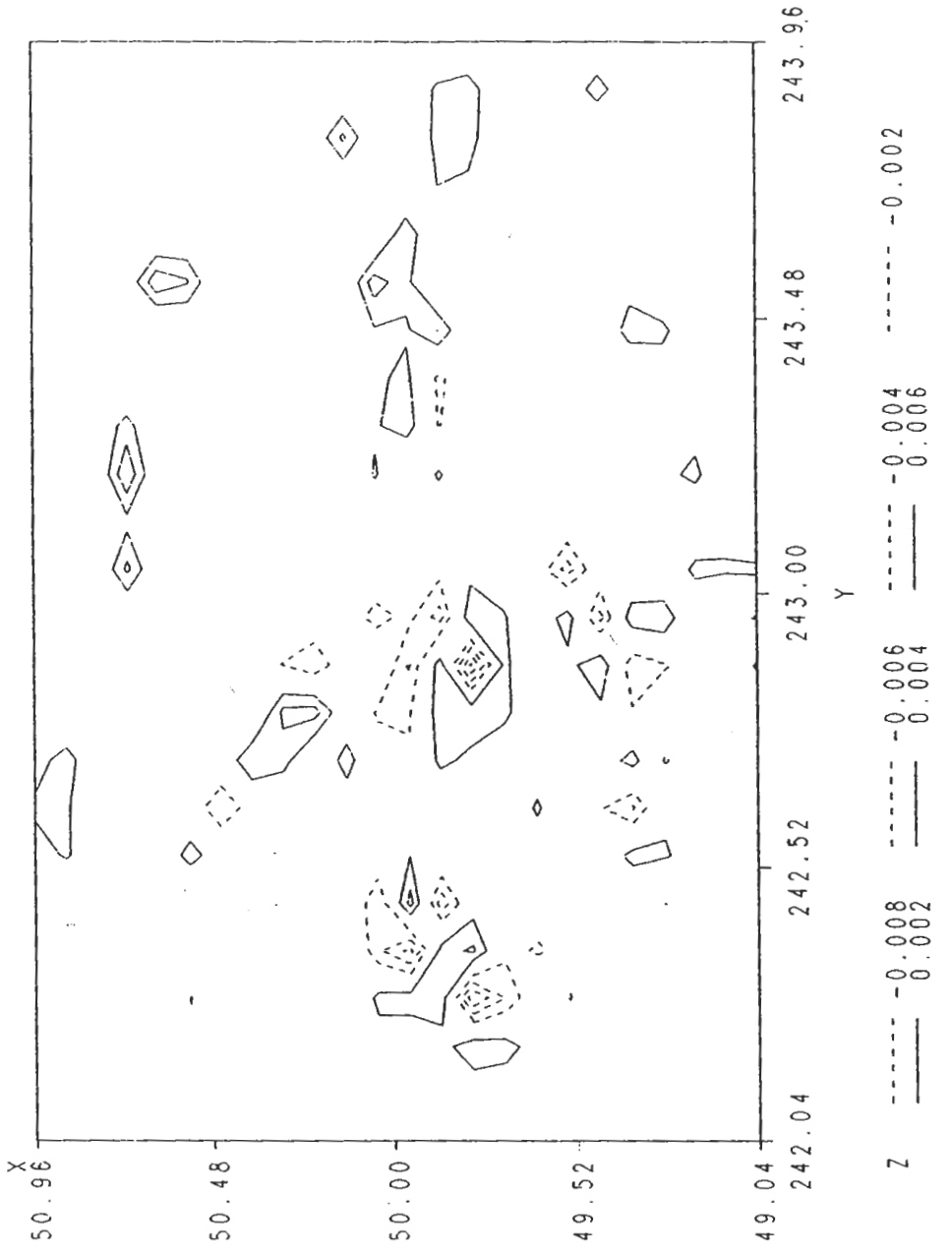

Figure 7.18: The geoidal heights $N^R_{pri,\delta\varrho}(\Omega)$ (in metres) induced by the laterally varying geological structure beneath the Purcell Mountains.

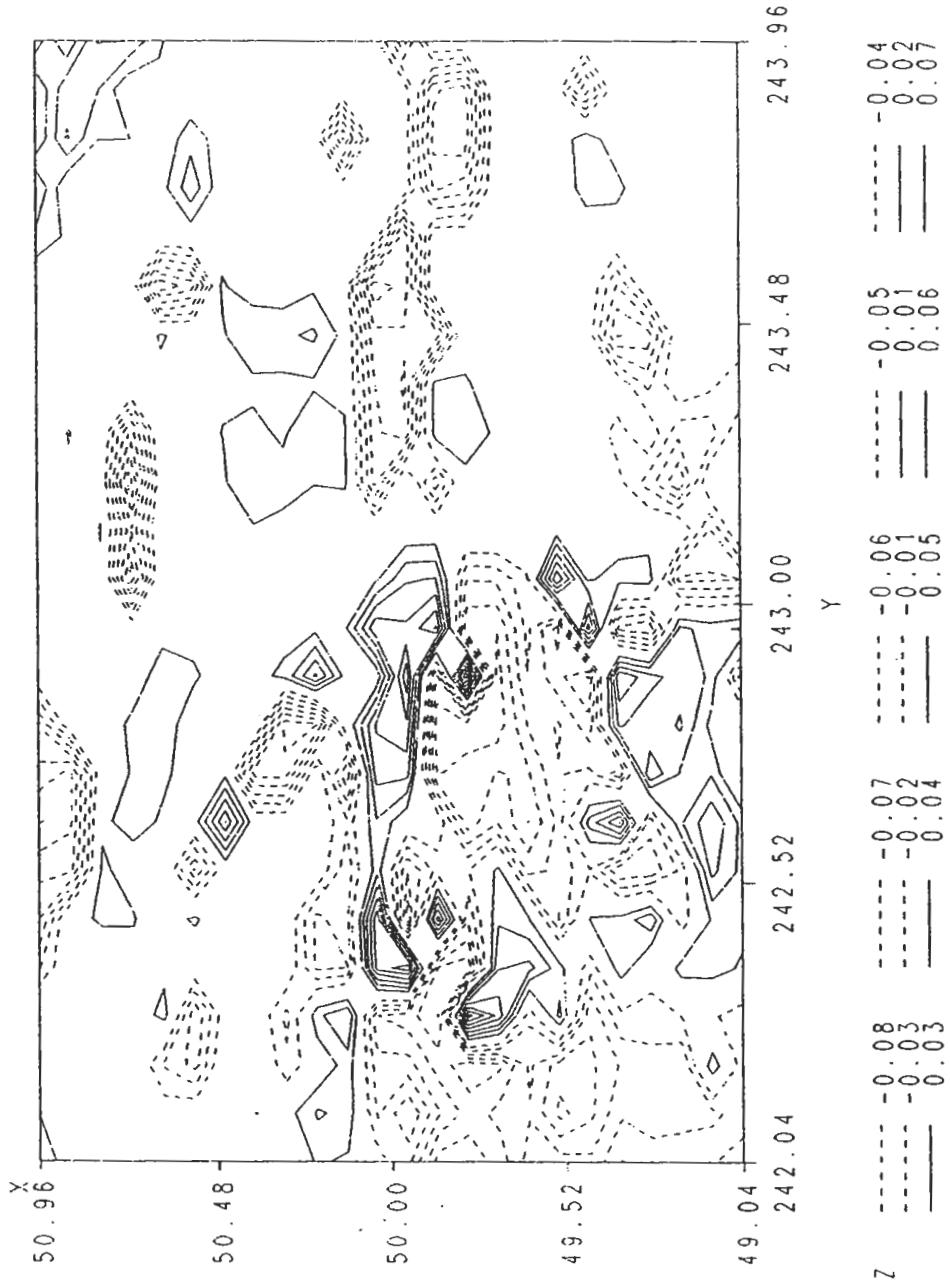

Figure 7.17: The geoidal heights $N^B_{pri,\delta\varrho}(\Omega)$ (in metres) induced by the laterally varying geological structure beneath the Purcell Mountains.

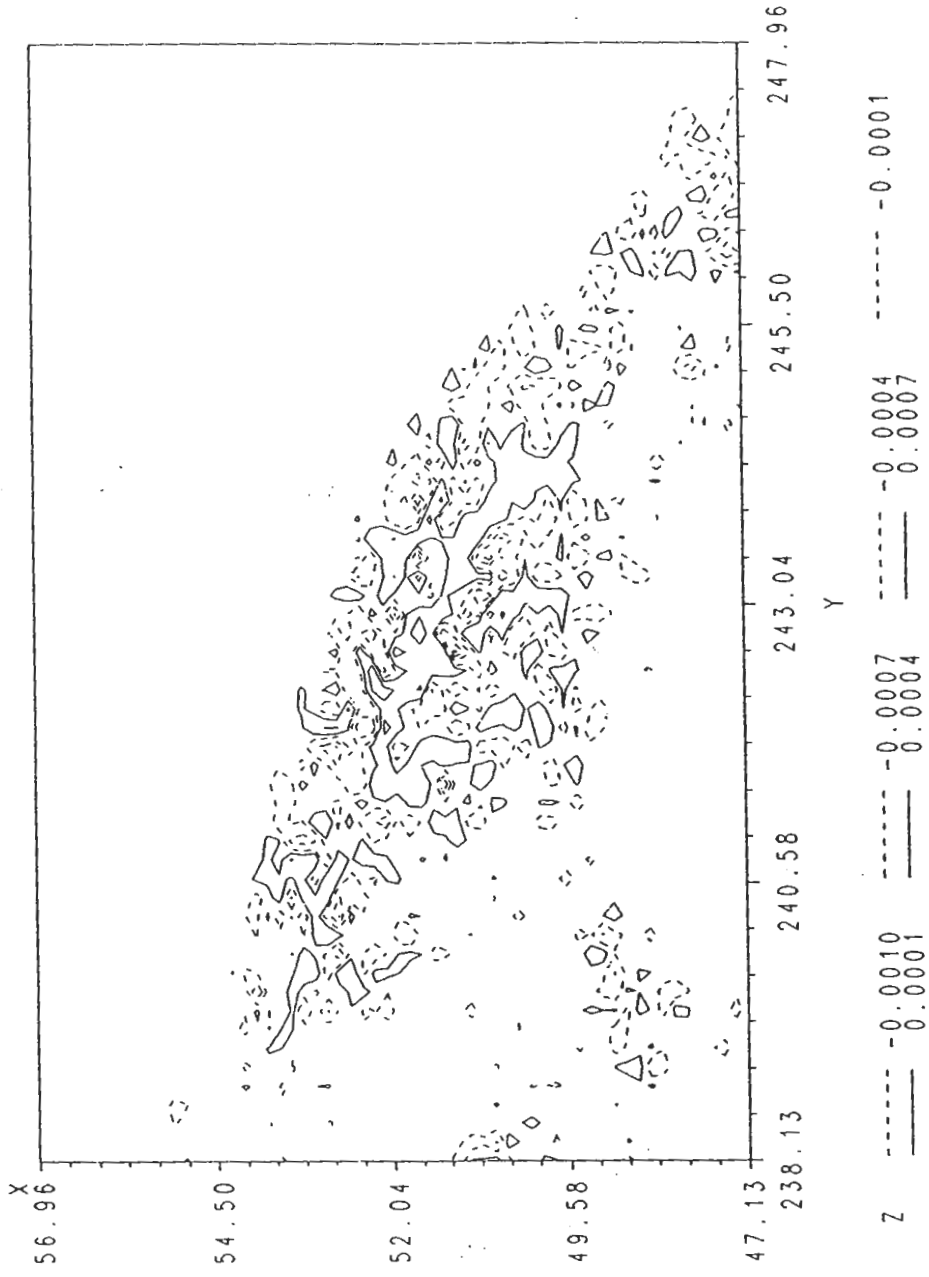

Figure 7.16: The geoidal heights $N^R_{pri,\delta\varrho}(\Omega)$ (in metres) induced by the Pratt-Hayford density anomalies (5.33) over area B.

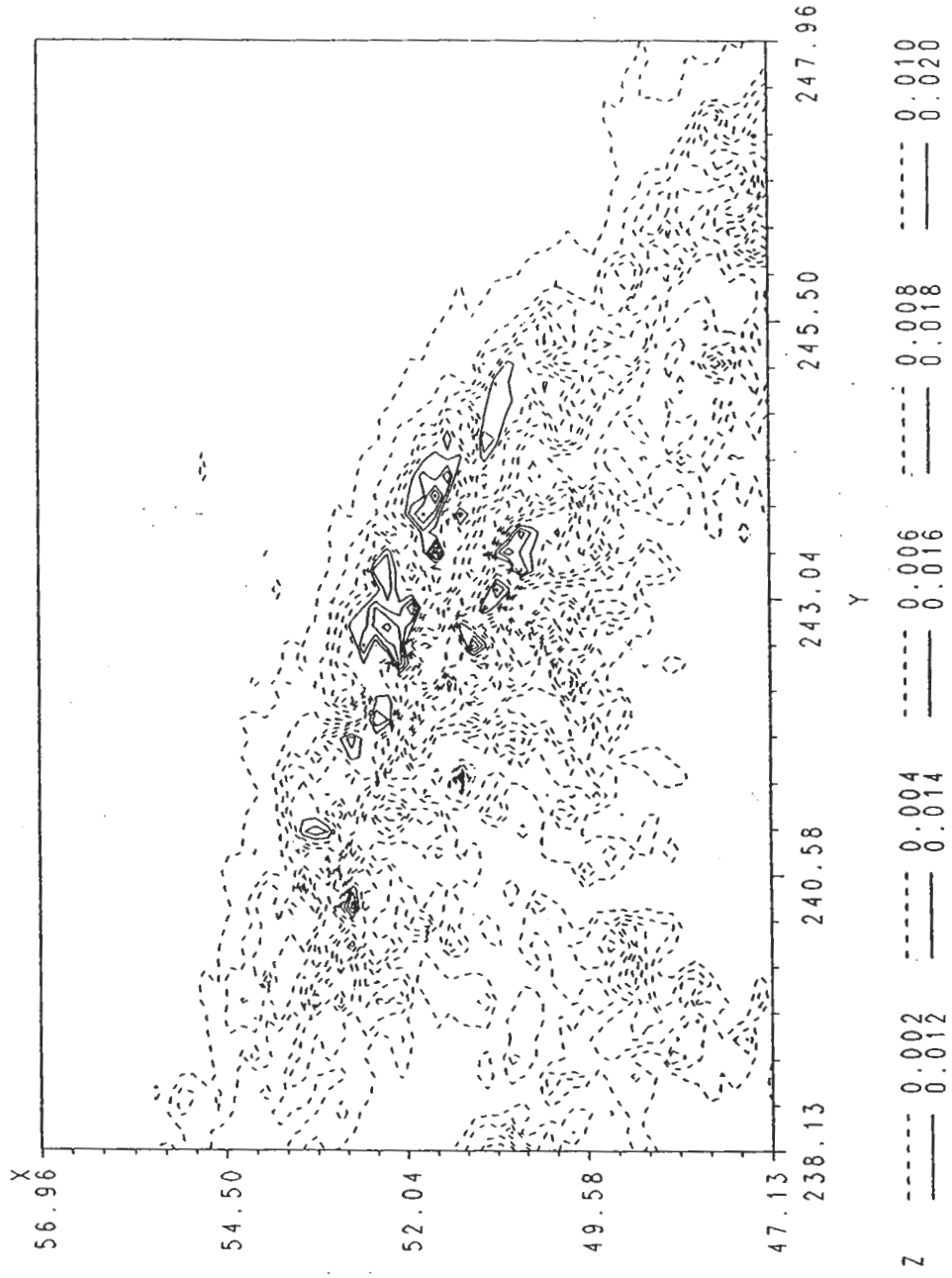

Figure 7.15: The geoidal heights $N^B_{pri,\delta\varrho}(\Omega)$ (in metres) induced by the Pratt-Hayford density anomalies (5.33) over area B.

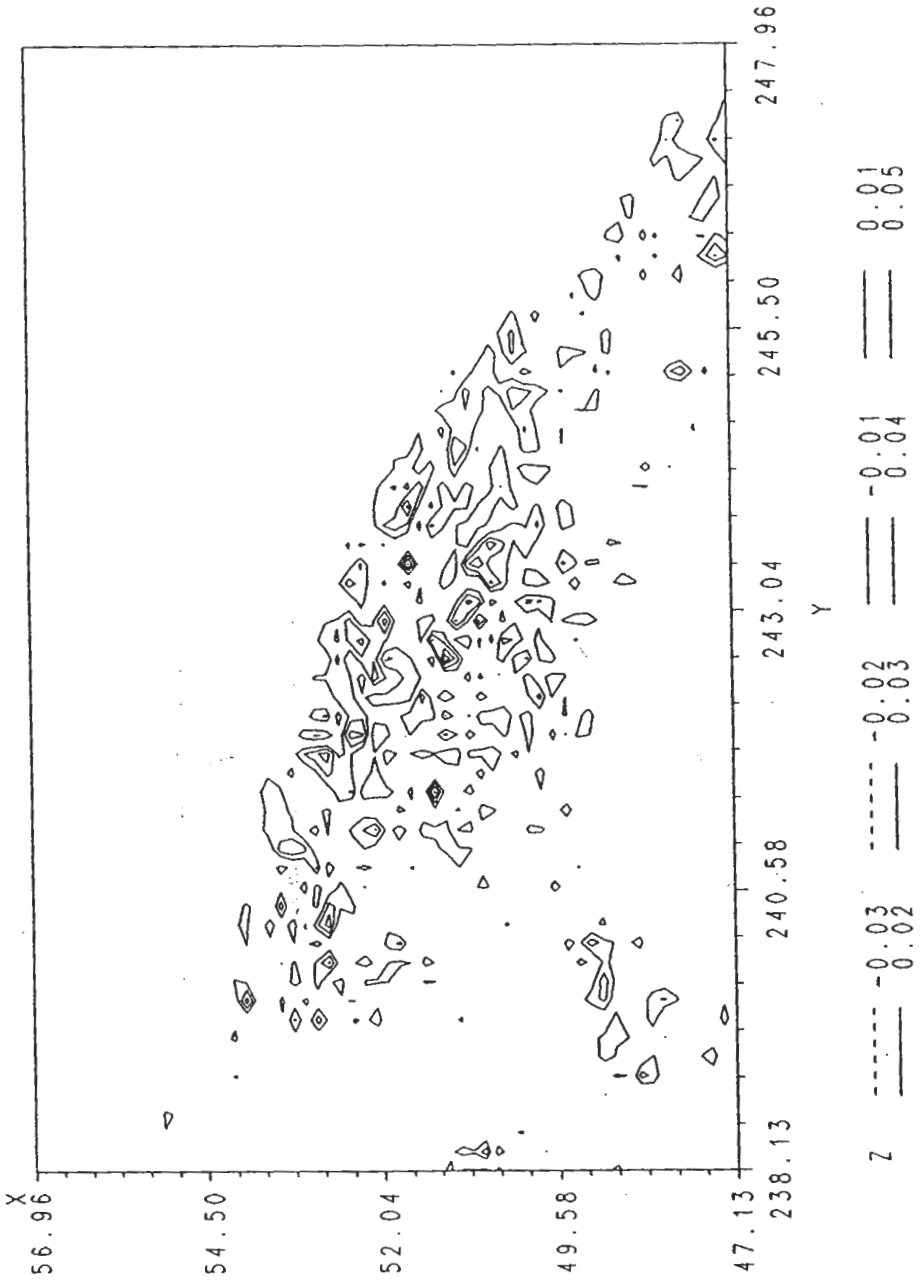

Figure 7.14: The geoidal heights (in metres) induced by term $N^R_{pri,0}(\Omega)$ over area B.

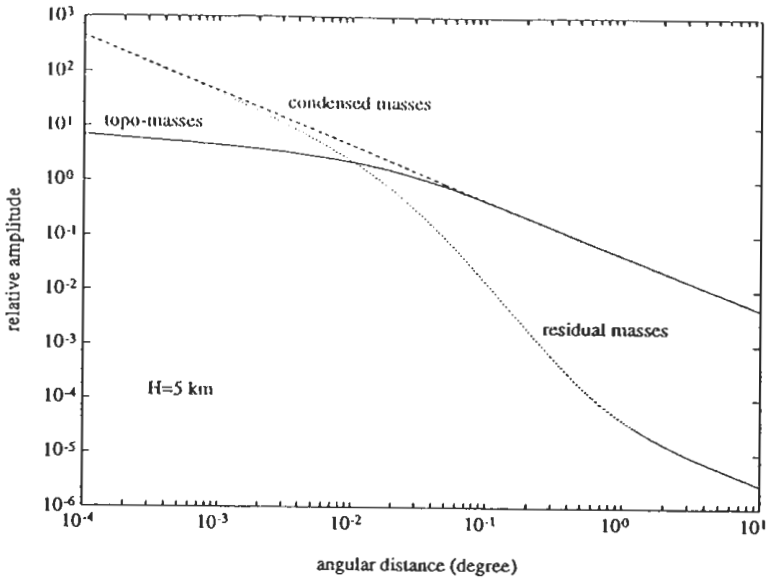

Figure 7.12: The same as Figure 7.10 for $H' = 5$km.

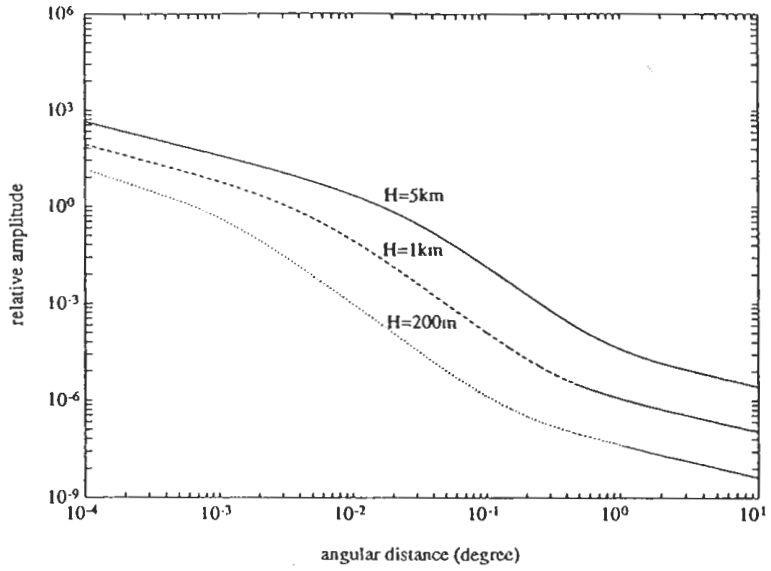

Figure 7.13: Integration kernel $\widetilde{N}(R,\psi,r')\Big|_{r'=R}^{R+H'} - R^2\tau(\Omega')N(R,\psi,R)$ for $H' = 5$km (solid), $H' = 1$km (dashed), and $H' = 200$m (dotted).

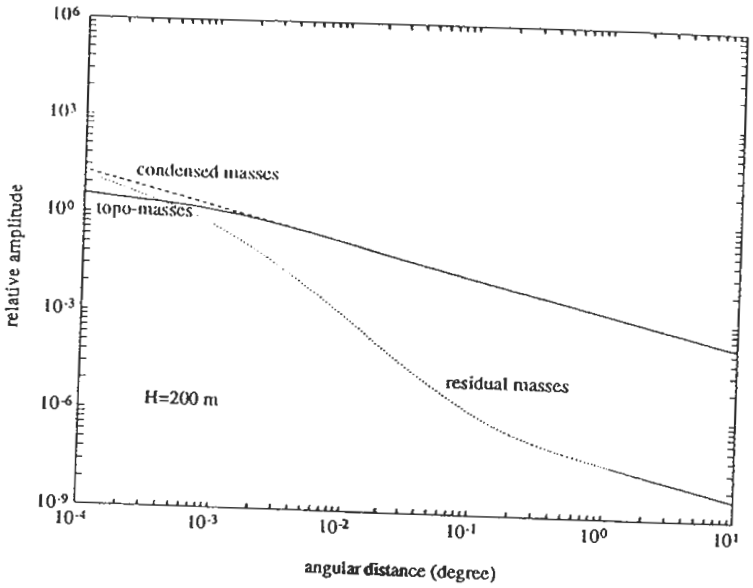

Figure 7.10: Integration kernels $\widetilde{N}(R,\psi,r')\Big|_{r'=R}^{R+H'}$ (solid), $R^2\tau(\Omega')N(R,\psi,R)$ (dashed), and their difference (dotted) for $H' = 200$m.

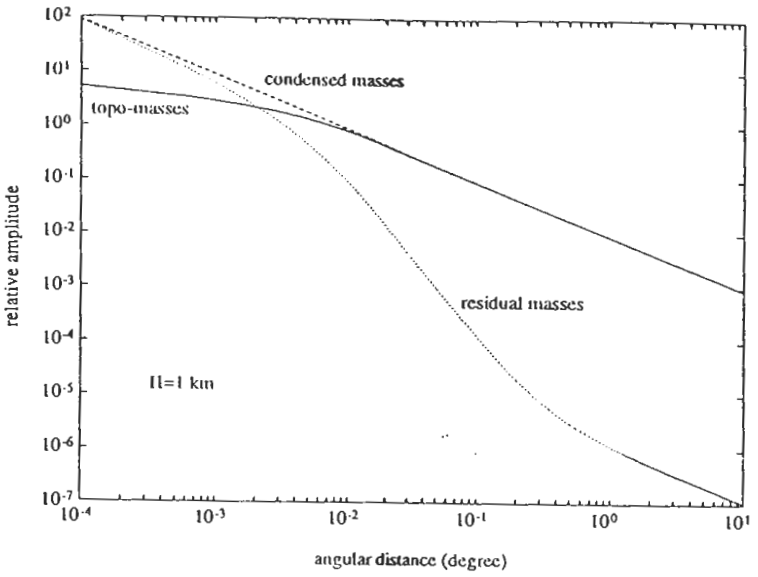

Figure 7.11: The same as Figure 7.10 for $H' = 1$km.

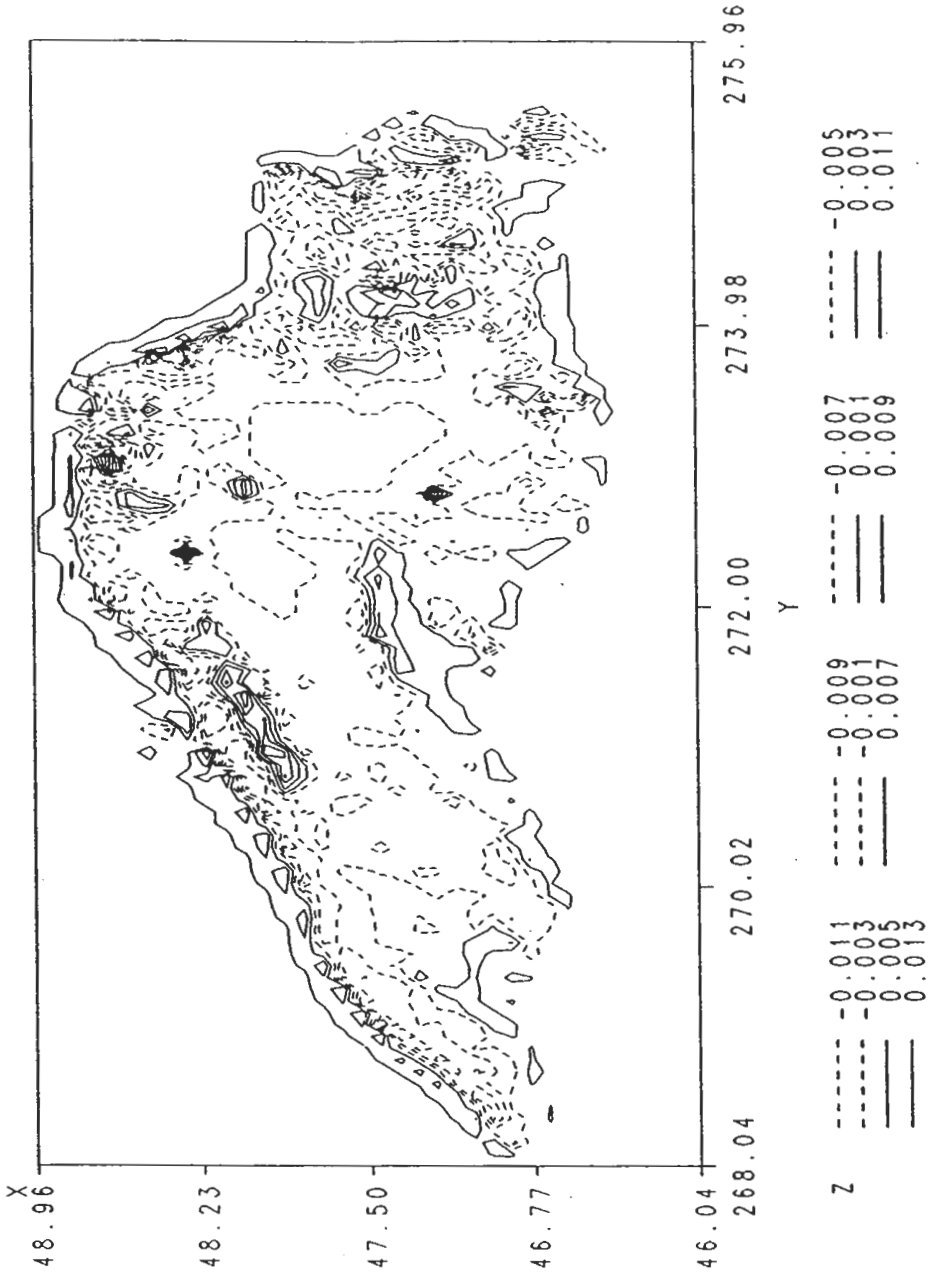

Figure 7.29: The geoidal heights $N_{dir,\delta\varrho}(\Omega)$ (in metres) generated by the gravitation $\delta A_{\delta\varrho}(\Omega)$ over the lake Superior. Truncation radius of the Stokes integration was 6^o.

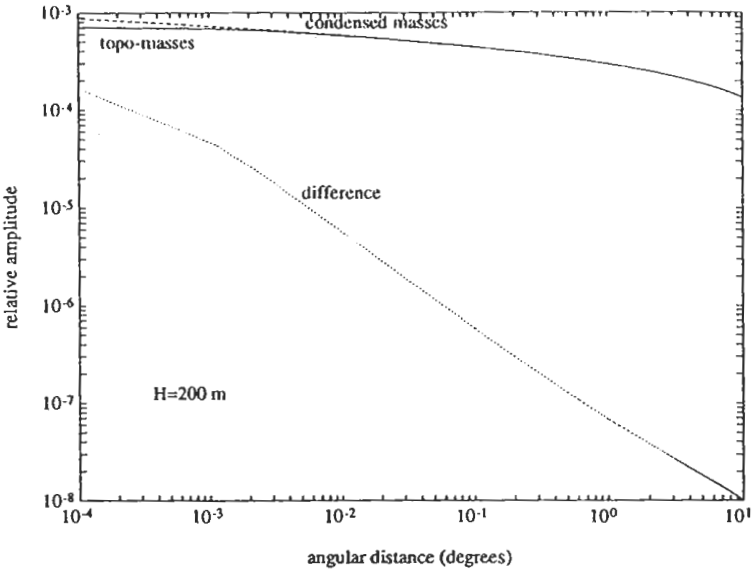

Figure 7.30: Integration kernels $\tilde{U}(R,\psi,r')\Big|_{r'=R}^{R+H'}$ (solid), $R^2\tau(\Omega')U(R,\psi,R)$ (dashed), and their difference (dotted) for $H' = 200$m.

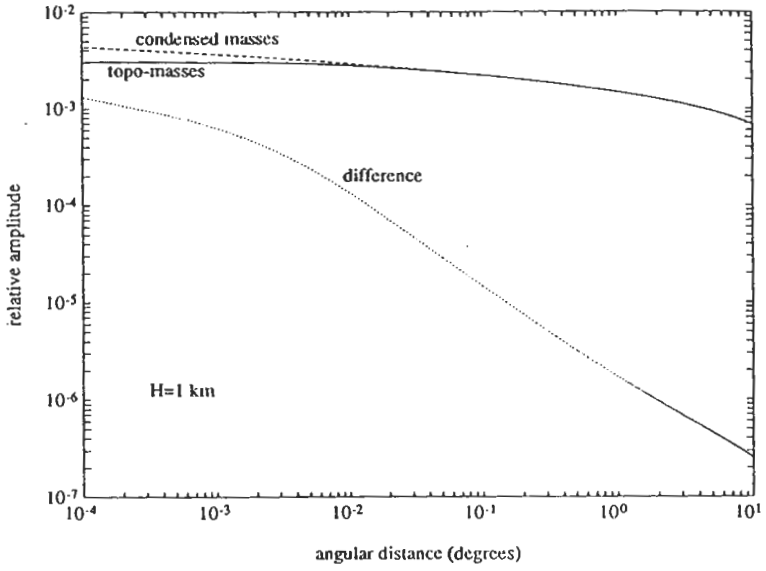

Figure 7.31: The same as Figure 7.30 for $H' = 1$km.

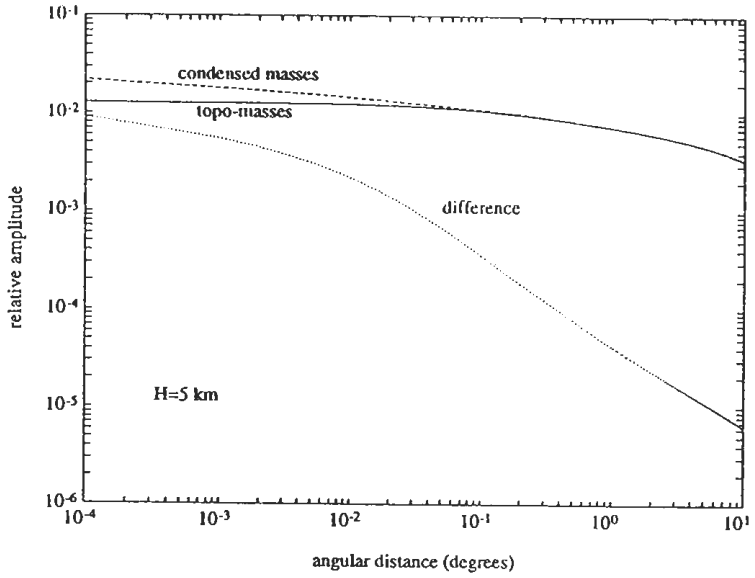

Figure 7.32: The same as Figure 7.30 for $H' = 5\text{km}$.

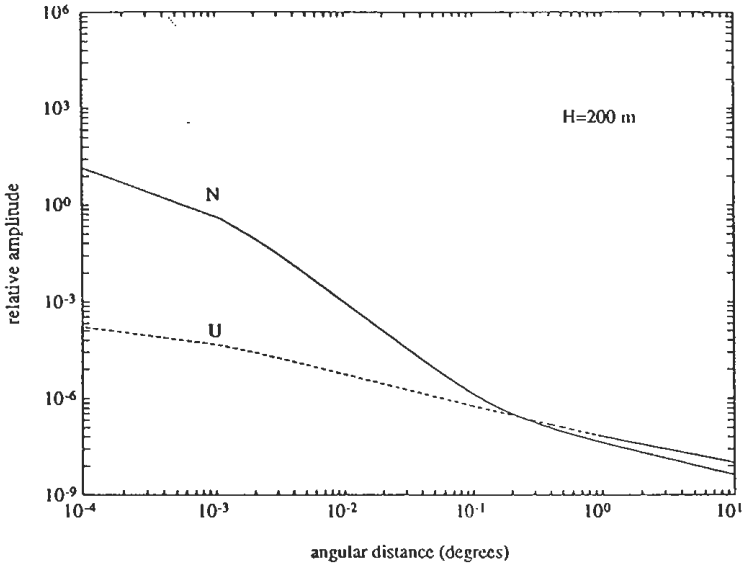

Figure 7.33: Integration kernels $\widetilde{N}(R,\psi,r')\Big|_{r'=R}^{R+H'} - R^2\tau(\Omega')N(R,\psi,R)$ (N-curve), and $\widetilde{U}(R,\psi,r')\Big|_{r'=R}^{R+H'} - R^2\tau(\Omega')U(R,\psi,R)$ (U-curve) for $H' = 200\text{m}$.

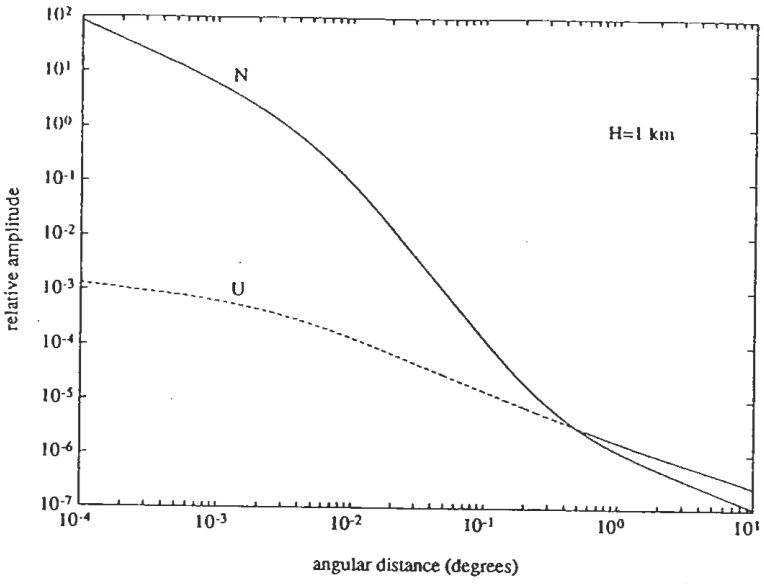

Figure 7.34: The same as Figure 7.33 for $H' = 1$km.

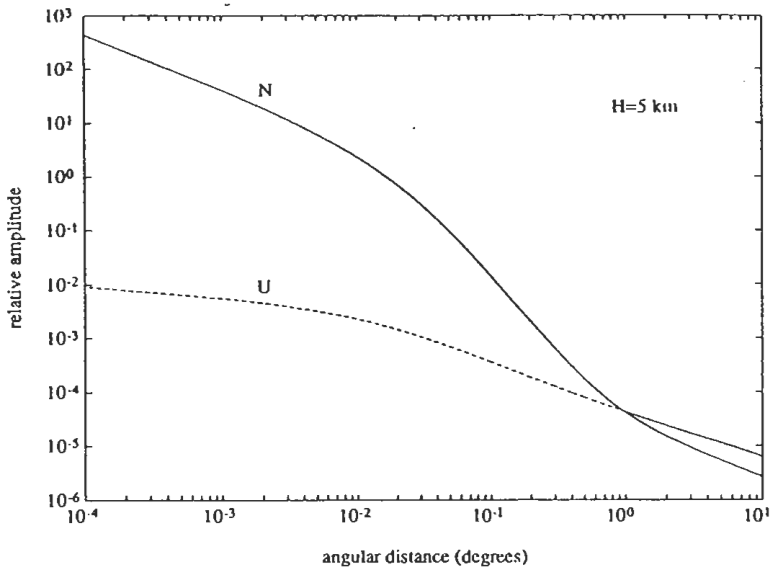

Figure 7.35: The same as Figure 7.33 for $H' = 5$km.

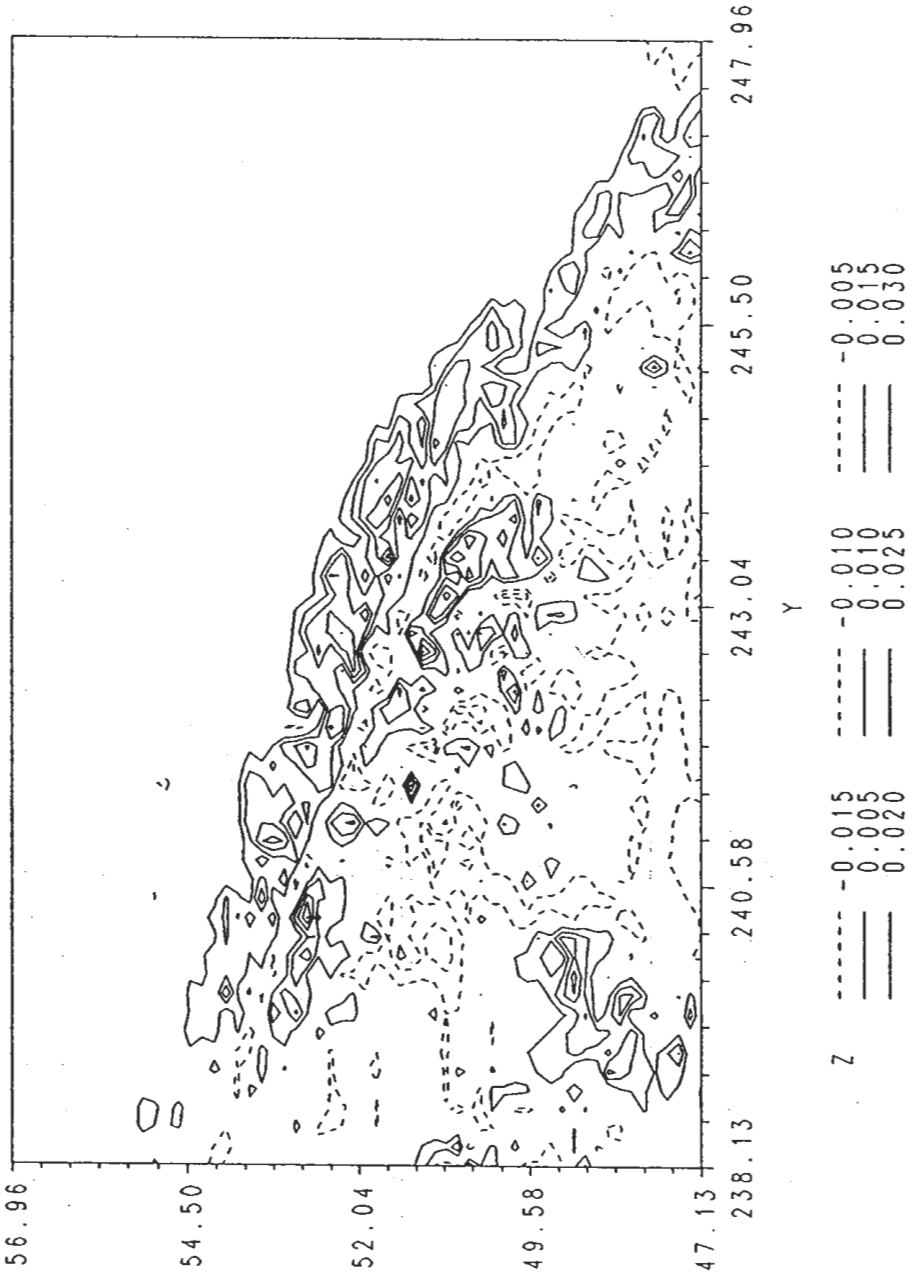

Figure 7.36: The geoidal heights (in metres) induced by the term $N_{sec,0}(\Omega)$ over area B.

Conclusions and recommendations

The report was focused on the problem wheather lateral changes of the density of topographical masses should be taken into consideration if the geoidal heights are to be determined with an absolute accuracy of 1 cm. To answer this question, we had to solve out some theoretical problems associated not only with the effect of lateral variations of the topographical density on the geoid, but also with the theory of finding the solution of the boundary-value problem for geoid determination.

In geodetical literature there is still not a unique formulation of the boundary-value problem for geoid determination. The existence of topographical masses and the question how to incorporate their gravitational effect into the solution of the problem are perhaps reasons of different formulations and solutions for the geoid. Geodesists still cannot decide wheather the boundary-value problem for the geoid (not the quasi-geoid) should be formulated on the earth's surface or on the geoid. Here, in Chapter 1, we have formulated the problem on the earth's surface and then continued the anomalous gravitational potential from the earth's surface to the geoid. It is not difficult to show that such a formulation leads to a non-singular integral for the downward continuation of the anomalous gravitation. On the contrary, if gravity anomalies are firstly continued from the earth's surface to the geoid, and then the boundary-value problem is formulated on the geoid, the downward continuation of gravity anomalies is represented by a strongly singular integral (Moritz, 1980, sect.45).

Strongly singular integrals also appear when the gravitational potential of the topographical masses is treated by the Taylor series expansion (Heck, 1992; Martinec and Vaníček, 1993a). To avoid this type of singularity and to

retain the character of the Newton integral as a weak singular integral, we did not use the Taylor series expansion of the Newton kernel but removed the singularity of the Newton kernel by a simple algebraic operation (Chapter 3).

Having solved these theoretical problems, we were able to investigate the effect of lateral variations of the topographical density on the geoidal heights. We split the laterally varying topographical density into a constant reference density and a lateral anomalous density and explored the terms separately. As a matter of fact, this enables to sort the topographical terms into three groups (sect. 7.4) according to their magnitudes.

The greatest contributions to geoidal heights come from terms of the first group; their magnitude may reach metres. They are determined by elevations of the earth's surface; the density of topographical masses for computing these terms is considered constant ($=2.67 g/cm^3$). The terms of the second group contribute to the geoid by decimetres at most over a rugged terrain of the Rocky Mountains and by milimetres over a flat terrain. They are determined by the elevations of the earth's surface as well as by laterally varying anomalous density of the topographical masses. The terms of the third group may be neglected for a 1-cm geoid computation. These facts also tell us that the effect of elevations of the earth's surface on the geoid is more prenounced than the effect of lateral changes of topographical density. Roughly saying, the topographical elevations contribute to geoidal heights by metres at most, whereas lateral density anomalies of topographical masses contribute to the geoid by decimetres at most.

We explored three types of lateral anomalies of the topographical density: the density contrast between water in a lake and surrounding rockies, the compensation density due to the Pratt-Hayford compensation mechanism of the topographical masses, and the density coming from the geological information. The first type of anomalous density may become important in the regions of a large lake. On the example of the lake Superior (lying in the central part of the North America), we demonstrated that errors due to neglecting the 'water' effect of the lake on the geoid may reach centimetres; in this particular case it was 2 cm at most. The anomalous densities coming from the Pratt-Hayford compensation model represent the maximal density changes within the topographical masses due to their compensation; the actual density variations due to compensation mechanism are probably smaller. Numerically, the Pratt-Hayford compensation densities contributes

to the geoid by centimetres at most.

The greatest lateral density variations occur due to a particular geological formation and local geological factors. These may affect the topographical density as much as 10% or even more. On a density pattern of geological structure beneath the Purcell Mountains, we demonstrated that the lateral changes of topographical density due to geological factors contribute to the geoid by decimetres at most.

Recommendations

The reported investigations of the gravitational effect of the topographical masses in context of 1-cm geoid determination result in the following recommendations.

(a) The gravitational effect of the topographical masses is described by three terms: the direct topographical effect on gravity, the primary indirect topographical effect on potential and the secondary indirect topographical effect on gravity. These topographical terms are defined **uniquely** by relations (1.24), (1.16), and (1.25), respectively. The contraversy between Vaníček and Kleusberg's (1987) and Wand ad Rapp's (1990) formulae for the direct topographical effect on gravity is easily to explain. Whereas the former describe the direct topographical effect on gravity only, the latter mix this phenomenon with the downward continuation of the gravity anomaly.

(b) Although Heck (1992) claims that there is no significant for 1-cm geoid determination wheather spherical or planar approximation of the geoid is used in expressions for the topographical terms, we beg to differ. The type of approximations significantly influences the Bouguer parts of the topographical terms; the differences of geoidal heights due to different approximations of the geoid may reach metres.

(c) In a rugged mountaineous terrain such as the Rocky Mountains, the Taylor series expansion of the Newton kernel does not converge. It may cause errors of the order of decimetres measured in the geoidal heights. Results are not possible to improve adding other terms of Taylor infinite series because of divergency of the series. The formulae derived in this report overcome the problem of divergency of the Taylor series. They may be used for an arbitrarily rugged terrain; the only condition is that the terrain must be star-shaped.

(d) For a rugged terrain of the Rocky Mountains a grid $5' \times 5'$ of to-

pographical heights is of such a poor resolution that it introduces errors of metres into the geoidal heights. It is highly recommended to use a more denser topographical grid, e.g. 1km× 1km to reduce this disretization error.

(e) For the same type of terrain, the geoid cannot be determined without knowledge of the density of the topographical masses. The numerical studies performed above show that for a 1-cm geoid the topographical density should be known with a relative accuracy of 1% or better.

(f) In a flat terrain, an approximation of the actual density of topographical masses by value of $2.67 g/cm^3$ is good enough for a 1-cm geoid determination.

(h) The 'water' effect of large lakes should be considered for a 1-cm geoid determination.

References

Cruz, J.Y., (1986). Ellipsoidal corrections to potential coefficients obtained from gravity anomaly data on the ellipsoid. Dept. of Geod. Sci. Rep., **371**, State Univ., Columbus.

Dziewonski, A.M., and D.L. Anderson (1981). Preliminary reference Earth model. *Phys. Earth Planet Inter.*, **25**, 297-356.

Featherstone, W.E., (1992). A G.P.S. controlled gravimetric determination of the geoid of the British Isles. PH.D. Thesis, University of Oxford, England, pp.252.

Forsberg, R. and M.G. Sideris (1993). Geoid computations by the multi-band spherical FFT aproach. *Manusc. geod.*, **18**, 82-90.

Geological Map of British Columbia (1962), Map (932), Geological Survey of Canada.

Geological Map of Canada (1962), Map 1045A, Geological Survey of Canada.

Gradshteyn, I.S., and I.M.Ryzhik (1980). *Table of Integrals, Series, and Products.* Corrected and enlarged edition, transl. by A.Jeffrey, Academic Press, New York.

Grafarend, E.W. (1989). The geoid and the gravimetric boundary value problem. The Royal Institute of Technology, Stockholm, TRITA GEOD series, **18**.

Heck, B. (1992): A revision of Helmert's second method of condensation in geoid and quasigeoid determination. Paper presented at 7th Int. Symposium Geodesy and Physics of the Earth, IAG-Symposium, No.112, Potsdam, October 1992.

Heiskanen, W.H., and F.A. Vening Meinesz (1958). *The Earth and Its Gravity Field.* Mc-Graw-Hill, New York.

Heiskanen, W.H., and H. Moritz (1967). *Physical Geodesy.* W.H.Freeman and Co., San Francisco.

Helmert, F.R. (1884). *Die mathematische und physikalische Theorien der höheren Geodäsie*, vol.2. Lepzig, B.G.Teubner.

Kellogg, O.D. (1929). *Foundations of Potential Theory.* Berlin, J.Springer (reprinted by Dover Publications, New York,1953).

Martinec, Z., (1990). A refined method of recovering potential coefficients from surface gravity data. *Studia geoph. et geod.*, **34**, 313-326.

Martinec, Z. (1992a). The minimum depth of compensation of topographic masses. Accepted for publication in *Geoph. J. Int.*.

Martinec, Z. (1992b). The density contrast at the Mohorovičič discontinuity. Accepted for publication in *Geoph. J. Int.*.

Martinec, Z. (1993a). Gravitational effect of residual topographical masses in the Stokes-Helmert technique for geoid determination. Progress rep. No.1 under the contract 'Effect of lateral density variations of topographical masses in view of improving on geoid model accuracy over Canada'. Dept. of Surv. Eng., Univ. of New Brunswick, Fredericton, N.B.

Martinec, Z. (1993b). The first and second indirect topographical effect. Progress report No.2 under the contract 'Effect of lateral density variations of topographical masses in view of improving on geoid model accuracy over Canada'. Dept. of Surv. Eng., Univ. of New Brunswick, Fredericton, N.B.

Martinec, Z. (1993c). The direct topographical effect on gravity. Stokes's integration. Progress report No.3 under the contract 'Effect of lateral density variations of topographical masses in view of improving on geoid model accuracy over Canada'. Dept. of Surv. Eng., Univ. of New Brunswick, Fredericton, N.B.

Martinec, Z., and P. Vaníček (1993a). The indirect effect of Stokes-Helmert's technique for a spherical approximation of the geoid. Submitted to *Manusc. geod.*, July 1992.

Martinec, Z., and P. Vaníček (1993b). Direct topographical effect of Helmert's condensation for a spherical geoid. Submitted to *Manusc. geod.*, February 1993.

Martinec, Z., and P. Vaníček (1993c). Correction of Moritz's formula for harmonic continuation of garvity anomaly (in preparation).

Martinec, Z., C. Matyska, E.W. Grafarend, and P. Vaníček (1993a). On Helmert's 2nd condensation technique. Submitted to *Manusc. geod.*, November 1992.

Martinec, Z., P. Vaníček, A. Mainville and M.Véronneau (1993b). The effect of lake water on geoid height computation (in preparation).

Martinec, Z., P. Vaníček, A. Mainville and M.Véronneau (1993c). Convergence of Taylor series expansion for the primary indirect topographical effect on potential (in preparation).

Molodenskij, M.S., V.F. Eremeev, and M.I. Yurkina: *Methods for Study of the External Gravitational Field and Figure of the Earth*, 1962 translation from Russian by the Israel Program for Scientific Translations for the Office of Technical Services, Department of Commerce, Washington, D.C., 1960.

Moritz, H. (1966). Linear solutions of the geodetic boundary-value problem. Dept. of Geod. Sci. Rep., **79**, Ohio State Univ., Columbus.

Moritz, H. (1968). On the use of the terrain correction in solving Molodensky's problem. Dept. of Geod. Sci. Rep., **108**, Ohio State Univ., Columbus.

Moritz, H. (1980). *Advanced Physical Geodesy.* H.Wichmann Verlag, Karlsruhe.

Olliver, J.G. (1980). The gravimetric geoid of Great Britain and Ireland. *Geoph. J. R. astr. Soc.*, **63**, pp.253-270.

Paul, M. (1973). A method of evaluating the truncation error coefficients for geoidal heights. *Bull. Geod.*, **110**, 413-425.

Pavlis, N.K. (1988). Modeling and estimation of a low degree geopotential model from terrestrial gravity data. Dept. of Geod. Sci. Rep., **386**, State Univ., Columbus.

Pellinen, L.P. (1962): Accounting for topography in the calculation of quasi-geoidal heights and plumb-line deflections from gravity anomalies. *Bull. Geod.*, **63**, 57-65.

Rapp, R.H., Y.M. Wang, and N.K. Pavlis (1991). The Ohio State 1991 geopotential and sea surface topography harmonic coefficients models. Dept. of Geod. Sci. Rep., **410**, State Univ., Columbus.